

UNCLASSIFIED

AD NUMBER

AD862285

LIMITATION CHANGES

TO:

Approved for public release; distribution is unlimited.

FROM:

Distribution authorized to U.S. Gov't. agencies and their contractors;  
Administrative/Operational Use; DEC 1969. Other requests shall be referred to Air Force Armament Lab., Eglin AFB, FL.

AUTHORITY

AFATL ltr 14 Nov 1975

THIS PAGE IS UNCLASSIFIED



**PARAMETRIC STUDY OF SEPARATION CHARACTERISTICS  
OF THE M-117 BOMB FROM THE F-4C AIRCRAFT  
AT TRANSONIC SPEEDS**

**E. G. Allee, Jr.**

**ARO, Inc.**

**December 1969**

This document has been approved for public release  
its distribution is unlimited

*Re: TAB 16-6  
Dtd 12 March 72*

This document is subject to special export controls and each transmittal to foreign governments or foreign nationals may be made only with prior approval of Air Force Armament Laboratory (AFATL) (ATII), Eglin AF Base, Florida 32542.

**PROPULSION WIND TUNNEL FACILITY  
ARNOLD ENGINEERING DEVELOPMENT CENTER  
AIR FORCE SYSTEMS COMMAND  
ARNOLD AIR FORCE STATION, TENNESSEE**

# ***NOTICES***

When U. S. Government drawings specifications, or other data are used for any purpose other than a definitely related Government procurement operation, the Government thereby incurs no responsibility nor any obligation whatsoever, and the fact that the Government may have formulated, furnished, or in any way supplied the said drawings, specifications, or other data, is not to be regarded by implication or otherwise, or in any manner licensing the holder or any other person or corporation, or conveying any rights or permission to manufacture, use, or sell any patented invention that may in any way be related thereto.

Qualified users may obtain copies of this report from the Defense Documentation Center.

References to named commercial products in this report are not to be considered in any sense as an endorsement of the product by the United States Air Force or the Government.

**PARAMETRIC STUDY OF SEPARATION CHARACTERISTICS  
OF THE M-117 BOMB FROM THE F-4C AIRCRAFT  
AT TRANSONIC SPEEDS**

**E.G. Allee, Jr.  
ARO, Inc.**

This document has been approved for public release  
and its distribution is unlimited. *La TAB 76-6  
2nd 12 March '76*

This document is subject to special export controls and each transmittal to foreign governments or foreign nationals may be made only with prior approval of Air Force Armament Laboratory (AEATL) (ATII), Eglin AF Base, Florida 32542.

## FOREWORD

The test reported herein was sponsored by the Air Force Armament Laboratory (AFATL) (ATII) under Program Element 62701F. Program Area 327B.

The results of the test were obtained by ARO, Inc. (a subsidiary of Sverdrup & Parcel and Associates, Inc.), contract operator of the Arnold Engineering Development Center (AEDC), Air Force Systems Command (AFSC), Arnold Air Force Station, Tennessee, under Contract F40600-69-C-0001. The test was conducted from August 12 through 16, 1969, under ARO Project No. PC0011, and the manuscript was submitted for publication on October 9, 1969.

Information in this report is embargoed under the Department of State International Traffic in Arms Regulations. This report may be released to foreign governments by departments or agencies of the U. S. Government subject to approval of Air Force Armament Laboratory (AFATL) (ATII), or higher authority within the Department of the Air Force. Private individuals or firms require a Department of State export license.

This technical report has been reviewed and is approved.

George F. Garey  
Major, USAF  
Acting AF Representative, PWT  
Directorate of Test

Roy R. Croy, Jr.  
Colonel, USAF  
Director of Test

**ABSTRACT**

A parametric study was conducted to determine the separation characteristics of an M-117 bomb from a Triple Ejection Rack (TER) located on the left-wing inboard pylon of an F-4C aircraft. Data were obtained using 0.05-scale models at Mach numbers from 0.50 to 1.30 and at simulated altitudes of 5000 and 20,000 ft. The effects of variations in mass, moment of inertia, center-of-gravity location, ejector force, initial store attitude on the TER, and presence of adjacent stores were investigated.

This document has been approved for public release  
its distribution is unlimited. *Per TAB 76-6  
D+4 March 76*

This document is subject to special export controls and each transmittal to foreign governments or foreign nationals may be made only with prior approval of Air Force Armament Laboratory (AFATL) (ATIL), Eglin AF Base, Florida 32542.

## CONTENTS

	<u>Page</u>
ABSTRACT . . . . .	iii
NOMENCLATURE . . . . .	vii
I. INTRODUCTION . . . . .	1
II. APPARATUS . . . . .	
2.1 Test Facility . . . . .	1
2.2 Test Articles . . . . .	1
2.3 Instrumentation . . . . .	2
III. PROCEDURE . . . . .	
3.1 General . . . . .	2
3.2 Trajectory Data Acquisition . . . . .	2
3.3 Precision of Data . . . . .	3
IV. RESULTS AND DISCUSSION . . . . .	
4.1 General . . . . .	4
4.2 Trajectories for Configuration I . . . . .	4
4.3 Trajectories for Configuration II . . . . .	4
4.4 Trajectories for Configuration III . . . . .	5
4.5 Trajectories for Configuration IV . . . . .	5
4.6 Trajectories for Configuration V . . . . .	5
4.7 Trajectories for Configuration VI . . . . .	6
4.8 Trajectories for Configuration VII . . . . .	6
V. CONCLUSIONS . . . . .	6

## APPENDIXES

### I. ILLUSTRATIONS

#### Figure

1. Isometric Drawing of a Typical Store Separation Installation and Block Diagram of the Computer Control Loop . . . . .	11
2. Tunnel Test Section and Model Installation Details . . . . .	12
3. Installation Photographs . . . . .	13
4. Dimensional Sketch of F-4C Parent Aircraft Model . . . . .	16
5. MER Installation and Configuration Details . . . . .	17
6. Dimensional Sketch of TER . . . . .	17
7. TER Installation Details . . . . .	19
8. Dimensional Sketch of M-117 Store Model . . . . .	20
9. Dimensional Sketch of 370-gal Fuel Tank Model . . . . .	21
10. Test Configurations . . . . .	22
11. Effect of Mach Number Variation for Configuration I; $\bar{m} = 23.31$ , $X_{cg} = 2.74$ , $F_{LZ} = 1200$ , $\theta = 0$ , $I_{yy} = 50$ , $h = 5000$ . . . . .	23
12. Effect of Center-of-Gravity Variation for Configuration I; $\bar{m} = 23.31$ , $F_{LZ} = 1200$ , $\theta = 0$ , $I_{yy} = 50$ , $h = 5000$ . . . . .	24

<u>Figure</u>	<u>Page</u>
13. Typical Effect of Ejector-Force Variation for Configuration I; $\bar{m} = 23.31, X_{cg} = 2.74, \theta = 0, I_{yy} = 50, M_{\infty} = 0.70, h = 5000$ . . . . .	28
14. Typical Effect of Moment-of-Inertia Variation for Configuration I; $X_{cg} = 2.74, F_{LZ} = 1200, \theta = 0, M_{\infty} = 0.90, h = 5000$ . . . . .	29
15. Typical Effect of Initial Store Attitude for Configuration I; $\bar{m} = 23.31, X_{cg} = 2.74, F_{LZ} = 1200, I_{yy} = 50,$ $M_{\infty} = 0.70, h = 5000$ . . . . .	31
16. Effect of Center-of-Gravity Variation for Configuration II; $\bar{m} = 23.31,$ $F_{LZ} = 1200, \theta = 0, I_{yy} = 50, h = 20,000$ . . . . .	32
17. Effect of Ejector-Force Variation for Configuration II; $\bar{m} = 23.31,$ $X_{cg} = 2.74, \theta = 0, I_{yy} = 50, h = 20,000$ . . . . .	34
18. Effect of Moment-of-Inertia Variation for Configuration II; $X_{cg} = 2.74, F_{LZ} = 1200, \theta = 0, h = 20,000$ . . . . .	36
19. Effect of Initial Store Attitude for Configuration II, $\bar{m} = 23.31,$ $X_{cg} = 2.74, F_{LZ} = 1200, I_{yy} = 50, h = 20,000$ . . . . .	40
20. Effect of Mach Number Variation for Configuration III; $\bar{m} = 23.31,$ $X_{cg} = 2.74, F_{LZ} = 1200, \theta = 0, I_{yy} = 50, h = 5000$ . . . . .	42
21. Effect of Center-of-Gravity Variation for Configuration III; $m = 23.31, F_{LZ} = 1200, \theta = 0, I_{yy} = 50, h = 5000$ . . . . .	43
22. Effect of Ejector Force Variation for Configuration III; $\bar{m} = 23.31,$ $X_{cg} = 2.74, \theta = 0, I_{yy} = 50, h = 5000$ . . . . .	47
23. Effect of Moment-of-Inertia Variation for Configuration III; $X_{cg} = 2.74, F_{LZ} = 1200, \theta = 0, h = 5000$ . . . . .	51
24. Typical Effect of Initial Store Attitude for Configuration III; $\bar{m} = 23.31, X_{cg} = 2.74, F_{LZ} = 1200, I_{yy} = 50, M_{\infty} = 0.90, h = 5000$ . . . . .	59
25. Effect of Center-of-Gravity Variation for Configuration IV; $\bar{m} = 23.31,$ $F_{LZ} = 1200, \theta = 0, I_{yy} = 50, h = 20,000$ . . . . .	60
26. Effect of Ejector-Force Variation for Configuration IV; $\bar{m} = 23.31,$ $X_{cg} = 2.74, \theta = 0, I_{yy} = 50, h = 20,000$ . . . . .	63
27. Effect of Moment-of-Inertia Variation for Configuration IV; $X_{cg} = 2.74, F_{LZ} = 0, \theta = 0, h = 20,000$ . . . . .	65
28. Effect of Initial Store Attitude for Configuration IV; $\bar{m} = 23.31,$ $X_{cg} = 2.74, F_{LZ} = 1200, I_{yy} = 50, h = 20,000$ . . . . .	72
29. Effect of Center-of-Gravity Variation for Configuration V; $\bar{m} = 23.31,$ $F_{LZ} = 1200, \theta = 0, I_{yy} = 50, M_{\infty} = 0.70, h = 5000$ . . . . .	75
30. Effect of Ejector-Force Variation for Configuration V; $\bar{m} = 23.31,$ $X_{cg} = 2.74, \theta = 0, I_{yy} = 50, M_{\infty} = 0.70, h = 5000$ . . . . .	76
31. Effect of Moment-of-Inertia Variation for Configuration V; $X_{cg} = 2.74, F_{LZ} = 1200, \theta = 0, h = 5000$ . . . . .	77
32. Effect of Mach Number Variation for Configuration VI; $\bar{m} = 23.31,$ $X_{cg} = 2.74, F_{LZ} = 1200, \theta = 0, I_{yy} = 50, h = 20,000$ . . . . .	79
33. Effect of Center-of-Gravity Variation for Configuration VI; $\bar{m} = 23.31,$ $X_{cg} = 2.74, F_{LZ} = 1200, \theta = 0, I_{yy} = 50, h = 20,000$ . . . . .	80
34. Effect of Ejector-Force Variation for Configuration VI; $\bar{m} = 23.31,$ $X_{cg} = 2.74, \theta = 0, I_{yy} = 50, h = 20,000$ . . . . .	82



<u>Figure</u>	<u>Page</u>
35. Effect of Moment-of-Inertia Variation for Configuration VI; $X_{cg} = 2.74, F_{LZ} = 1200, \theta = 0, h = 20,000$ . . . . .	84
36. Effect of Initial Store Attitude for Configuration VI; $\bar{m} = 23.31$ , $X_{cg} = 2.74, F_{LZ} = 1200, I_{yy} = 50, h = 20,000$ . . . . .	88
37. Effect of Center-of-Gravity Variation for Configuration VII; $\bar{m} = 23.31, F_{LZ} = 1200, \theta = 0, I_{yy} = 50, h = 20,000$ . . . . .	90
38. Effect of Ejector-Force Variation for Configuration VII; $\bar{m} = 23.31$ , $X_{cg} = 2.74, \theta = 0, I_{yy} = 50, h = 20,000$ . . . . .	92
39. Effect of Moment-of-Inertia Variation for Configuration VII; $X_{cg} = 2.74, F_{LZ} = 1200, \theta = 0, h = 20,000$ . . . . .	94
40. Effect of Initial Store Attitude for Configuration VII; $\bar{m} = 23.31$ , $X_{cg} = 2.74, F_{LZ} = 1200, I_{yy} = 50, h = 20,000$ . . . . .	98

## II. TABLES

I. Test Constants . . . . .	100
II. Range of Test Variables . . . . .	101

## NOMENCLATURE

$b$	Store lateral reference length, ft
$C_{\ell_p}$	Roll-damping coefficient
$C_{m_q}$	Pitch-damping coefficient
$C_{n_r}$	Yaw-damping coefficient
$\bar{c}$	Store longitudinal reference length, ft
$F_{LZ}$	Ejector force, lb
$h$	Simulated flight altitude, ft
$I_{xx}$	Full-scale store roll moment of inertia, slug-ft <sup>2</sup>
$I_{xz}$	Full-scale store product of inertia, slug-ft <sup>2</sup>
$I_{yy}$	Full-scale store pitch moment of inertia, slug-ft <sup>2</sup>
$I_{zz}$	Full-scale store yaw moment of inertia, slug-ft <sup>2</sup>
$M_\infty$	Free-stream Mach number
$\bar{m}$	Full-scale store mass, slugs

$q_\infty$	Free-stream dynamic pressure, psf
$S$	Store reference area, ft <sup>2</sup>
$t$	Real trajectory time from launch position, sec
$X_{cg}$	Longitudinal location of store cg from nose, ft
$X$	Travel of store cg parallel to the flight-axis system $X_F$ direction, ft
$Y$	Travel of store cg parallel to the flight-axis system $Y_F$ direction, ft
$Z$	Travel of store cg parallel to the flight-axis system $Z_F$ direction, ft
$\alpha_p$	Parent aircraft model angle of attack relative to the tunnel centerline, deg
$\eta$	Change in store yaw angle referenced to the store launch attitude, deg
$\theta$	Angle between the store centerline and the TER surface at each TER station, deg
$\lambda$	Model scale
$\nu$	Change in store pitch angle referenced to the store launch attitude, deg

## FLIGHT-AXIS SYSTEM COORDINATES

### Directions

$X_F$	Parallel to the projection of the wind vector in the aircraft plane of symmetry; positive forward as seen by the pilot
$Y_F$	Perpendicular to the aircraft plane of symmetry; positive to the right as seen by the pilot
$Z_F$	Perpendicular to the projection of the wind vector in the aircraft plane of symmetry; positive downward

### Angles

Pitch	Angle between the projection of the store longitudinal axis in the $X_F$ - $Z_F$ plane and the $X_F$ axis; positive nose up as seen by the pilot
Yaw	Angle between the store longitudinal axis and its projection in the $X_F$ - $Z_F$ plane; positive store nose right as seen by the pilot

## SECTION I INTRODUCTION

A wind tunnel investigation was conducted to determine the effect of various parameters on the separation characteristics of an M-117 bomb shape released from the F-4C aircraft. Seven configurations were investigated with the store launched from a Triple Ejection Rack (TER) mounted on the left-wing inboard pylon. Parameters varied included store mass, center of gravity, moment of inertia, ejector force, and initial store angle on the TER. Trajectories were calculated for simulated altitudes of 5000 and 20,000 ft at Mach numbers of 0.5, 0.7, 0.9, 1.1, and 1.3.

## SECTION I APPARATUS

### 2.1 TEST FACILITY

The AEDC Aerodynamic Wind Tunnel, Transonic (4T) is a closed-loop, continuous flow, variable density wind tunnel with a Mach number range from 0.10 to 1.40. Stagnation pressure can be varied from 300 to 3700 psfa at all Mach numbers within this range. The 4-ft square test section is 12.5 ft long and has variable porosity (0.5 to 10 percent) walls to provide minimum wall interference at all Mach numbers.

For captive trajectory testing, two independent support systems are used for mounting the parent aircraft and store models. The parent model is mounted inverted on a sting attached to the main pitch sector. The store model is mounted on the Captive Trajectory System (CTS) which extends from the top wall of the tunnel and provides six degrees of freedom of movement independent of the parent model.

Store movement during a trajectory is controlled by a digital-analog control loop (Fig. 1, Appendix I). The two systems work as an integrated unit and, with the required input information, provide automatic store movement during a trajectory. The store is positioned by six d-c electric motors. Maximum CTS translation is  $\pm 15$  in. from the tunnel centerline in the lateral and vertical directions and 36 in. in the axial direction. Angular displacement is limited to  $\pm 45$  deg in pitch and yaw and  $\pm 360$  deg in roll. A more complete test facility description can be found in the Test Facilities Handbook.<sup>1</sup>

Test section and model installation details are shown in Figs. 2 and 3.

### 2.2 TEST ARTICLES

Models used for this test were 0.05-scale models of the F-4C aircraft, M-117 bomb, and 370-gal. fuel tank. All trajectories in this test were launched from a TER mounted on a pylon located on the left-wing inboard station. In addition, a dummy TER

---

<sup>1</sup>Test Facilities Handbook (Seventh Edition), "Propulsion Wind Tunnel Facility", Vol. 5, Arnold Engineering Development Center, July 1968.

and pylon were attached to the right-wing inboard station. For the first five configurations, 370-gal. fuel tanks were attached to the outboard pylon stations of both wings. A forward-shifted Multiple Ejection Rack (MER) was attached to the centerline of the F-4C model at a -1.0-deg incidence angle. Dummy M-117 bomb models were attached to all three forward stations and to the two aft-outboard stations of the MER. The MER remained in this configuration during all trajectories.

Sketches of all models are shown in Figs. 4 through 9. Diagrams of all test configurations are shown in Fig. 10. The locations of the suspension points on the M-117 bomb and the TER are shown in Figs. 7 and 8. These sketches also show the location of the ejector. The ejector force always acts normal to the store mounting surface on the TER.

## 2.3 INSTRUMENTATION

A six-component, internal strain-gage balance was used to obtain store aerodynamic force and moment data. Translational and angular positions of the store were obtained from the CTS analog outputs, while parent model angle of attack was determined by an angular position indicator on the main pitch sector. The left-wing inboard TER contained a touch wire system which enabled the store to be accurately positioned for launch. The system was also wired to automatically stop the CTS motion should the store or sting support make contact with any surface other than the touch wire.

## SECTION III PROCEDURE

### 3.1 GENERAL

The general operating conditions for this investigation were as follows:

$M_\infty$	$q_\infty$ , psf	$\alpha_p$ , deg
0.50	240	3.0
0.70	300	1.4
0.90	300	0.1
1.10	400	0.0
1.30	500	0.1

Dynamic pressure was restricted to a maximum of 500 psf by structural limitations of the F-4C model. At the lower Mach numbers,  $q_\infty$  was further reduced to keep the vibration-induced axial dynamic forces within balance limitations.

### 3.2 TRAJECTORY DATA ACQUISITION

To obtain a trajectory, test conditions were established in the tunnel, and the parent model was positioned at the desired angle of attack. The store model was then oriented to a position corresponding to the store attachment point on the TER. After the

store was set at the desired initial position, operational control of the CTS was switched to the digital computer which controlled the store movement during the trajectory through commands to the CTS analog system (see block diagram, Fig. 1). Data from the wind tunnel, consisting of measured model forces and moments, wind tunnel operating conditions, and CTS rig positions, were input to the digital computer for use in the full-scale trajectory calculations. In applying the wind tunnel data to the calculations of the full-scale store trajectories, the measured forces and moments are reduced to coefficient form and then applied with proper full-scale store dimensions and flight dynamic pressure. The digital computer was programmed to solve the six-degree-of-freedom equations to calculate the angular and linear displacements of the store relative to the parent aircraft pylon. In general, the program involves using the last two successive measured values of each static aerodynamic coefficient to predict the magnitude of the coefficients over the next time interval of the trajectory. These predicted values are used to calculate the new position and attitude of the store at the end of the time interval.

The CTS is then commanded to move the store model to this new position, and the aerodynamic loads are measured. If these new measurements agree with the predicted values, the process is continued over another time interval of the same magnitude. If the measured and predicted values do not agree within the desired precision, the calculation is redone over a time interval one-half the previous value. This process is repeated until a complete trajectory has been obtained.

Pertinent test information is presented in Tables I and II of Appendix II. Pitch and yaw aerodynamic damping coefficients were supplied by the Air Force Armament Laboratory (AFATL) (ATII).

### 3.3 PRECISION OF DATA

Accuracy of the data presented is affected by such quantities as the CTS rig position error, uncertainties in setting tunnel conditions, and the sensitivity of the balance which measures aerodynamic loads. Estimated uncertainty in Mach number setting is  $\pm 0.005$ . Position accuracy for the CTS was  $\pm 0.05$  in. for X, Y, and Z axes and  $\pm 0.15$  deg about the pitch and yaw axes.

Uncertainties attributed to the balance were calculated as follows:

$t$	$\Delta X$	$\Delta Y$	$\Delta Z$	$\Delta \nu$	$\Delta \eta$
0.5	$\pm 0.04$	$\pm 0.04$	$\pm 0.04$	$\pm 0.16$	$\pm 0.12$

Roll data are not presented in this report because the forces experienced about the roll axis were less than the uncertainty of the balance roll element.

## SECTION IV RESULTS AND DISCUSSION

### 4.1 GENERAL

The data acquired from this test consisted of launch trajectories of the M-117 bomb from the F-4C aircraft. Seven weapon loading configurations were tested (see Fig. 10) at Mach numbers of 0.50, 0.70, 0.90, 1.1, and 1.3 at angles of attack varying with Mach number. Data were obtained for the various store parameters listed in Table II at a simulated altitude of 5000 ft for Configurations I, III, and V and 20,000 ft for Configurations II, IV, VI, and VII. The store was set at an angle of 0 deg ( $\theta = 0$ ) with respect to each launch surface of the TER for most of the trajectories. However, trajectories were also run with  $\theta = \pm 2$  deg to assess the influence of this parameter. The normal center of gravity for the store was located at  $X_{cg} = 2.74$  ft; therefore, this location is used as the reference on all plots showing effects of  $X_{cg}$  variation.

Generally, the major effect of varying the store characteristics was evidenced in the pitch and yaw angles. The X, Y, and Z displacements were similar for each parameter with any particular configuration.

Under some test conditions, only a very short trajectory was obtained because of store model contact with some part of the TER. Any such contact caused a store ground which resulted in automatic trajectory termination.

### 4.2 TRAJECTORIES FOR CONFIGURATION I

All trajectories for Configuration I were characterized by a rapid negative pitching motion which resulted in the CTS sting contacting the trailing edge of the wing and stopping the trajectory after a very short run time. Therefore, all Configuration I data are presented with an expanded time scale. The effect of Mach number variation is shown in Fig. 11. Data for this configuration were obtained at  $M_\infty = 0.70, 0.90, 1.10, \text{ and } 1.30$ . Trajectories resulting from center-of-gravity variation are presented in Fig. 12. At  $M_\infty = 0.70$ , an  $X_{cg} = 2.99$  resulted in a store ground on the TER and, therefore, early trajectory termination. Typical trajectories resulting from ejector-force variation are shown in Fig. 13. All ejector forces used resulted in store separation without contact with the TER. Typical trajectories resulting from moment-of-inertia variation are presented in Fig. 14. At  $M_\infty = 0.70$  and  $\bar{m} = 7.771$ , an  $I_{yy} = 50$  resulted in the store contacting the TER. All other combinations resulted in separation without store contact at all test Mach numbers. Typical trajectories resulting from varying the initial store attitude on the pylon are shown in Fig. 15. Store separation without contacting the TER was achieved at all three values of  $\theta$ .

### 4.3 TRAJECTORIES FOR CONFIGURATION II

Data for Configuration II are presented only for Mach numbers of 0.50 and 0.70. At  $M_\infty = 0.90$ , the store contacted the TER and caused early termination of all

trajectories. Trajectories resulting from variation of center of gravity are presented in Fig. 16. Trajectories resulting from ejector-force variation are presented in Fig. 17. At  $M_\infty = 0.70$ , an  $F_{LZ} = 600$  lb was not sufficient to prevent the store contacting the TER and stopping the trajectory. Trajectories resulting from moment-of-inertia variation are presented in Fig. 18. Trajectories resulting from variation of the initial store attitude on the pylon are presented in Fig. 19. At  $M_\infty = 0.70$  and  $\theta = -2$  deg, the store contacted the TER and stopped the trajectory.

#### 4.4 TRAJECTORIES FOR CONFIGURATION III

Trajectories for Configuration III showing the effect of Mach number variation for a typical set of input parameters are shown in Fig. 20. Data for this configuration were obtained at  $M_\infty = 0.70, 0.90, 1.10$ , and  $1.30$ . Trajectories resulting from center-of-gravity variation are presented in Fig. 21. At all Mach numbers, the store exhibited large pitch and yaw oscillations. Generally, the farther aft the  $X_{cg}$  location and the higher the Mach number, the greater the oscillations exhibited by the store. Trajectories resulting from ejector-force variation are presented in Fig. 22. At  $M_\infty = 1.3$ , an  $F_{LZ} = 600$  lb was not sufficient to allow the store to separate without contacting the TER. Trajectories resulting from moment-of-inertia variation are presented in Fig. 23. A typical trajectory comparison for variation of initial store attitude on the TER is shown in Fig. 24. A  $\theta$  of other than  $0$  deg resulted in store contact with the TER for all Mach numbers except  $M_\infty = 0.90$ . At that Mach number, the store cleared the TER at all three values of  $\theta$ .

#### 4.5 TRAJECTORIES FOR CONFIGURATION IV

Data were obtained at Mach numbers of  $0.50, 0.70$ , and  $0.90$  for Configuration IV. Trajectories resulting from center-of-gravity variation are presented in Fig. 25. At  $M_\infty = 0.90$ , an  $X_{cg}$  location at, or aft of, the ejector force caused such a rapid negative pitching and yawing motion that the store contacted the TER and terminated the trajectory. Trajectories resulting from variation of ejector force are presented in Fig. 26. At  $M_\infty = 0.90$ , only the  $1800$ -lb ejector force was sufficient to allow the store to separate without contacting the TER. Trajectories resulting from moment-of-inertia variation are presented in Fig. 27. At  $M_\infty = 0.90$  and  $\bar{m} = 23.31$ , an  $I_{yy} = 50$  allowed the store to contact the TER and stop the trajectory. Trajectories resulting from variation of the initial store attitude on the TER are presented in Fig. 28. At  $M_\infty = 0.50$ ,  $\theta = +2$  deg resulted in rapid store rotation and thus contact with the TER. However, at  $M_\infty = 0.90$ ,  $\theta = +2$  deg was the only condition which resulted in store separation without contact with the TER.

#### 4.6 TRAJECTORIES FOR CONFIGURATION V

Although trajectories for Configuration V were attempted at Mach numbers of  $0.70, 0.90, 1.10$ , and  $1.30$ , useful data were obtained only at  $M_\infty = 0.70$ . At all other Mach numbers, the store contacted the TER and caused early trajectory termination. Trajectories resulting from center-of-gravity variation are presented in Fig. 29. Trajectories resulting from ejector-force variation are presented in Fig. 30. An  $F_{LZ} = 600$  lb was not

sufficient to allow the store to separate from the TER without contact. Trajectories resulting from moment-of-inertia variation are presented in Fig. 31. An initial store attitude on the pylon of other than 0 deg ( $\theta = 0$ ) resulted in the store contacting the TER and causing an early trajectory termination.

#### 4.7 TRAJECTORIES FOR CONFIGURATION VI

Trajectories for Configuration VI were attempted at Mach numbers of 0.50, 0.70, and 0.90. At  $M_\infty = 0.90$ , the store exhibited a rapid pitch and yaw motion which resulted in the store contacting some part of the TER and caused an early trajectory as shown in Fig. 32. Therefore, data are presented only for  $M_\infty = 0.50$  and 0.70. Trajectories resulting from variation of center-of-gravity location are presented in Fig. 33. At  $M_\infty = 0.50$ , an  $X_{cg} = 2.24$  ft resulted in a rapid pitch-up motion causing the store to contact the TER and producing early trajectory termination. Trajectories resulting from ejector-force variation are presented in Fig. 34, trajectories resulting from variation of moment of inertia are presented in Fig. 35, and trajectories resulting from variation of initial store attitude on the TER are presented in Fig. 36.

#### 4.8 TRAJECTORIES FOR CONFIGURATION VII

Trajectories for Configuration VII were attempted at Mach numbers 0.50, 0.70, and 0.90. However, at  $M_\infty = 0.90$ , the store contacted some part of the TER and caused early termination. Therefore, data are presented only for  $M_\infty = 0.50$  and 0.70. Trajectories resulting from variation of center-of-gravity location are presented in Fig. 37. Rather severe yaw oscillations were experienced at  $M_\infty = 0.70$ . Trajectories resulting from variation of ejector force are presented in Fig. 38. At  $M_\infty = 0.70$ , an  $F_{LZ} = 600$  lb was not sufficient to permit separation without the store contacting the TER and causing early trajectory termination. Trajectories resulting from variation of moment of inertia are presented in Fig. 39. Trajectories resulting from variation of the initial store attitude on the TER are presented in Fig. 40. At  $M_\infty = 0.70$ ,  $\theta = -2$  deg resulted in store contact with the TER and early termination of the trajectory.

### SECTION V CONCLUSIONS

Conclusions drawn from this test were as follows:

1. The major effect of the various store parameters was evidenced in the pitch and yaw motions.
2. Generally, the 600-lb ejector force was insufficient to insure that the store would separate from the TER without contact.
3. All Configuration I trajectories had a rapid initial pitch rate. However, only two of the trajectories resulted in the store contacting the TER upon separation.



4. Configuration III trajectories showed store pitch and yaw oscillations at certain center-of-gravity locations at each Mach number tested. Generally, the farther aft the center of gravity was located and the higher the Mach number, the greater the magnitude of the oscillations.
5. For Configuration V at Mach numbers greater than 0.70, the store contacted the TER and caused early trajectory termination.
6. Launch from the TER outboard shoulder position at  $M_\infty = 0.90$  was difficult, even with the reduced aerodynamic loads of flight at 20,000-ft altitude. Rapid pitch and yaw motions caused the store to contact the TER for all trajectories attempted with Configurations II, VI, and VII, and for all but a few of the trajectories with Configuration IV.

## **APPENDIXES**

- I. ILLUSTRATIONS**
- II. TABLES**

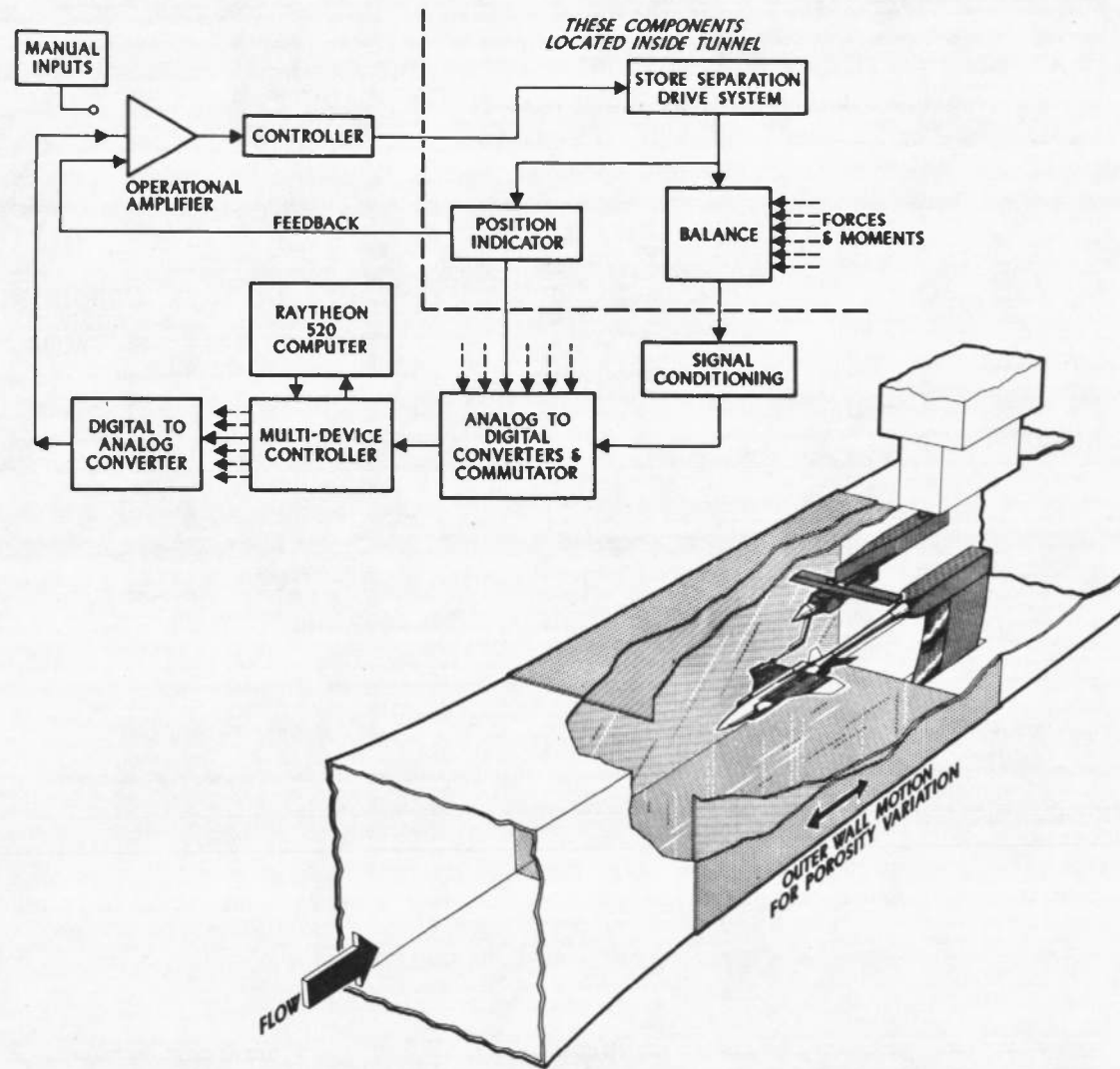
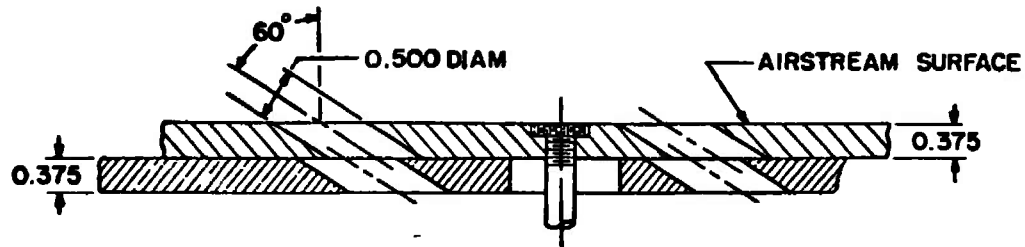


Fig. 1 Isometric Drawing of a Typical Store Separation Installation and Block Diagram of the Computer Control Loop



TYPICAL PERFORATED WALL CROSS SECTION

NOTE: TUNNEL STATIONS AND DIMENSIONS ARE IN INCHES

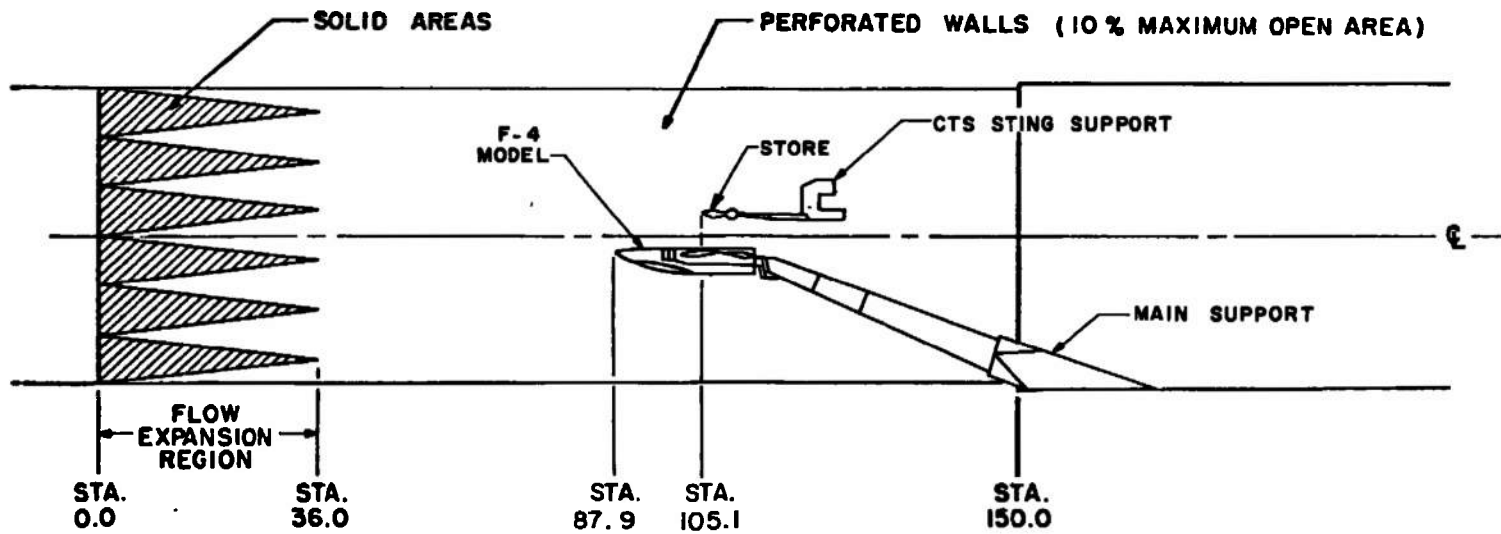
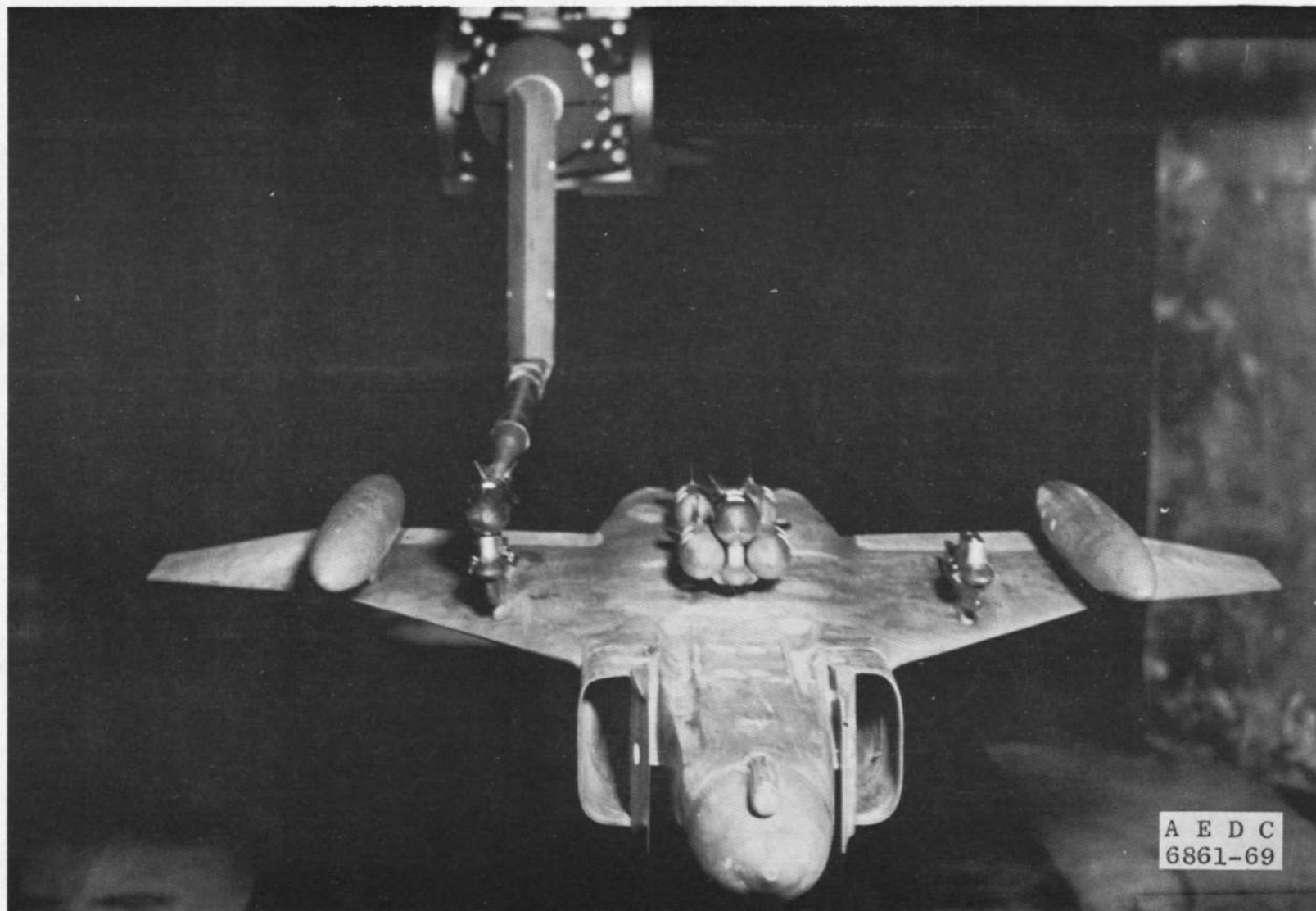
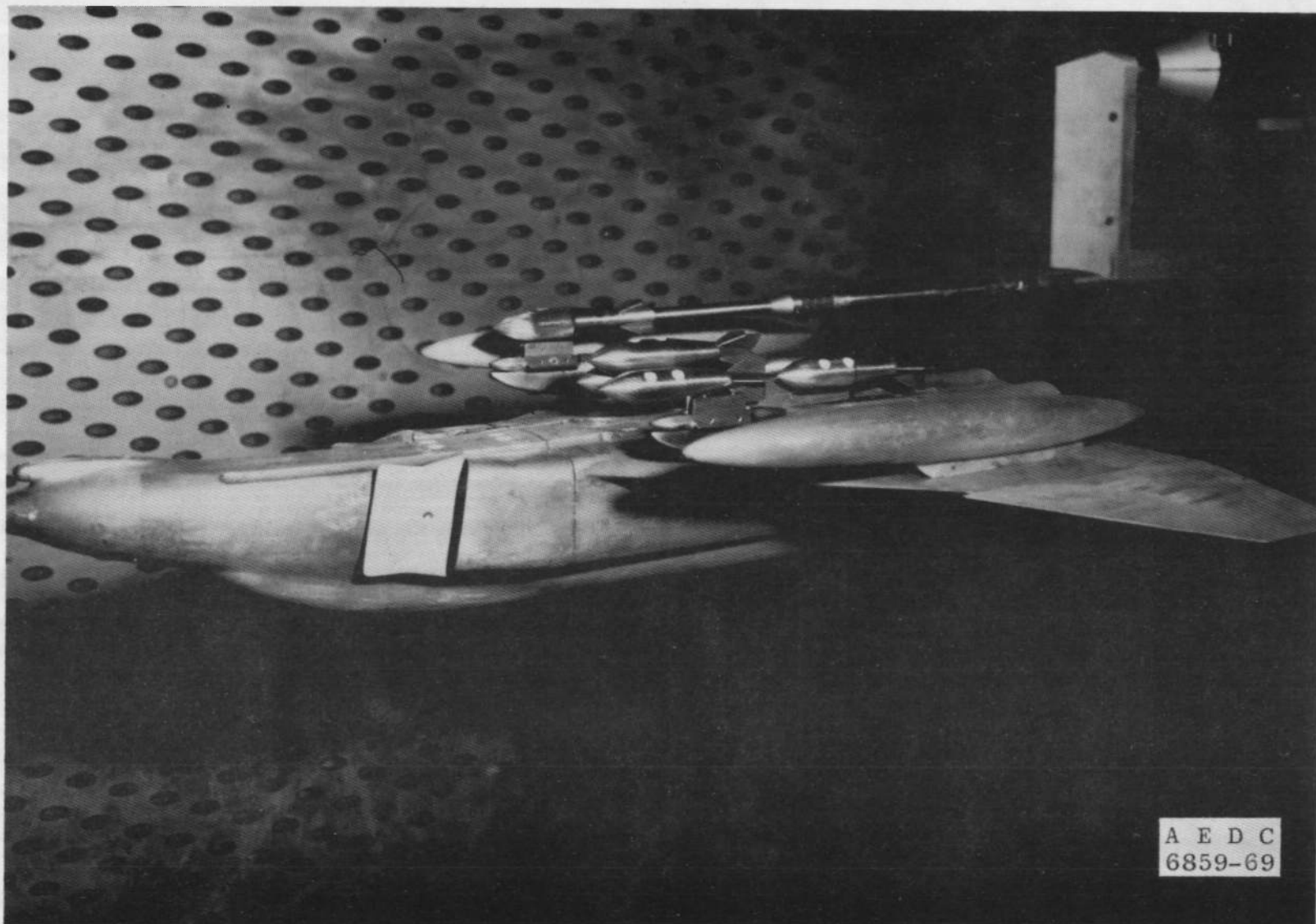


Fig. 2 Tunnel Test Section and Model Installation Details

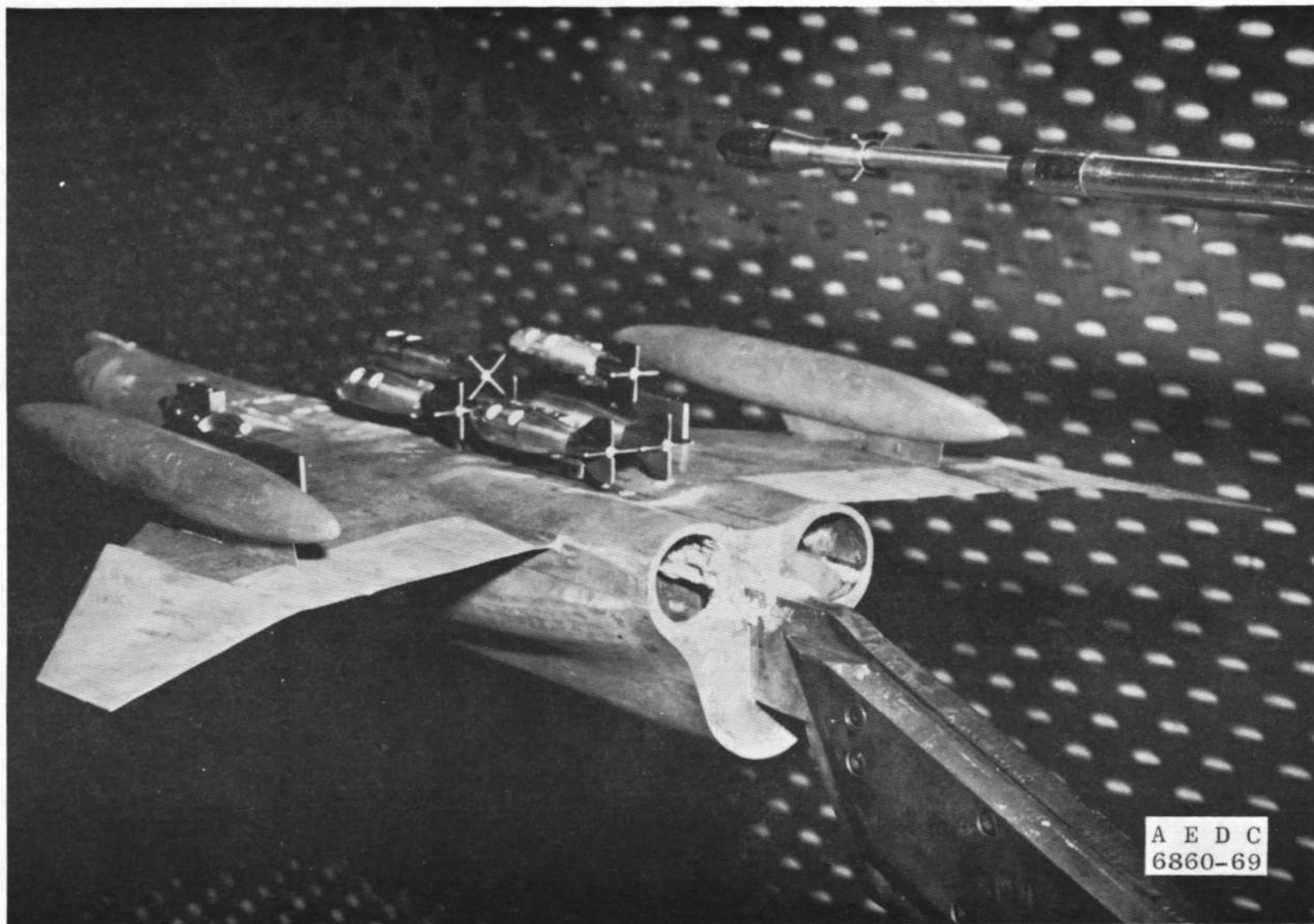


a. Store on TER  
Fig. 3 Installation Photographs

A E D C  
6861-69



b. Side View—Store on TER  
Fig. 3 Continued



c. Aft View—Store off TER  
Fig. 3 Concluded

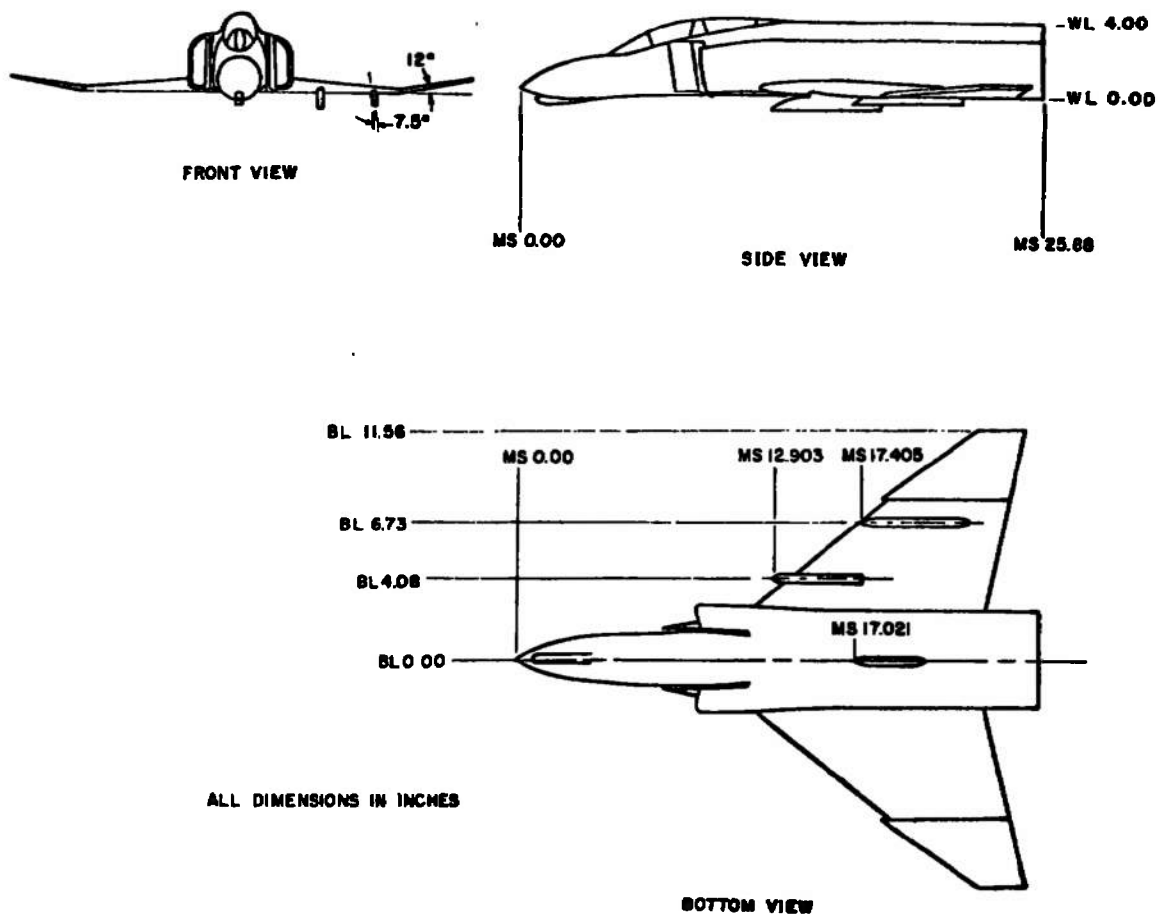


Fig. 4 Dimensional Sketch of F-4C Parent Aircraft Model



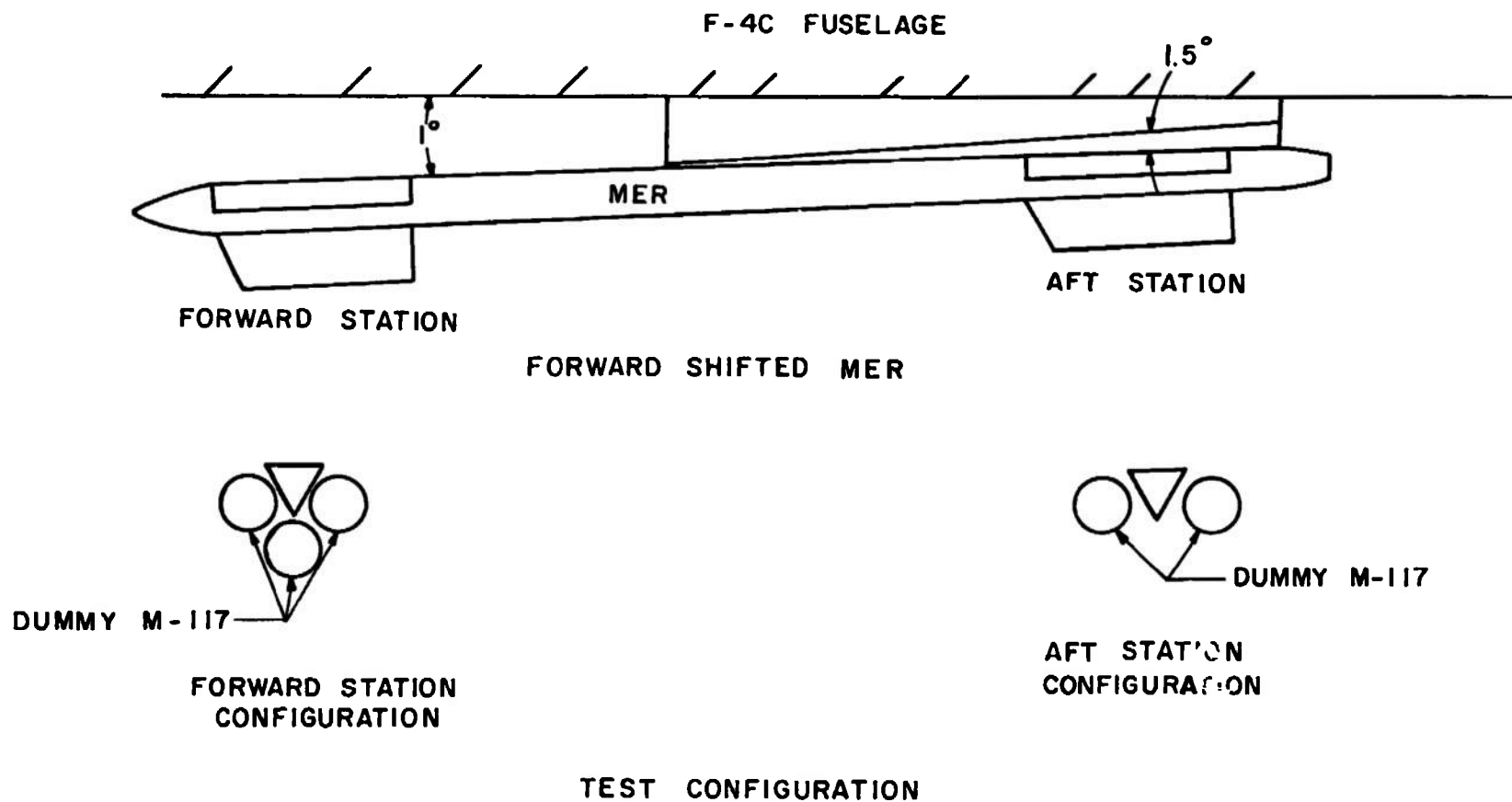
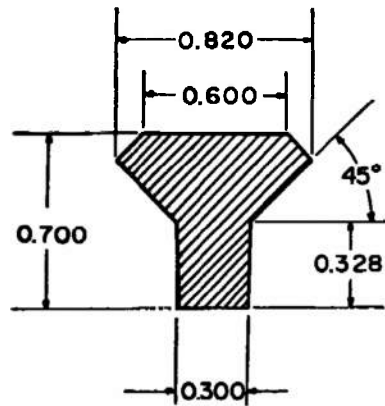


Fig. 5 MER Installation and Configuration Details



SECTION A-A

ALL DIMENSIONS IN INCHES

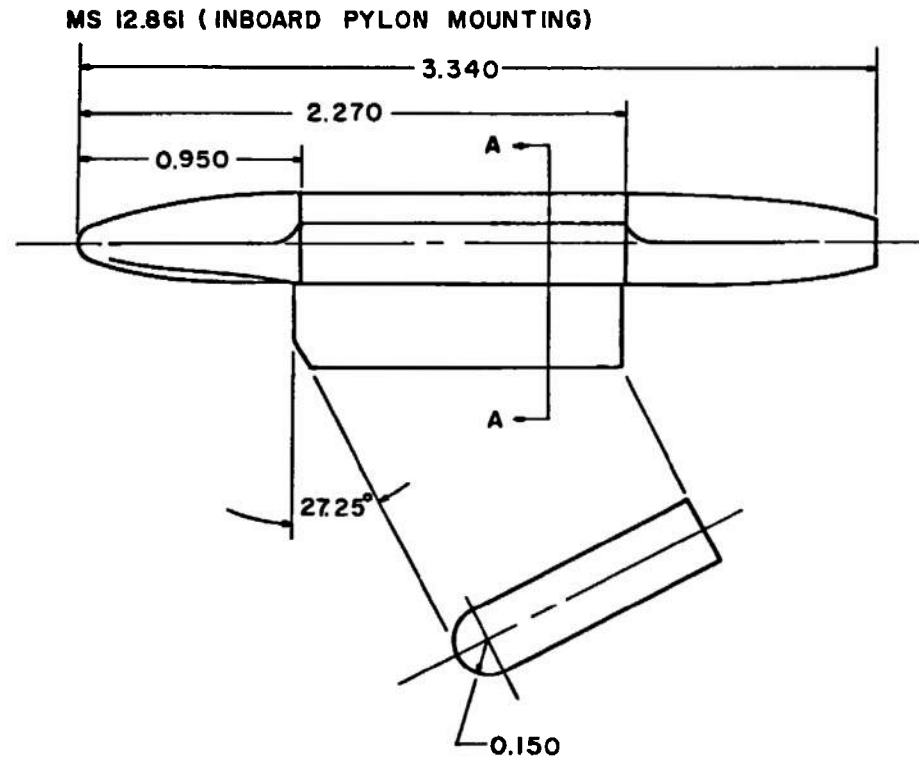
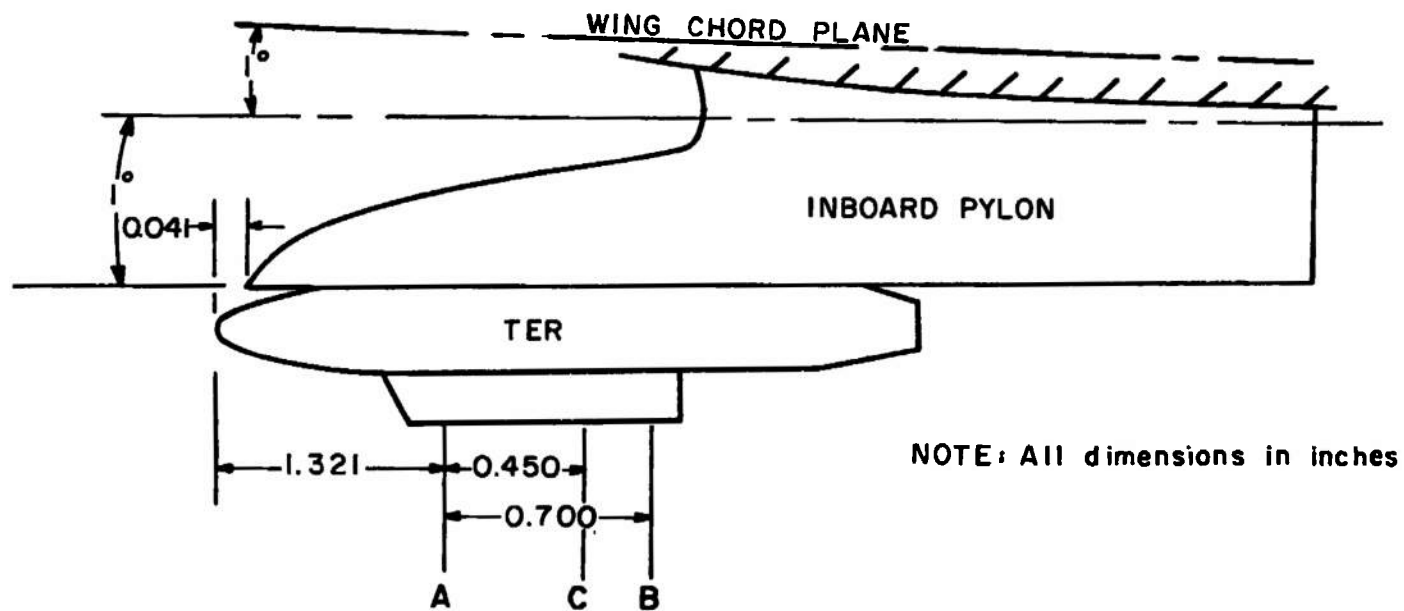


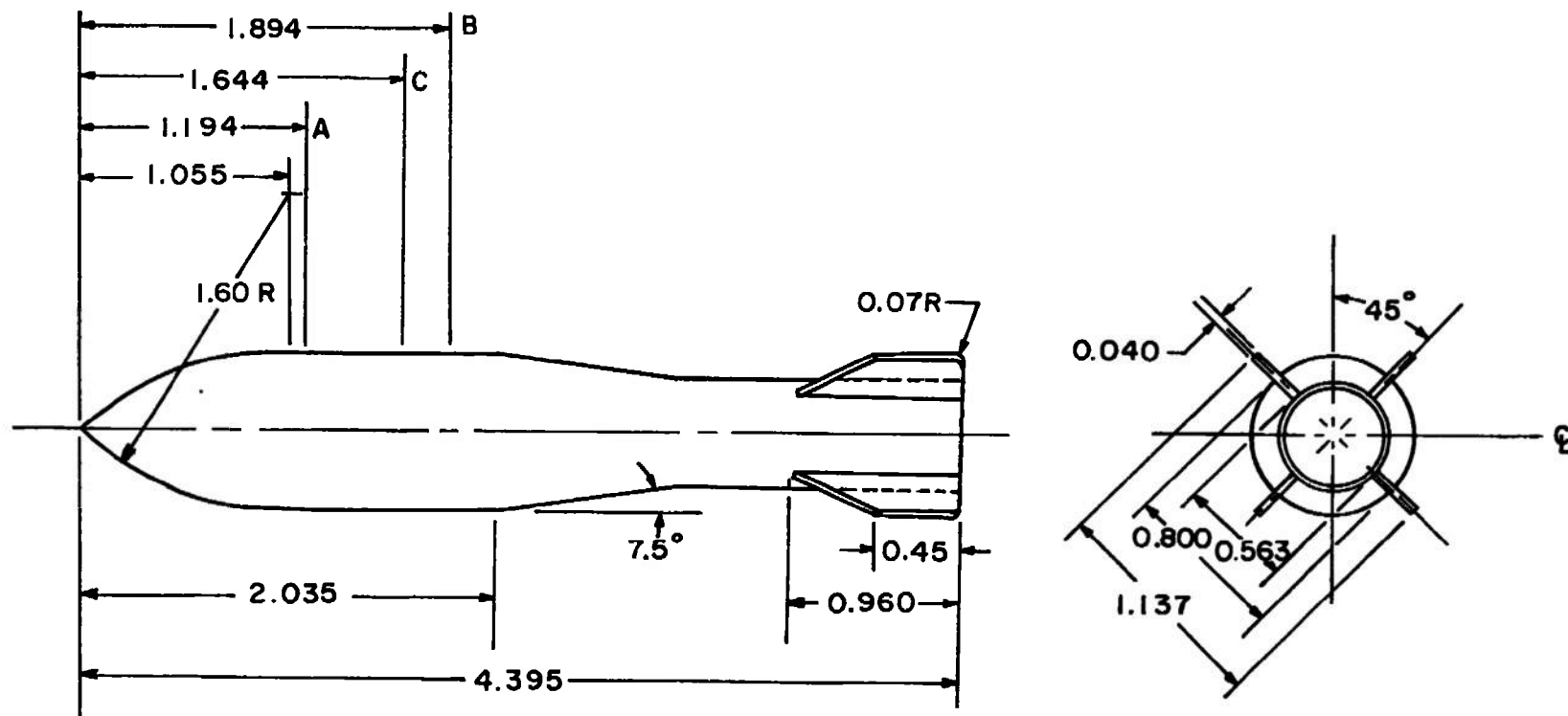
Fig. 6 Dimensional Sketch of TER



- A. Forward 14" suspension point
- B. Aft 14" suspension point
- C. Ejector location

Fig. 7 TER Installation Details

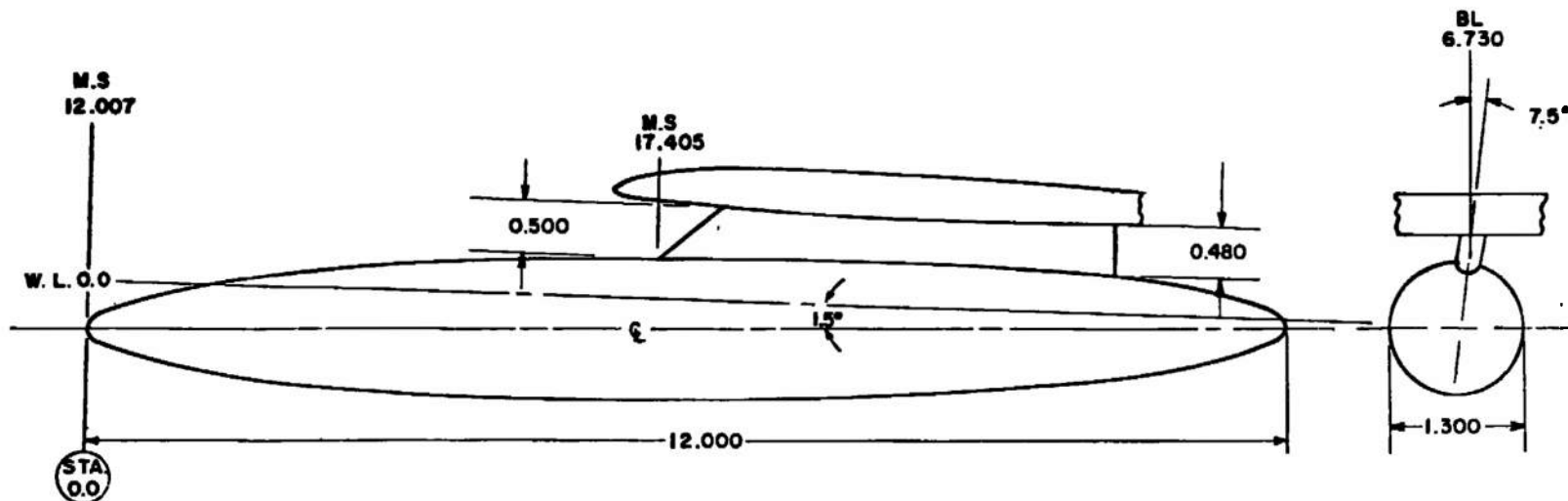
20



- A. Forward 14" suspension point
- B. Aft 14" suspension point
- C. Ejector location

NOTE: All dimensions in inches

Fig. 8 Dimensional Sketch of M-117 Store Model

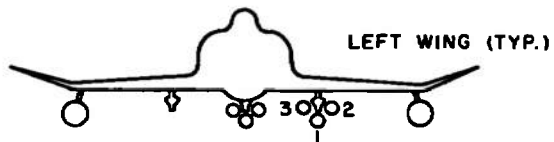


NOTE: MODEL STATIONS AND  
DIMENSIONS IN INCHES

BODY CONTOUR, TYPICAL BOTH ENDS

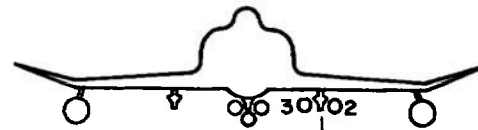
STATION	BODY DIAM	STATION	BODY DIAM
0.000	0.000	2.500	1.116
0.025	0.100	2.750	1.156
0.050	0.144	3.000	1.190
0.150	0.258	3.250	1.218
0.250	0.340	3.500	1.242
0.500	0.498	3.750	1.260
0.750	0.622	4.000	1.274
1.000	0.724	4.250	1.286
1.250	0.812	4.500	1.294
1.500	0.890	4.750	1.298
1.750	0.958	5.000	1.300
2.000	1.016	6.000	1.300
2.250	1.070		

Fig. 9 Dimensional Sketch of 370-gal. Fuel Tank Model



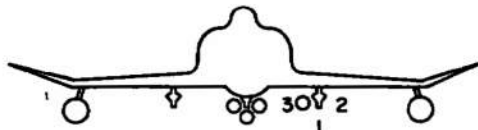
**CONFIGURATION I**

TER STATION 1: LAUNCH  
 TER STATION 2: DUMMY M-117  
 TER STATION 3: DUMMY M-117  
 OUTBOARD STATIONS: 370 GALLON FUEL TANKS



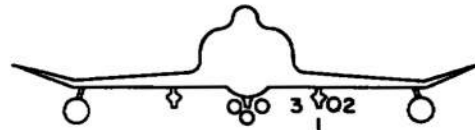
**CONFIGURATION II**

TER STATION 1: EMPTY  
 TER STATION 2: LAUNCH  
 TER STATION 3: DUMMY M-117  
 OUTBOARD STATIONS: 370 GALLON FUEL TANKS



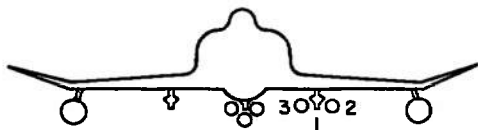
**CONFIGURATION III**

TER STATION 1: EMPTY  
 TER STATION 2: EMPTY  
 TER STATION 3: LAUNCH  
 OUTBOARD STATIONS: 370 GALLON FUEL TANKS



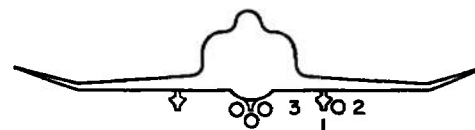
**CONFIGURATION IV**

TER STATION 1: EMPTY  
 TER STATION 2: LAUNCH  
 TER STATION 3: EMPTY  
 OUTBOARD STATIONS: 370 GALLON FUEL TANKS



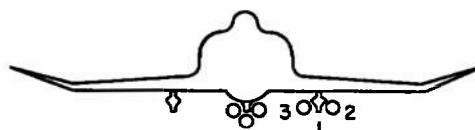
**CONFIGURATION V**

TER STATION 1: EMPTY  
 TER STATION 2: DUMMY M-117  
 TER STATION 3: LAUNCH  
 OUTBOARD STATIONS: 370 GALLON FUEL TANKS



**CONFIGURATION VI**

TER STATION 1: EMPTY  
 TER STATION 2: LAUNCH  
 TER STATION 3: EMPTY  
 OUTBOARD STATIONS: EMPTY



**CONFIGURATION VII**

TER STATION 1: EMPTY  
 TER STATION 2: LAUNCH  
 TER STATION 3: DUMMY M-117  
 OUTBOARD STATIONS: EMPTY

**Fig. 10 Test Configurations**

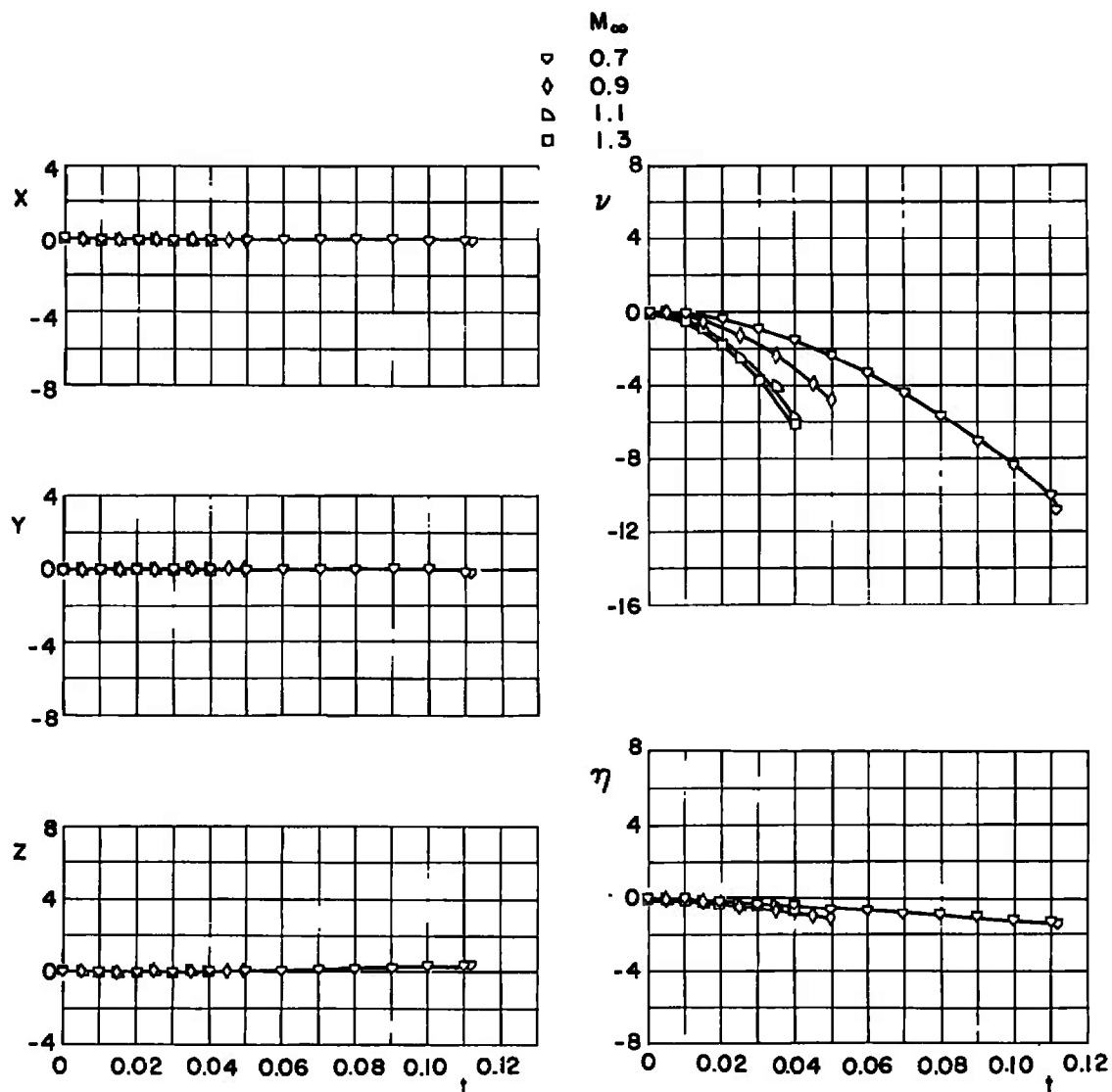
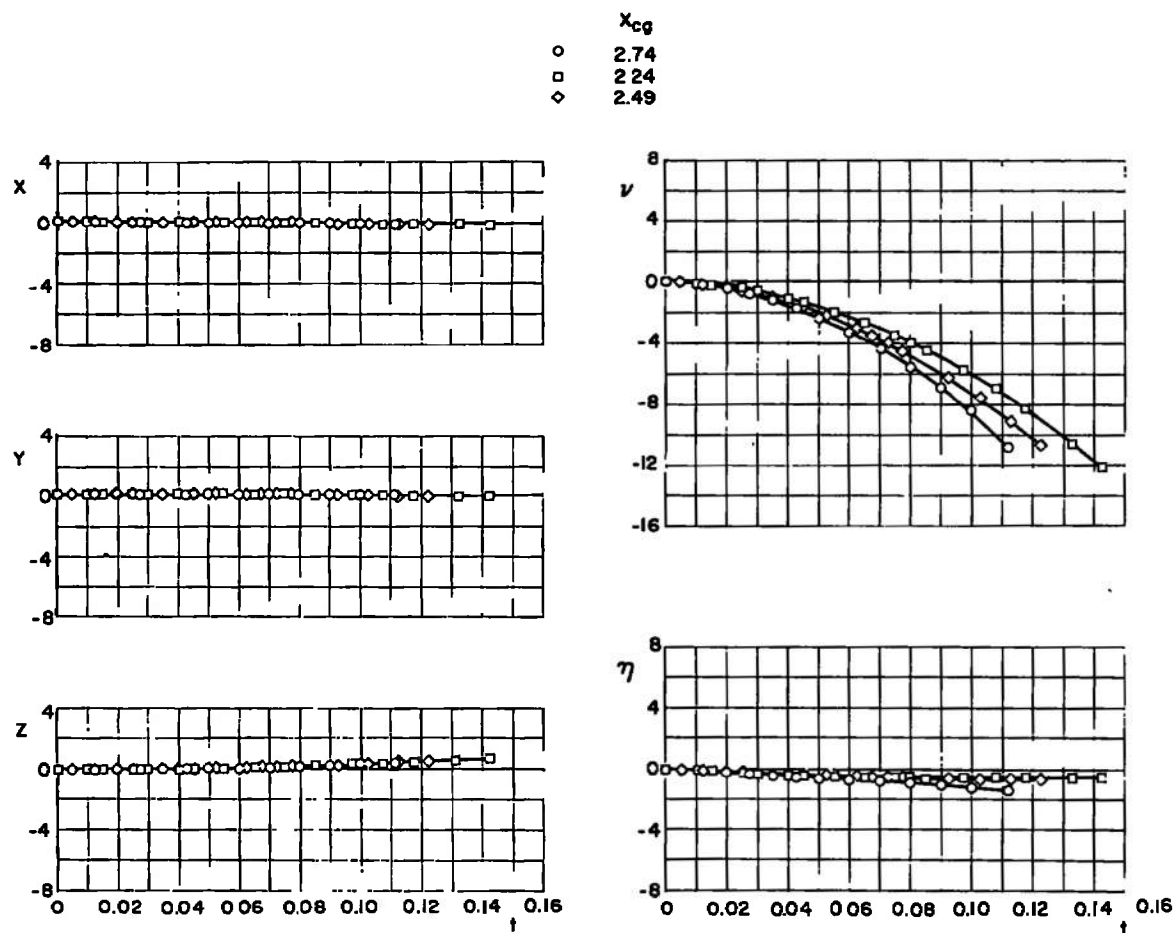
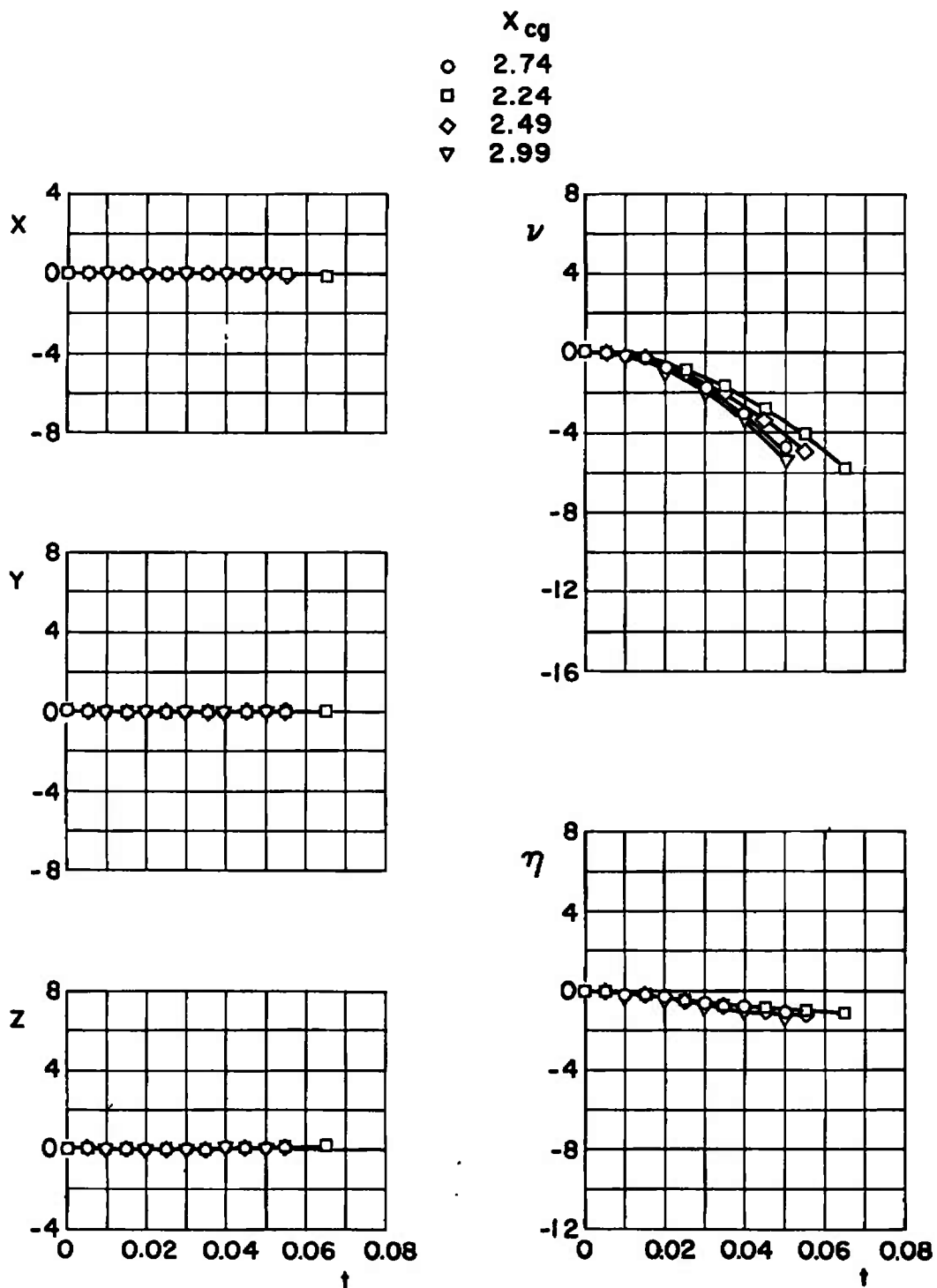


Fig. 11 Effect of Mach Number Variation for Configuration I;  $\bar{m} = 23.31$ ,  
 $X_{cg} = 2.74$ ,  $F_{LZ} = 1200$ ,  $\theta = 0$ ,  $I_{yy} = 50$ ,  $h = 5000$



a.  $M_\infty = 0.70$   
 Fig. 12 Effect of Center-of-Gravity Variation for Configuration I;  $\bar{m} = 23.31$ ,  
 $F_{LZ} = 1200$ ,  $\theta = 0$ ,  $I_{yy} = 50$ ,  $h = 5000$

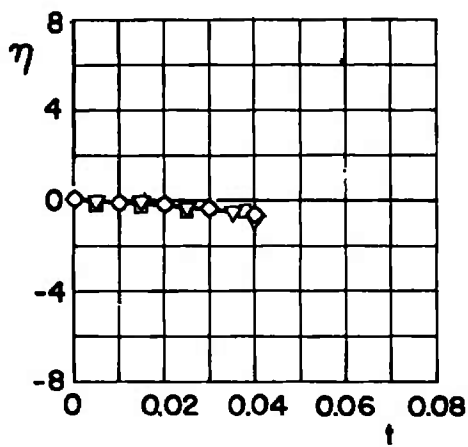
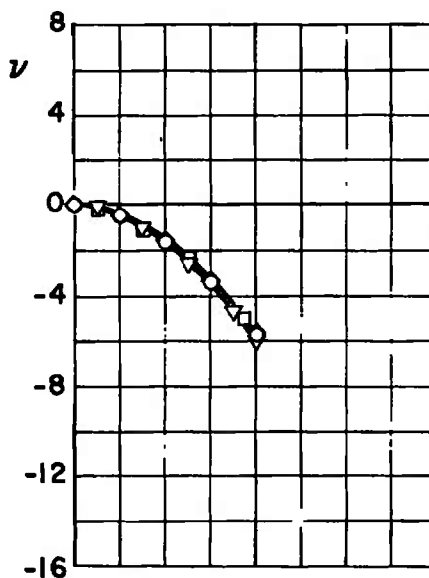
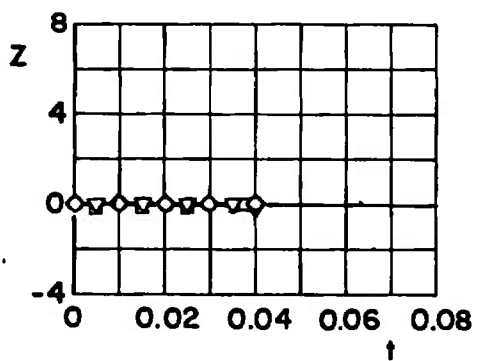
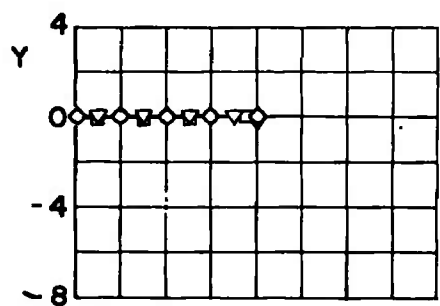
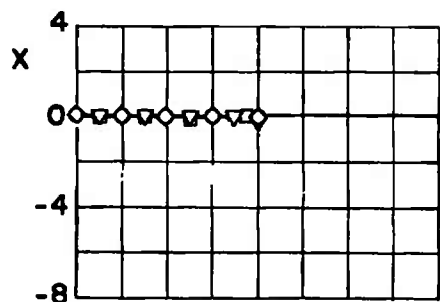




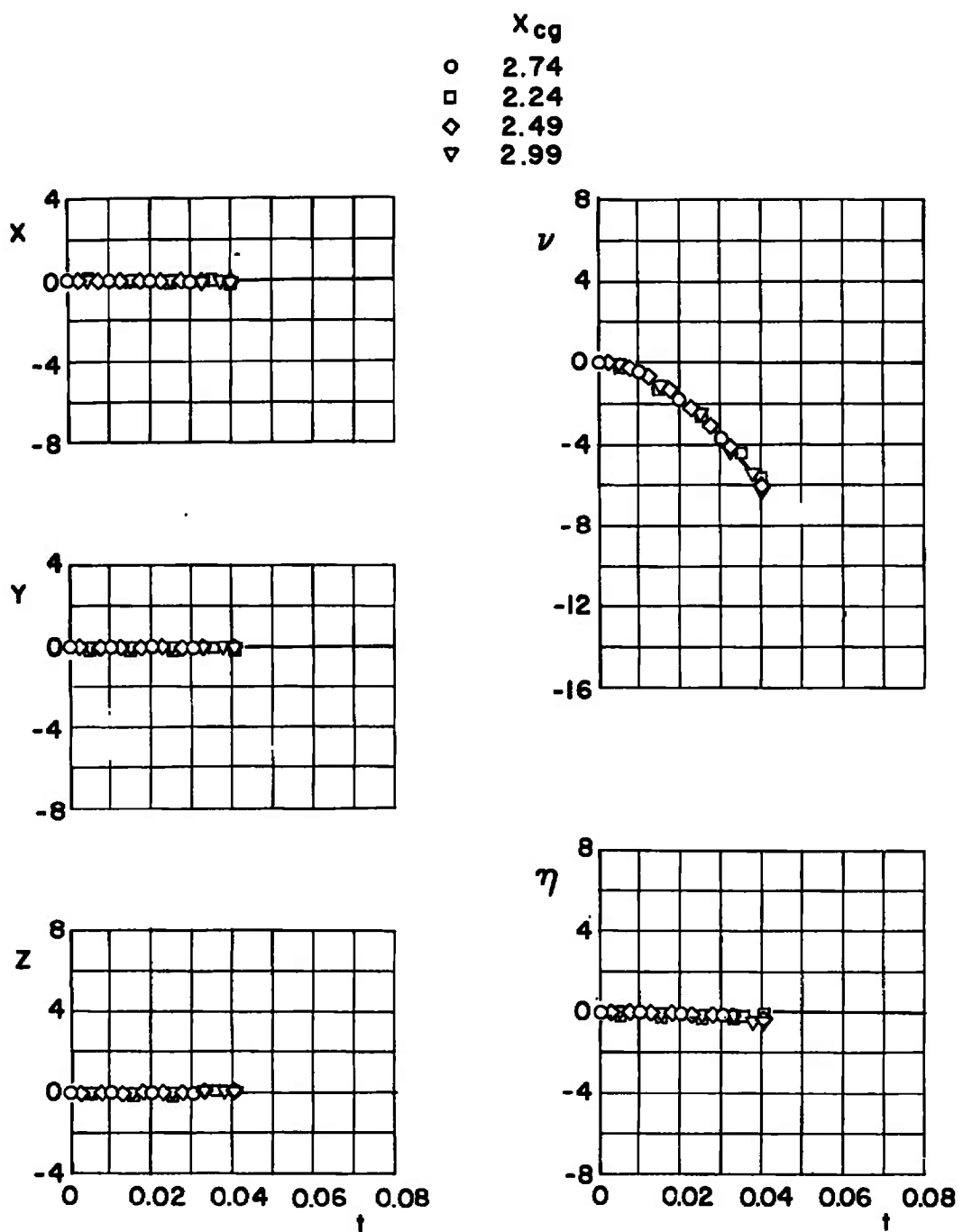
b.  $M_\infty = 0.90$   
Fig. 12 Continued

$x_{cg}$

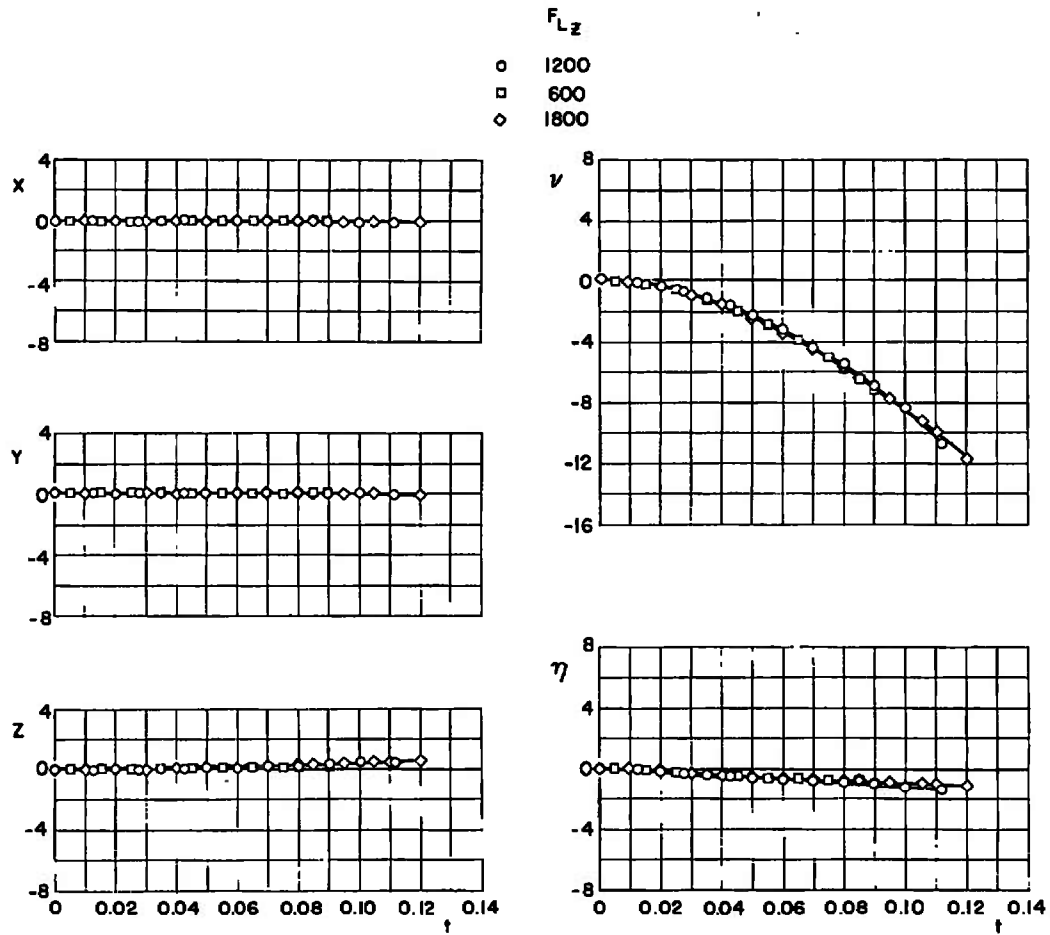
○	2.74
□	2.24
◇	2.49
▽	2.99



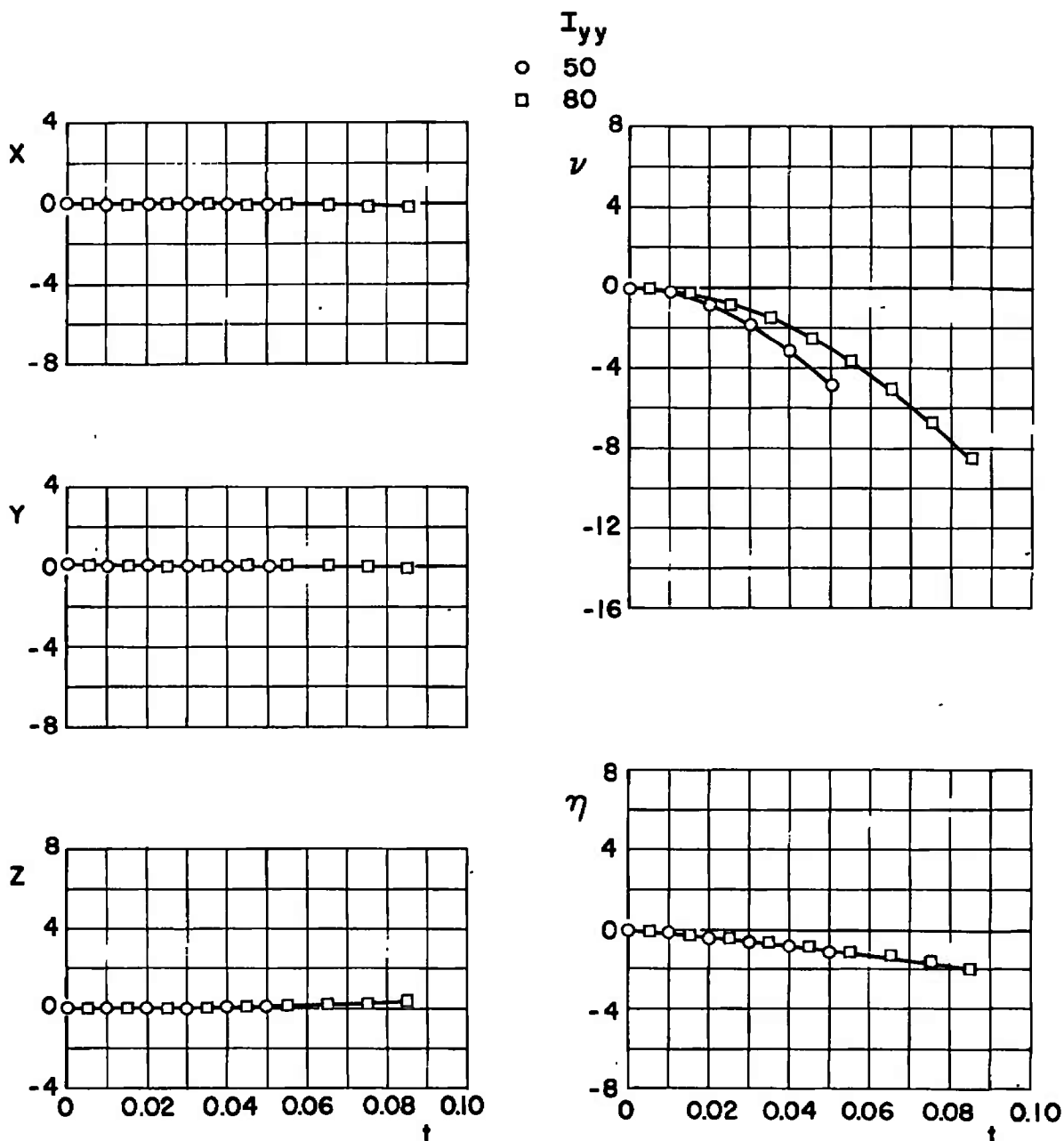
c.  $M_\infty = 1.10$   
Fig. 12 Continued



d.  $M_\infty = 1.30$   
 Fig. 12 Concluded

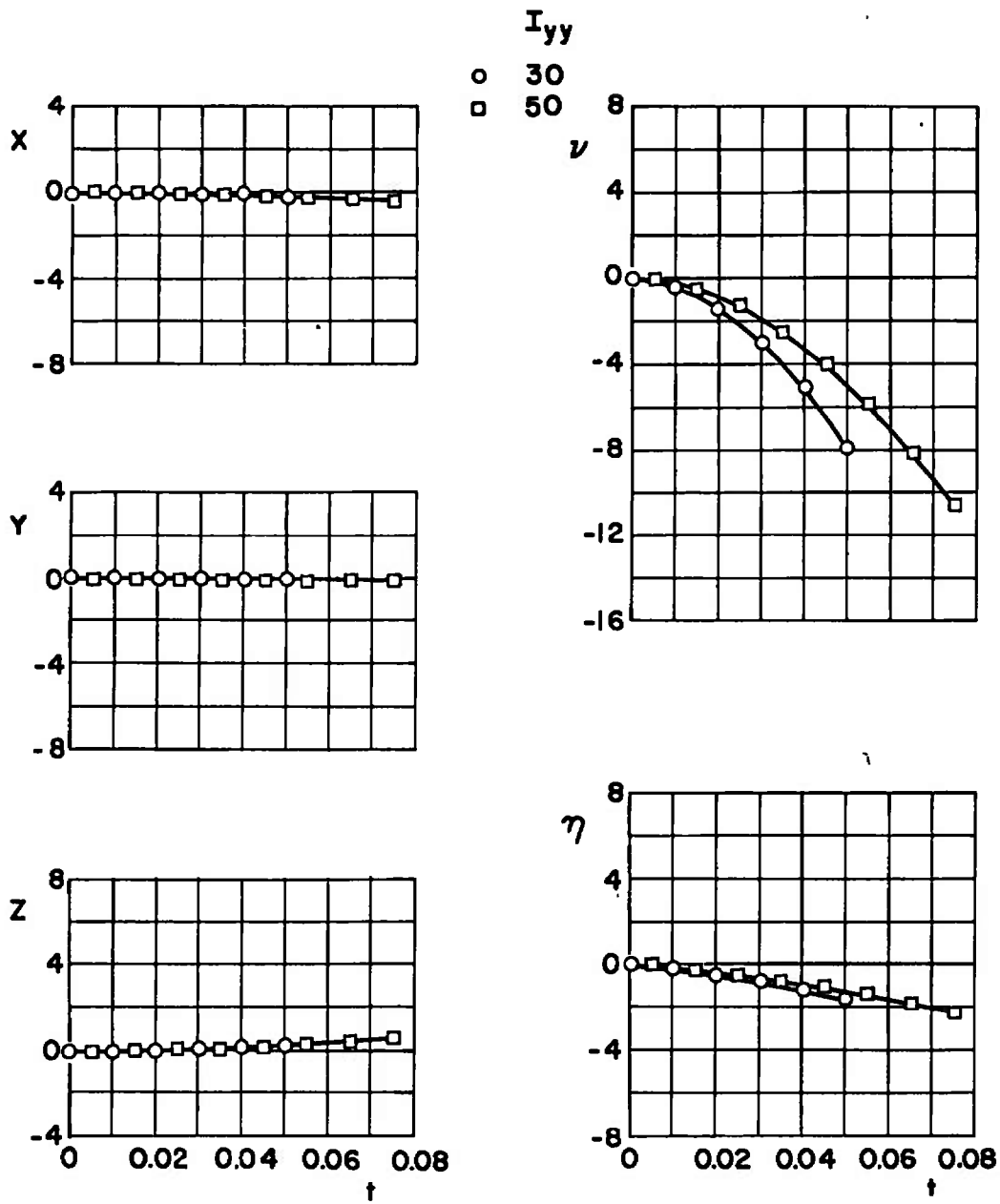


**Fig. 13 Typical Effect of Ejector-Force Variation for Configuration I;**  
 $\bar{m} = 23.31, X_{cg} = 2.74, \theta = 0, I_{yy} = 50, M_{\infty} = 0.70, h = 5000$



a.  $\bar{m} = 23.31$

Fig. 14 Typical Effect of Moment-of-Inertia Variation for Configuration I;  
 $X_{cg} = 2.74$ ,  $F_{Lz} = 1200$ ,  $\theta = 0$ ,  $M_\infty = 0.90$ ,  $h = 5000$



b.  $\bar{m} = 7.771$   
Fig. 14 Concluded

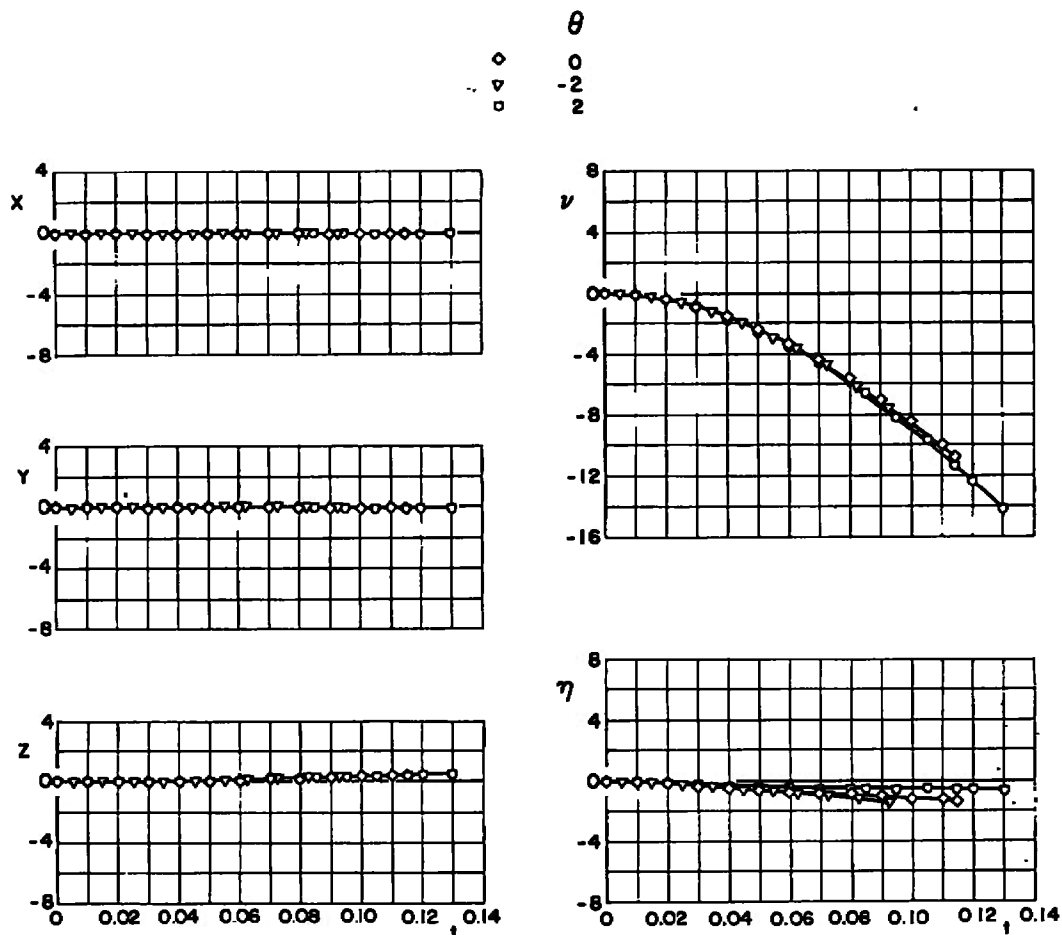


Fig. 15 Typical Effect of Initial Store Attitude for Configuration I;  $\bar{m} = 23.31$ ,  $X_{cg} = 2.74$ ,  $F_{LZ} = 1200$ ,  $I_{yy} = 50$ ,  $M_\infty = 0.70$ ,  $h = 5000$

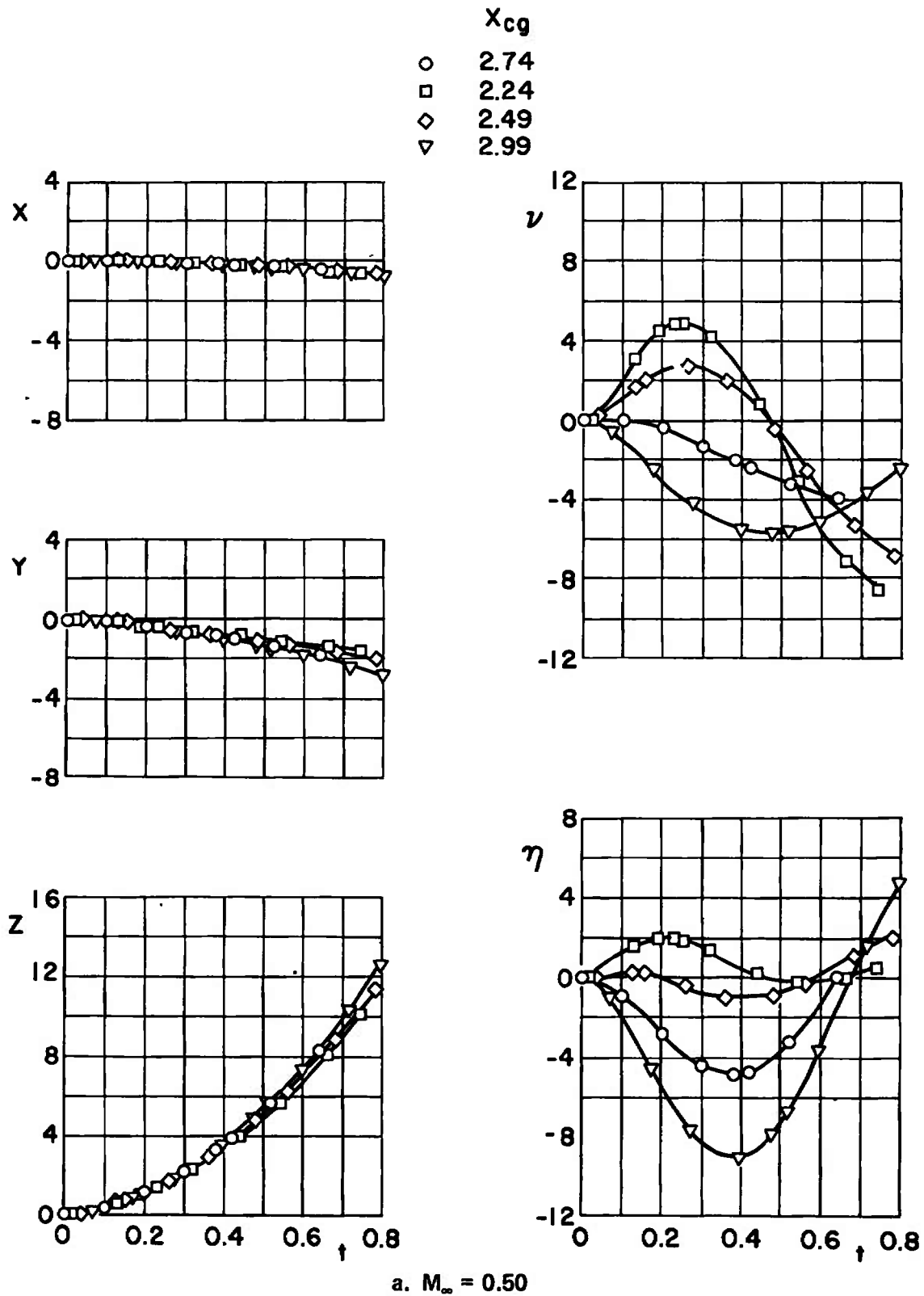
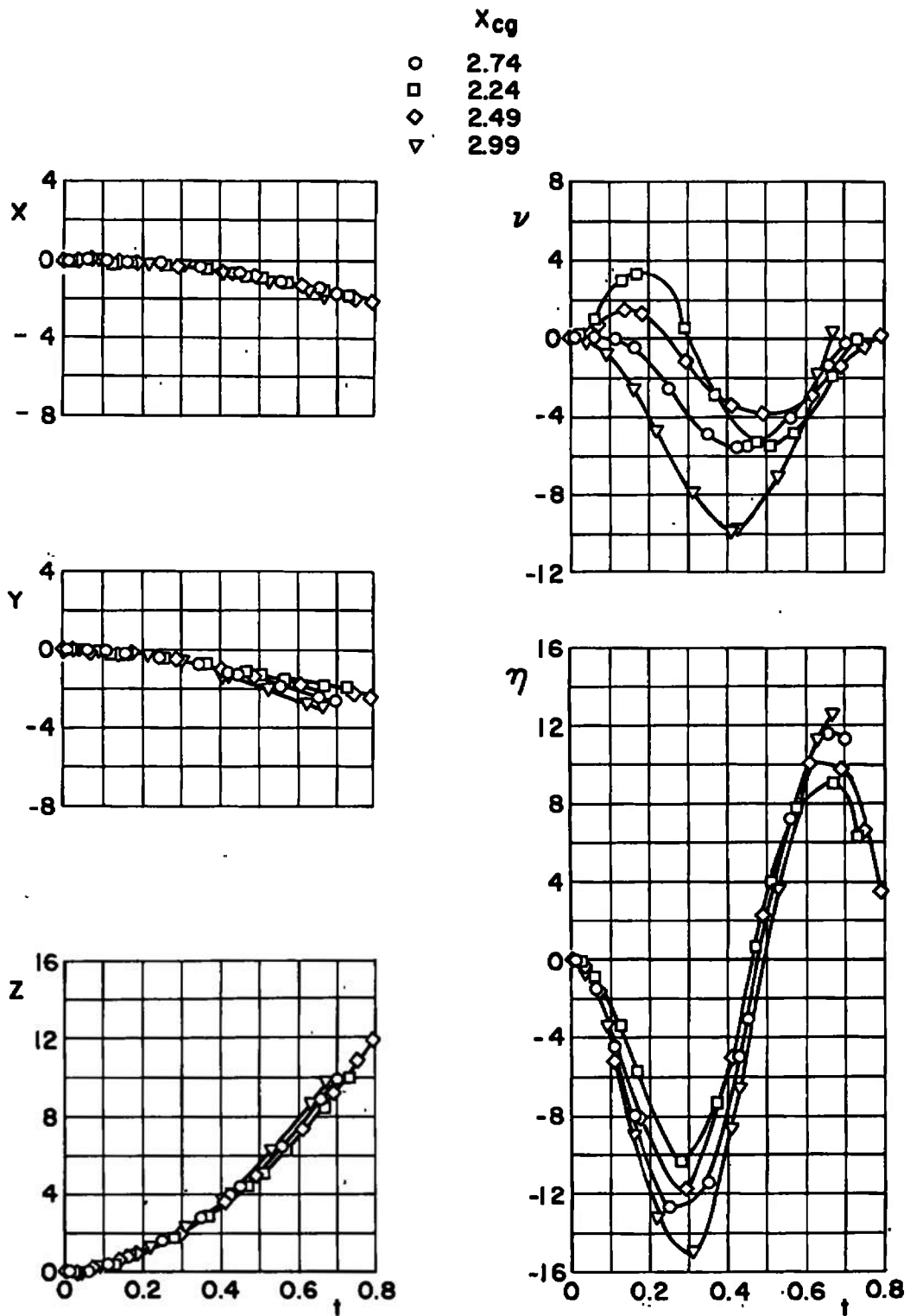


Fig. 16 Effect of Center-of-Gravity Variation for Configuration II;  
 $\bar{m} = 23.31$ ,  $F_{Lz} = 1200$ ,  $\theta = 0$ ,  $I_{yy} = 50$ ,  $h = 20,000$





b.  $M_\infty = 0.70$   
Fig. 16 Concluded

$F_{Lz}$ 

- 1200  
 □ 600  
 ◇ 1800

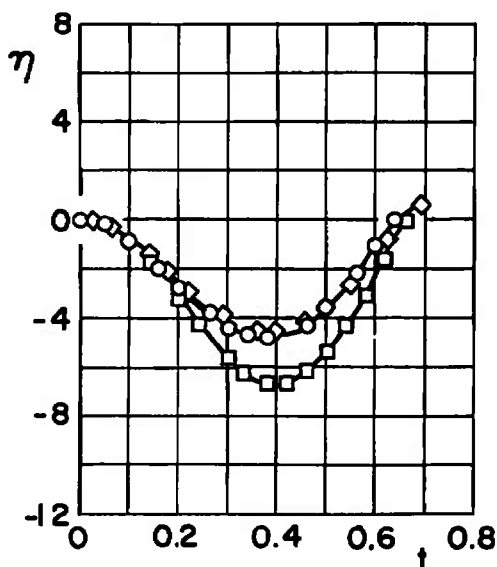
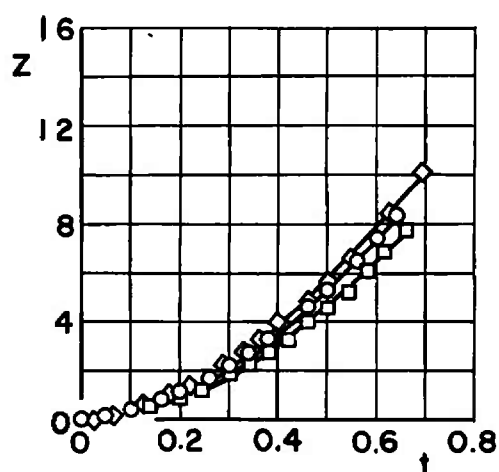
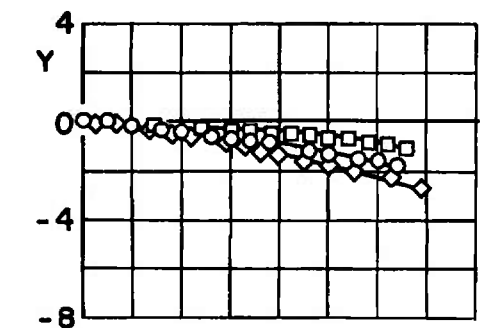
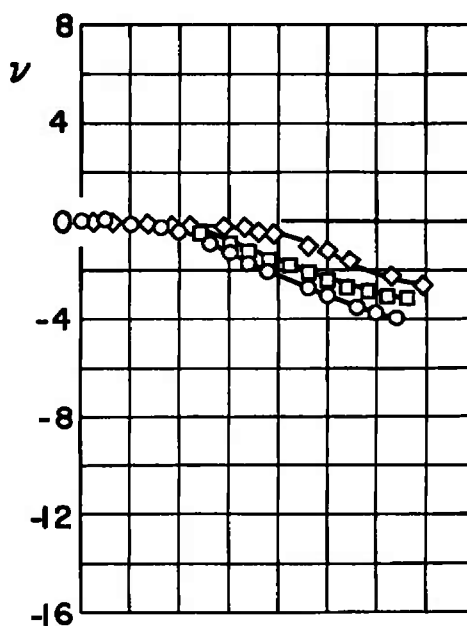
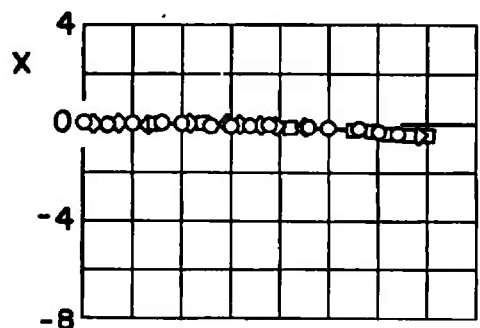
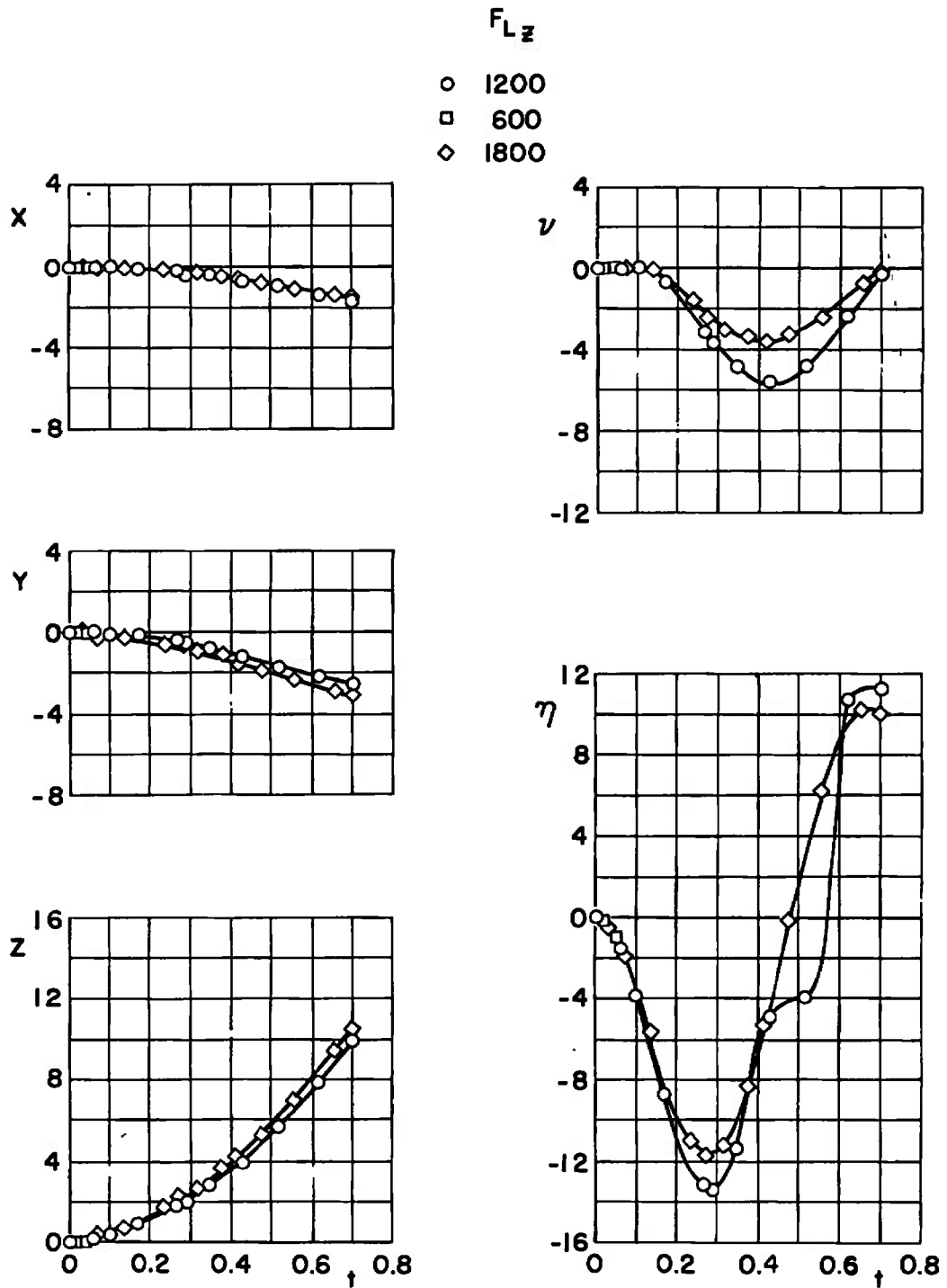
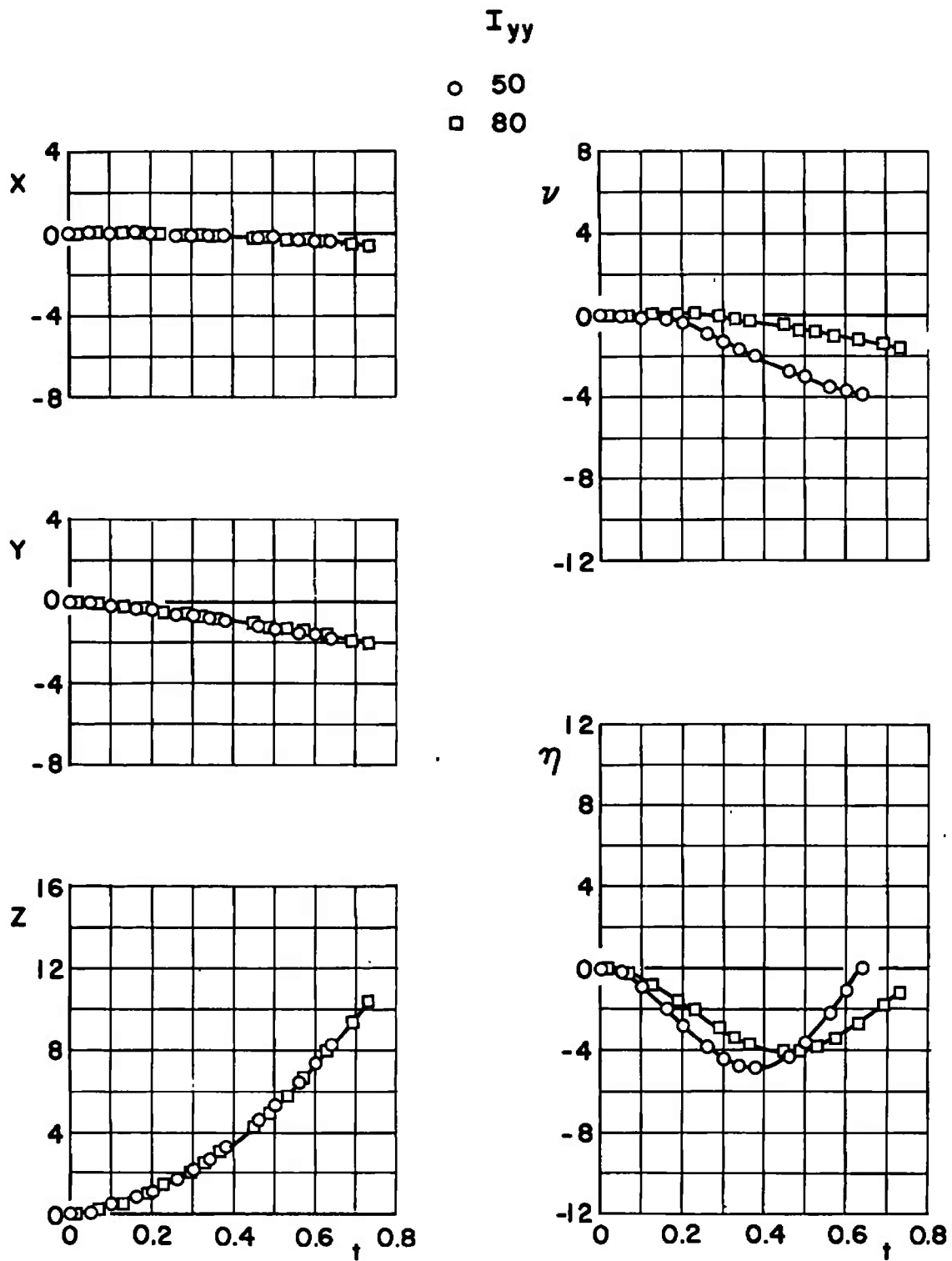
a.  $M_\infty = 0.50$ 

Fig. 17 Effect of Ejector-Force Variation for Configuration II;  $\bar{m} = 23.31$ ,  
 $X_{cg} = 2.74$ ,  $\theta = 0$ ,  $I_{yy} = 50$ ,  $h = 20,000$



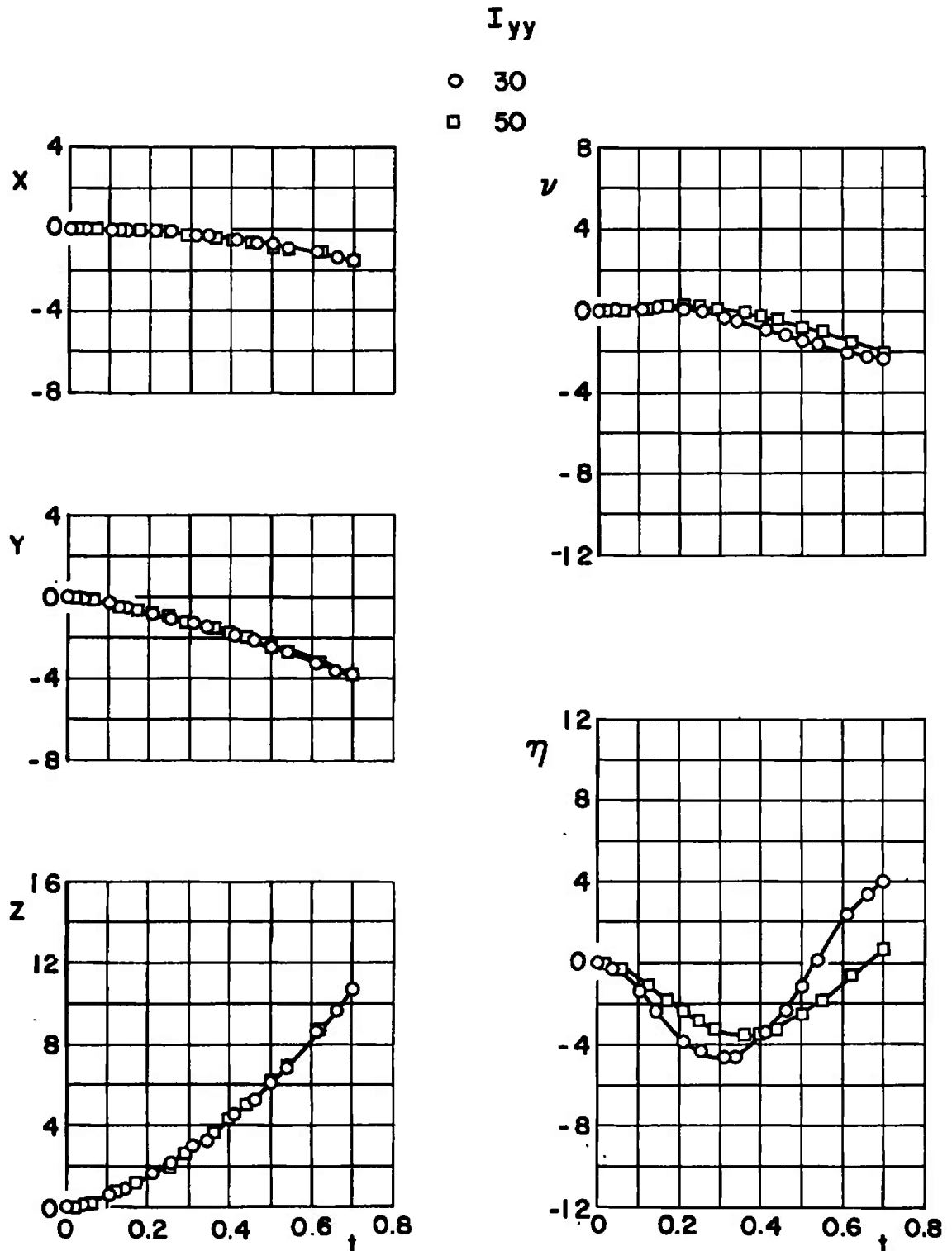
b.  $M_\infty = 0.70$   
Fig. 17 Concluded



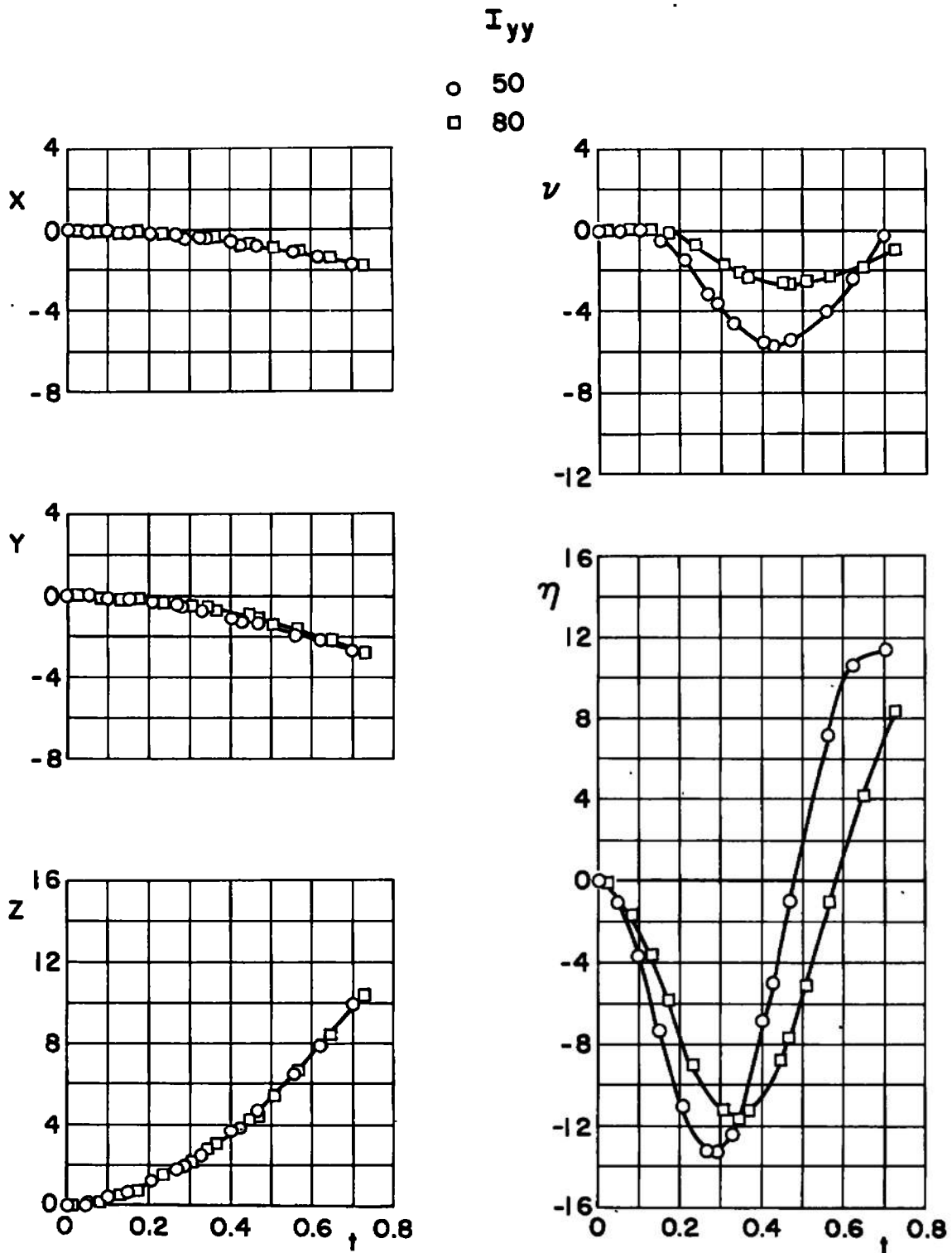
a.  $M_\infty = 0.50$ ,  $\bar{m} = 23.31$

Fig. 18 Effect of Moment-of-Inertia Variation for Configuration II;

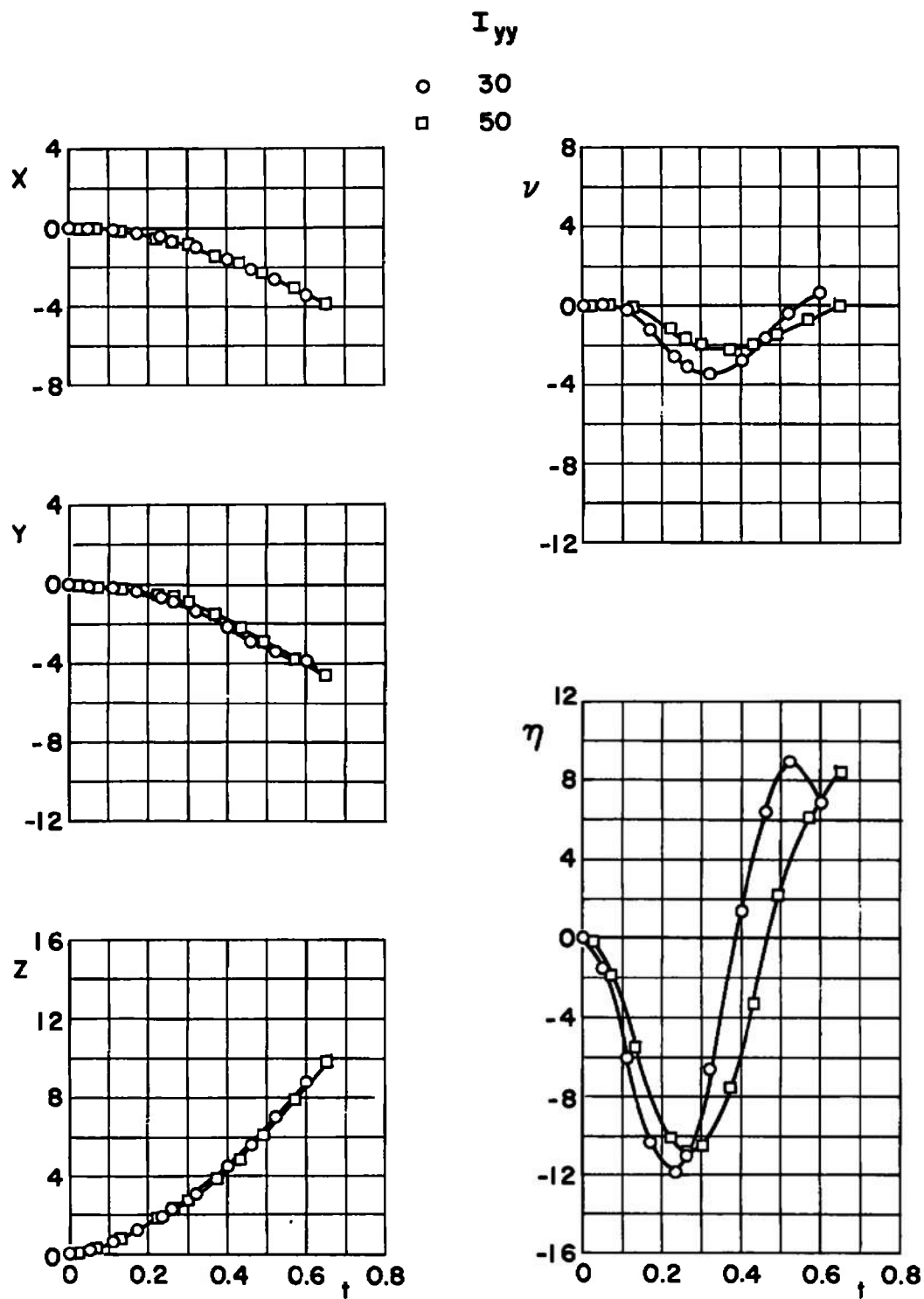
$X_{cg} = 2.74$ ,  $F_{Lz} = 1200$ ,  $\theta = 0$ ,  $h = 20,000$



b.  $M_\infty = 0.50$ ,  $\bar{m} = 7.331$   
Fig. 18 Continued



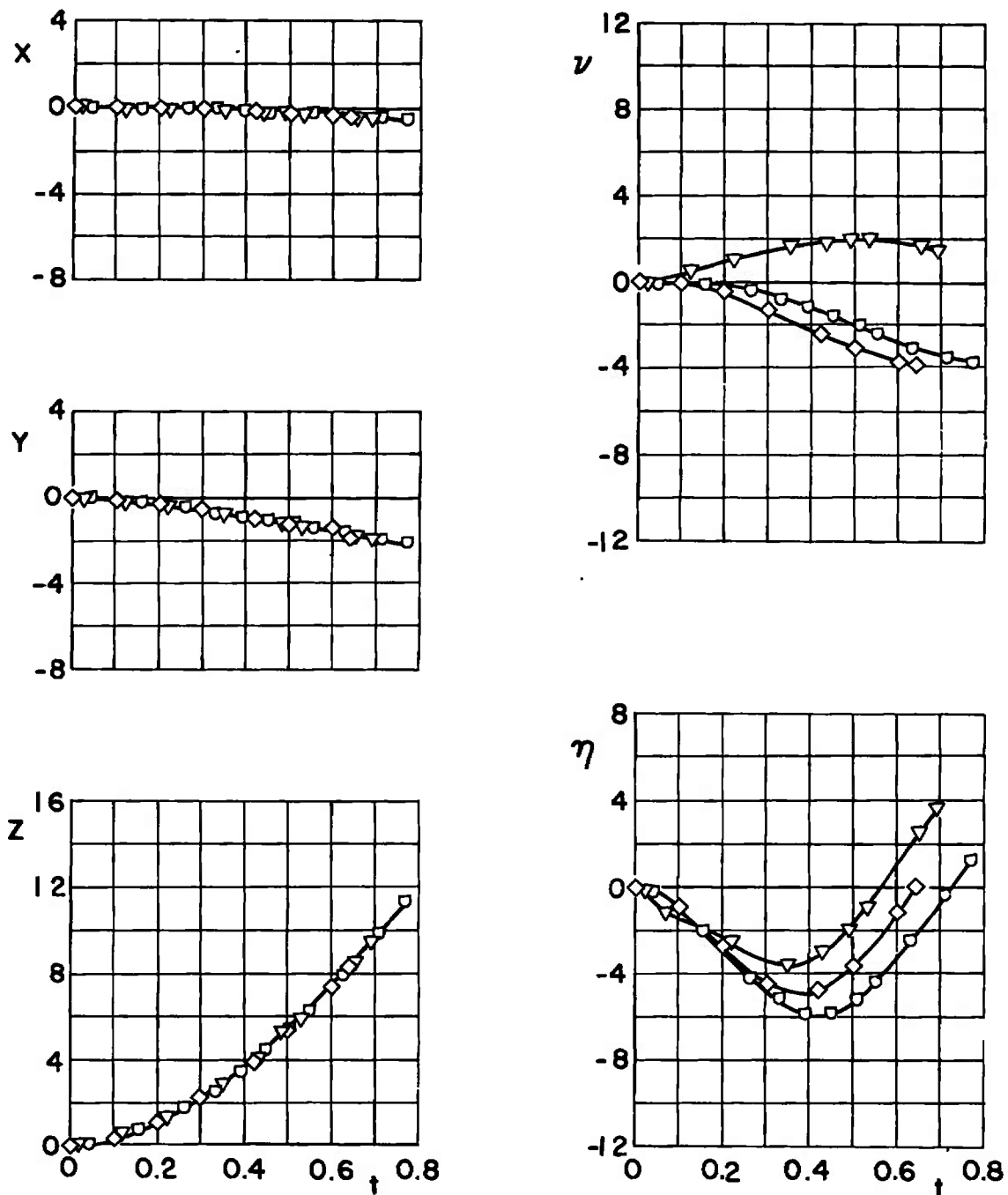
c.  $M_\infty = 0.70$ ,  $\bar{m} = 23.31$   
Fig. 18 Continued



d.  $M_\infty = 0.70$ ,  $\bar{m} = 7.331$   
Fig. 18 Concluded

$\theta$

$\diamond$  0  
 $\nabla$  -2  
 $\square$  2



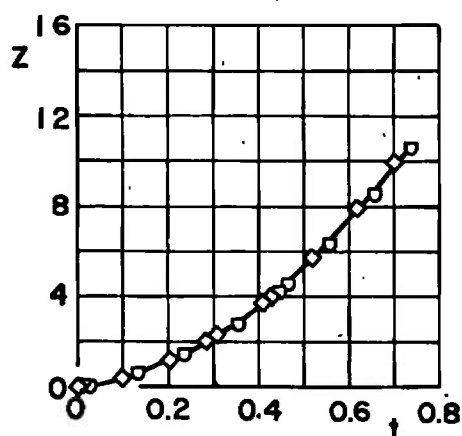
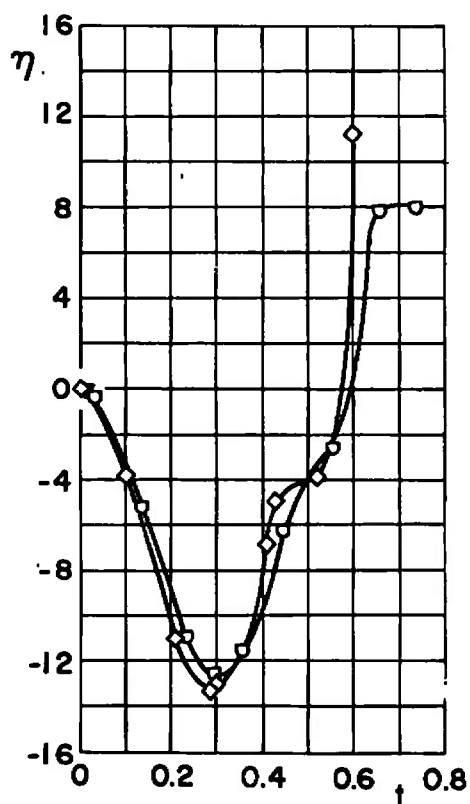
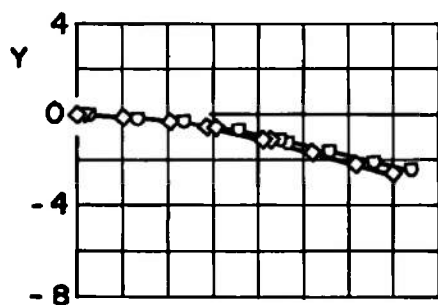
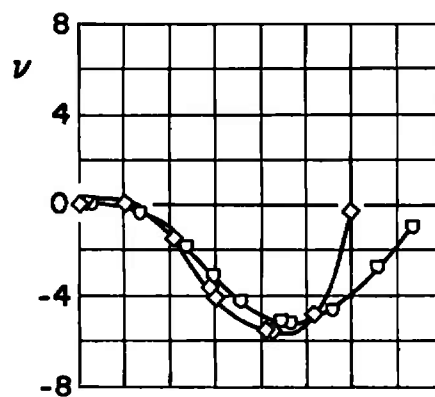
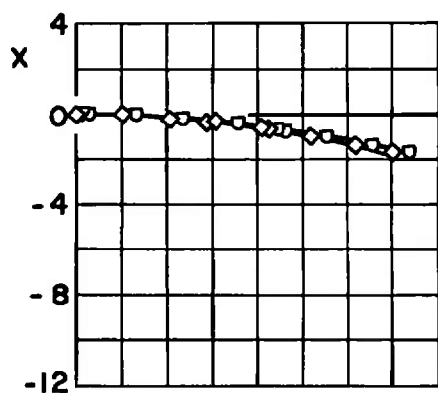
a.  $M_\infty = 0.50$

Fig. 19 Effect of Initial Store Attitude for Configuration II,  $\bar{m} = 23.31$ ,  
 $X_{cg} = 2.74$ ,  $F_{LZ} = 1200$ ,  $I_{yy} = 50$ ,  $h = 20,000$



$\theta$

$\diamond$	0
$\nabla$	-2
$\square$	2



b.  $M_\infty = 0.70$   
Fig. 19 Concluded

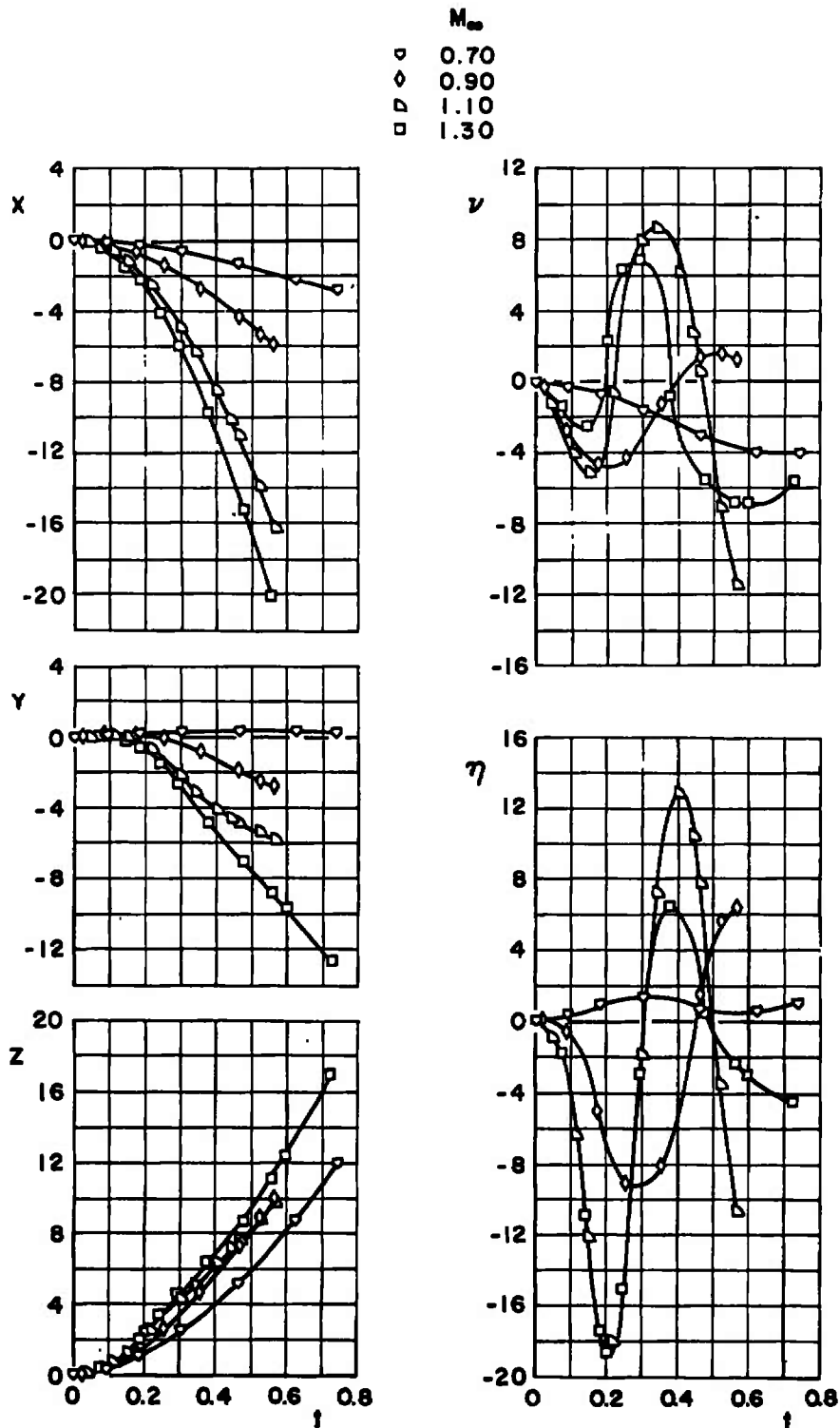


Fig. 20 Effect of Mach Number Variation for Configuration III;  $\bar{m} = 23.31$ ,  $X_{cg} = 2.74$ ,  $F_{LZ} = 1200$ ,  $\theta = 0$ ,  $I_{yy} = 50$ ,  $h = 5000$

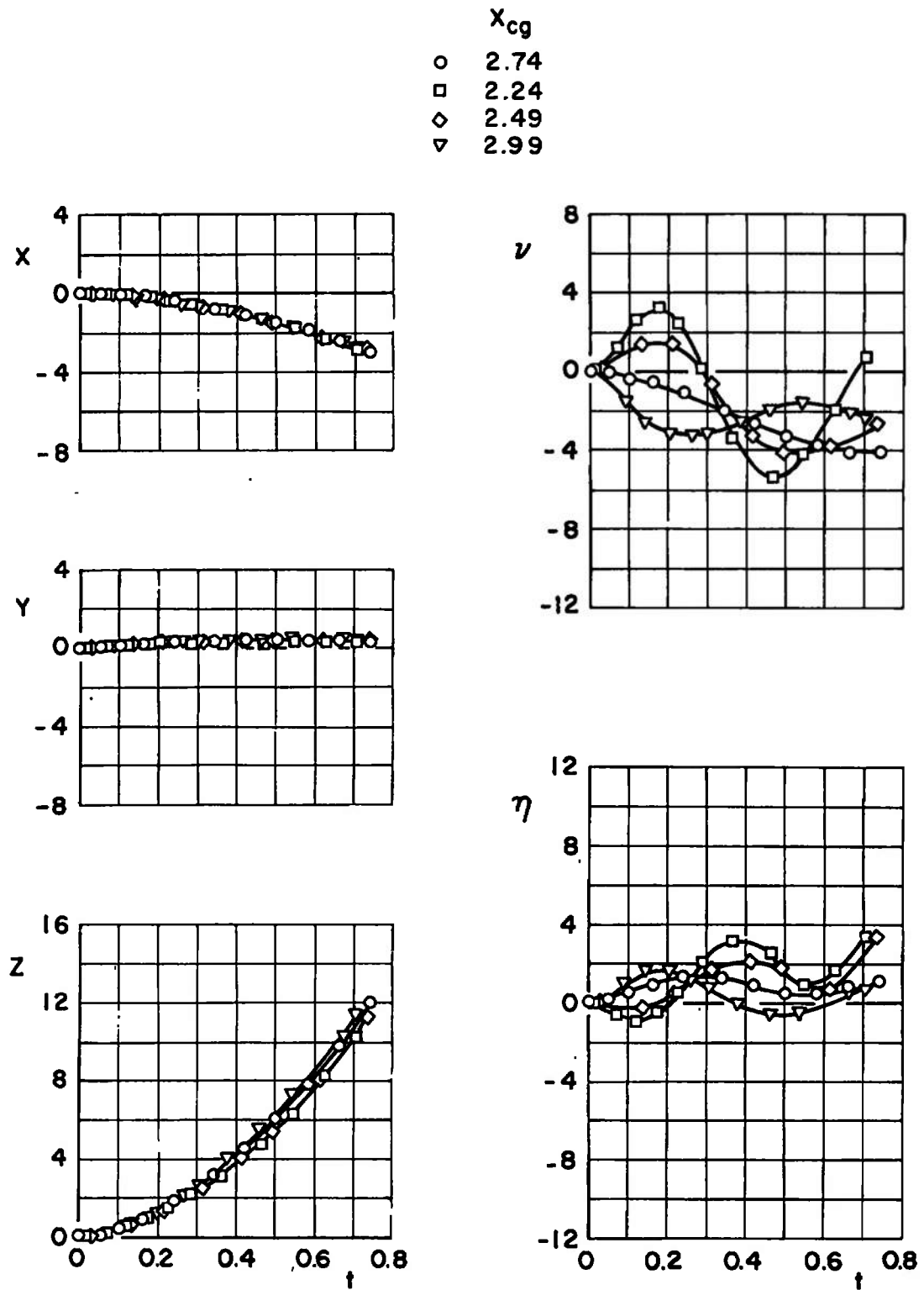
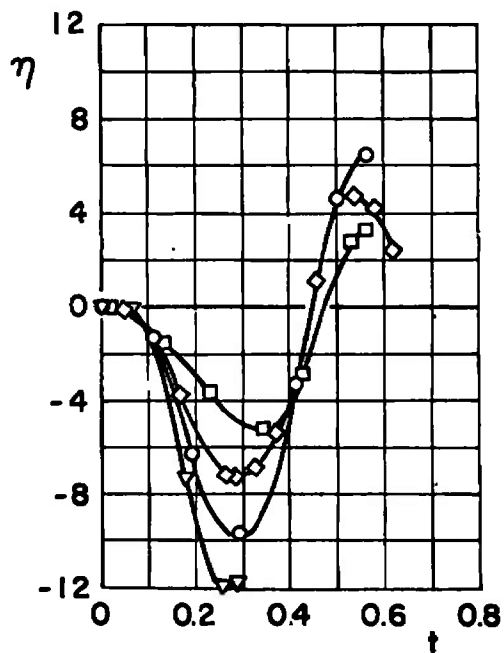
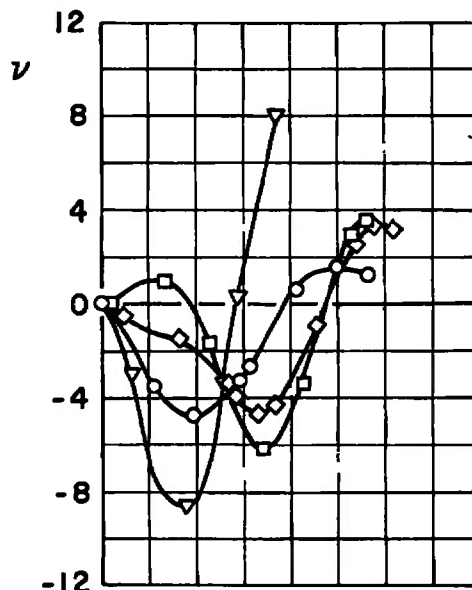
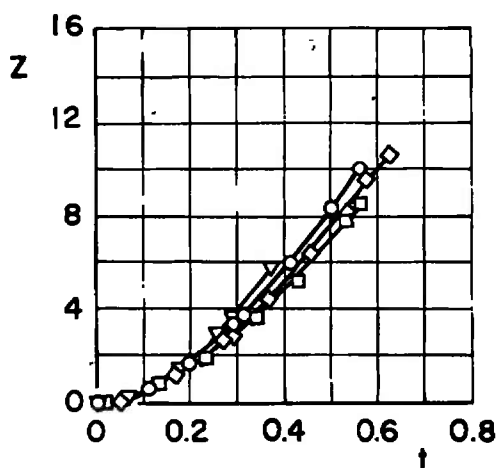
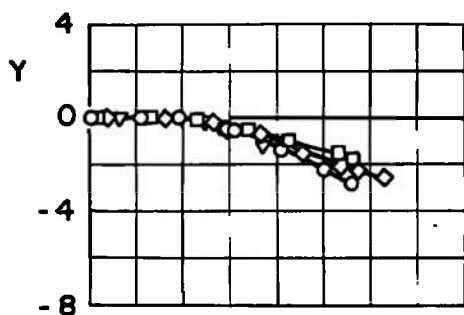
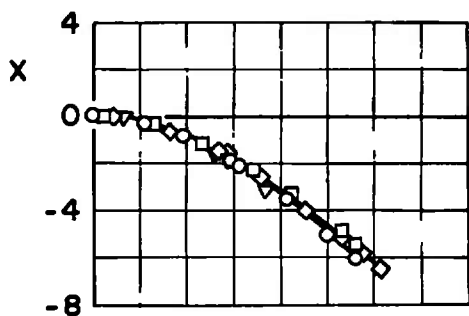
a.  $M_\infty = 0.70$ 

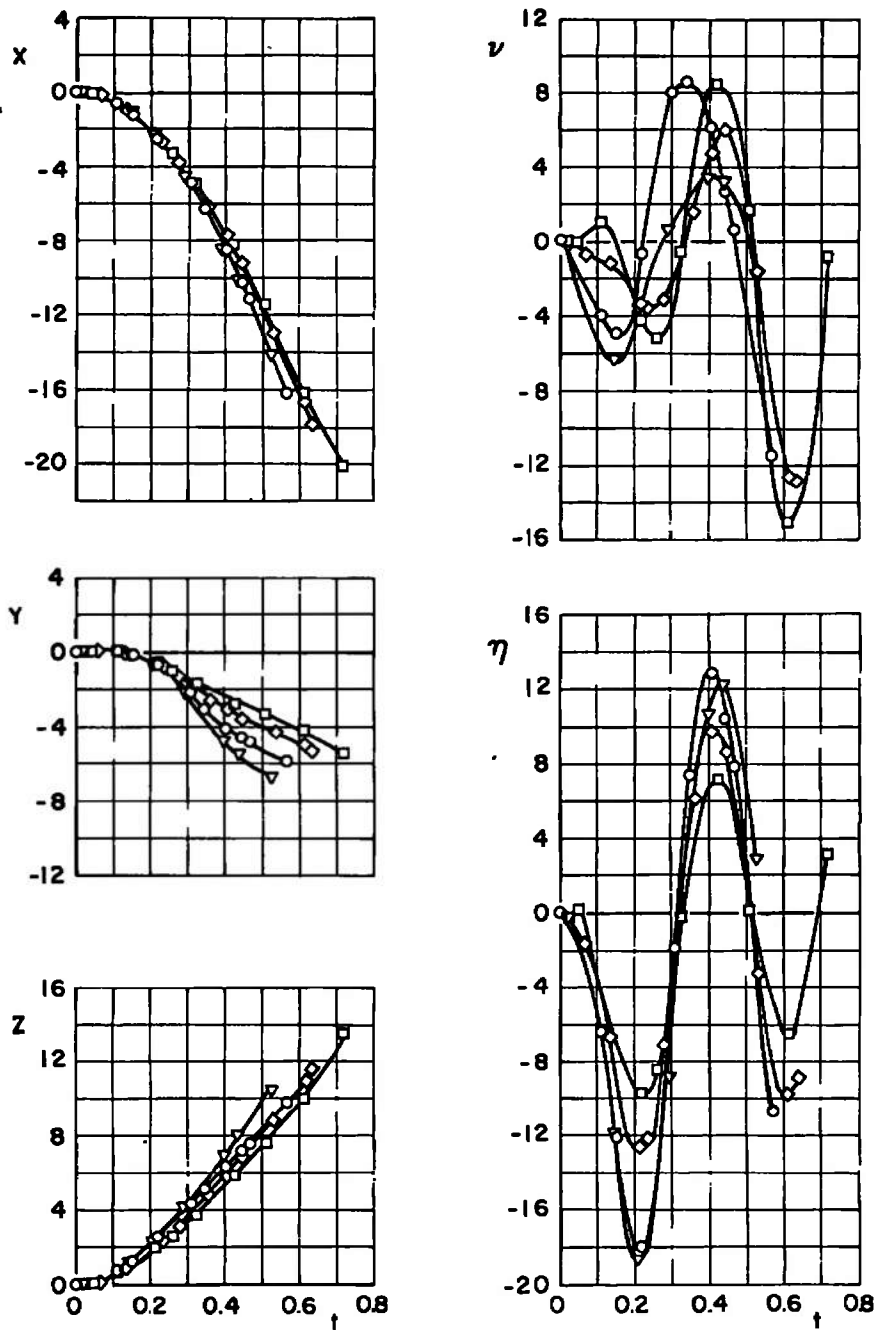
Fig. 21 Effect of Center-of-Gravity Variation for Configuration III;  $\bar{m} = 23.31$ ,  
 $F_{Lz} = 1200$ ,  $\theta = 0$ ,  $I_{yy} = 50$ ,  $h = 5000$

$X_{cg}$   
 ○ 2.74  
 □ 2.24  
 ◇ 2.49  
 ▽ 2.99



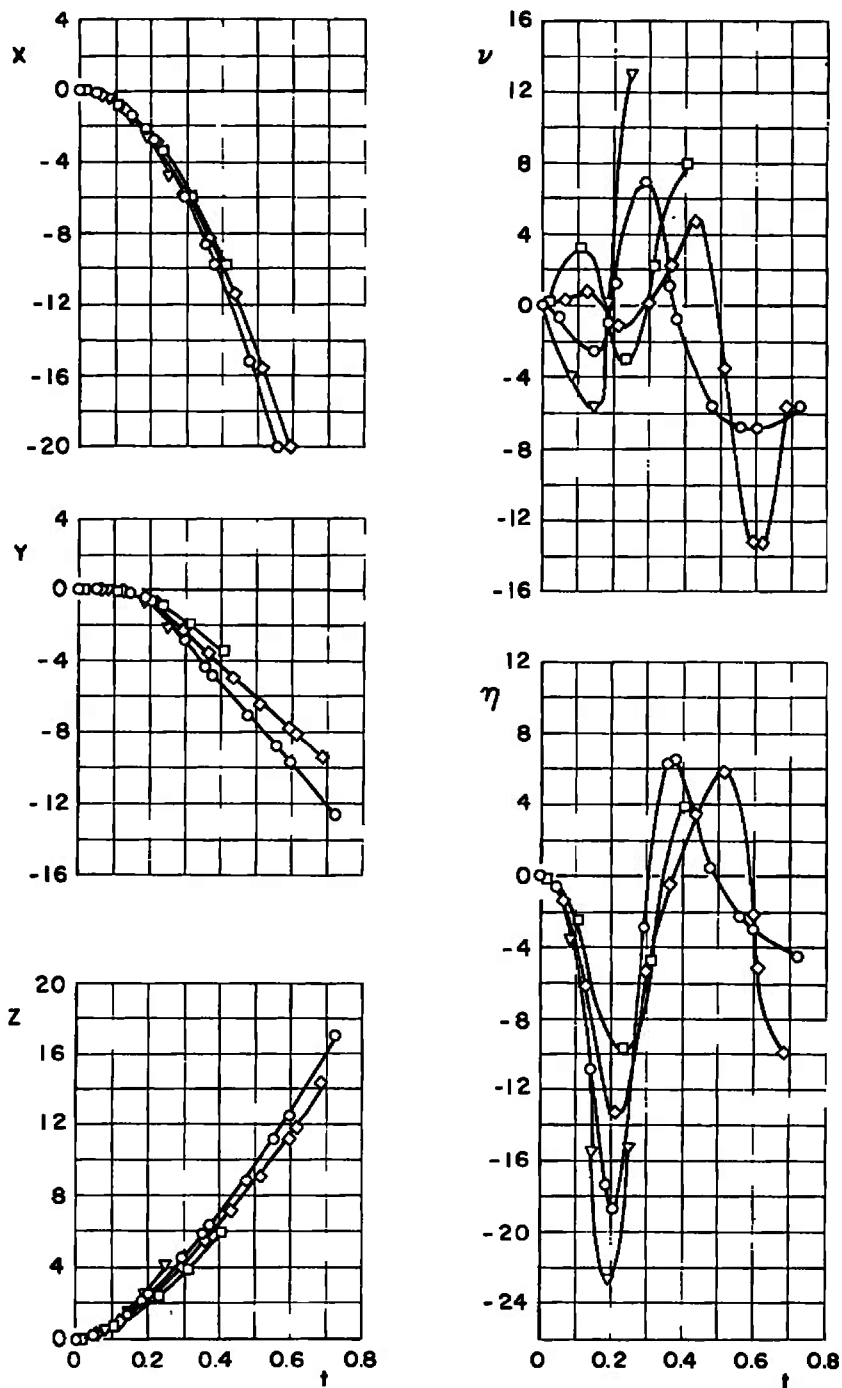
b.  $M_\infty = 0.90$   
 Fig. 21 Continued

$x_{cg}$   
 ○ 2.74  
 □ 2.24  
 ◇ 2.49  
 ▼ 2.99



c.  $M_\infty = 1.10$   
 Fig. 21 Continued

$x_{cg}$   
 ○ 2.74  
 □ 2.24  
 ◇ 2.49  
 ▽ 2.99



d.  $M_\infty = 1.30$   
 Fig. 21 Concluded

$F_{Lz}$ 

○ 1200

□ 600

◇ 1800

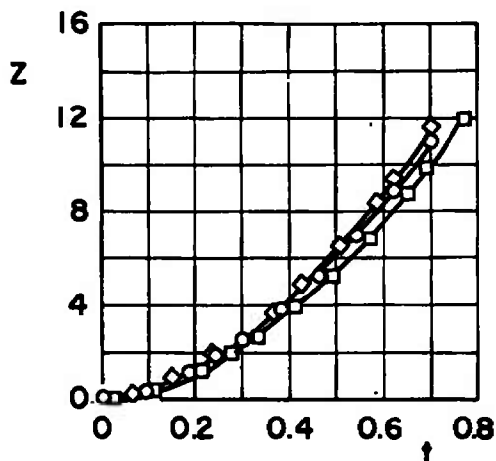
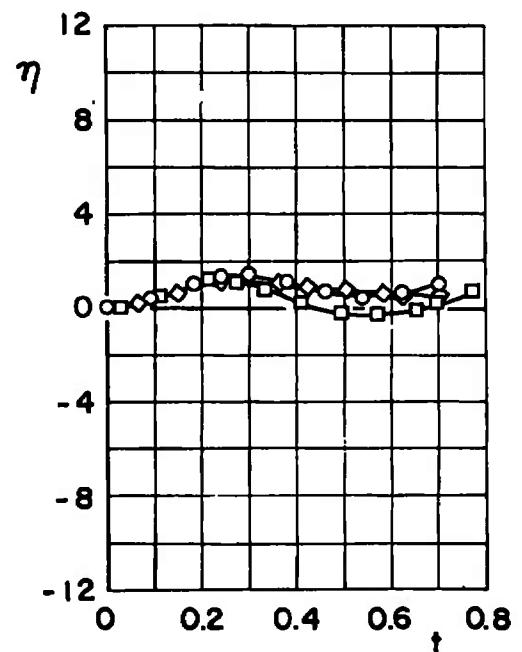
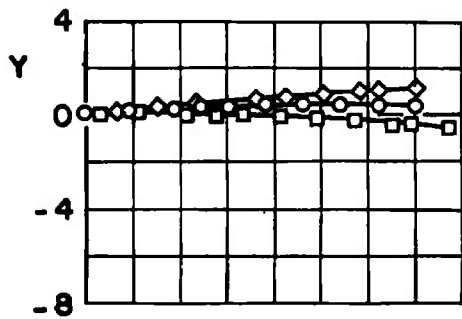
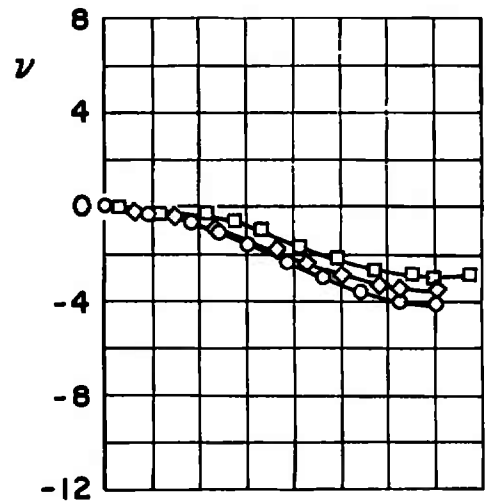
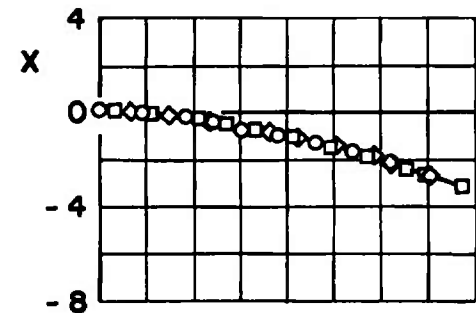
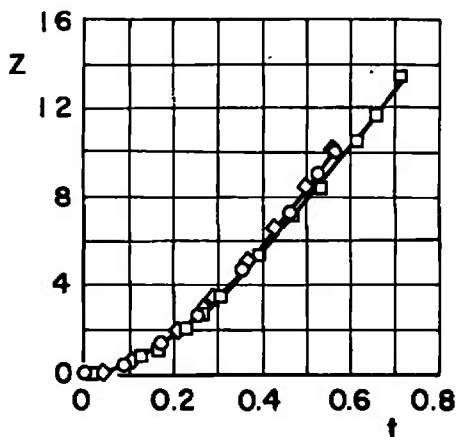
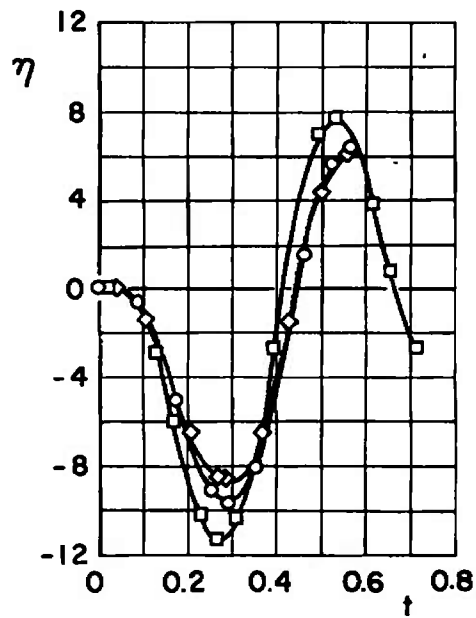
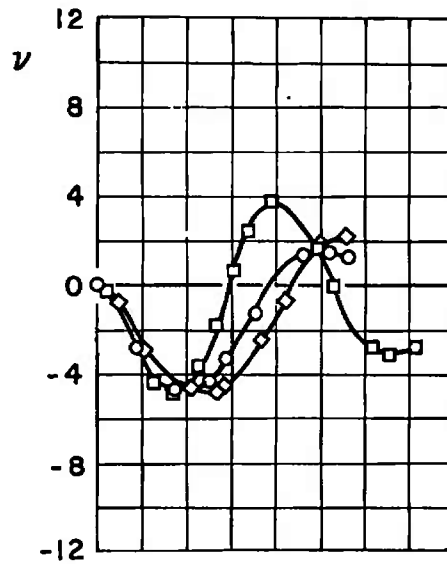
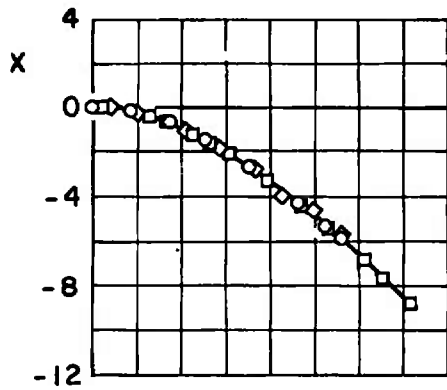
a.  $M_\infty = 0.70$ 

Fig. 22 Effect of Ejector-Force Variation for Configuration III;  $\bar{m} = 23.31$ ,  
 $X_{cg} = 2.74$ ,  $\theta = 0$ ,  $I_{yy} = 50$ ,  $h = 5000$

$F_{Lz}$

- 1200
- 600
- ◇ 1800

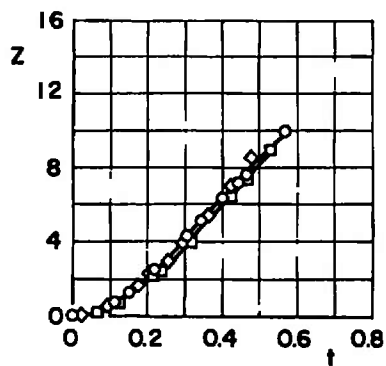
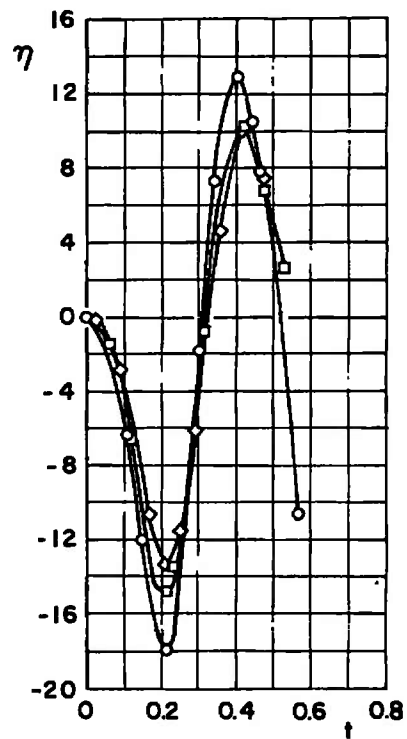
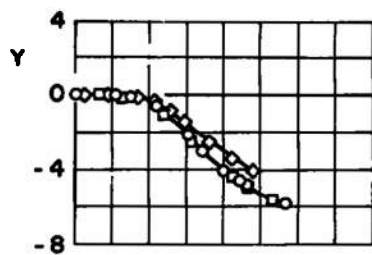
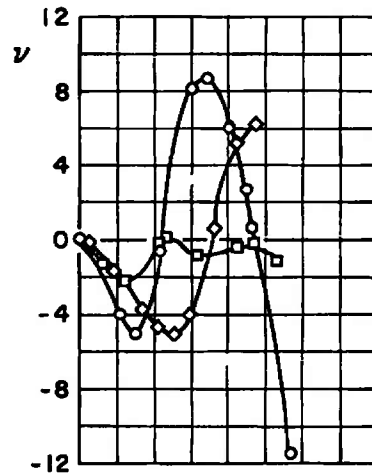
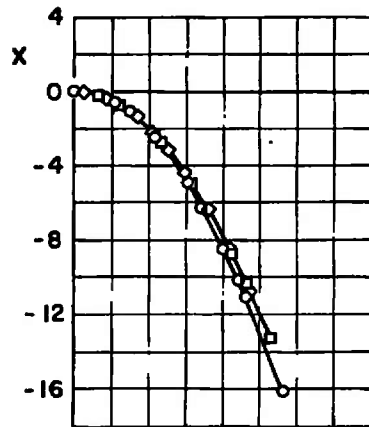


b:  $M_\infty = 0.90$   
Fig. 22 Continued

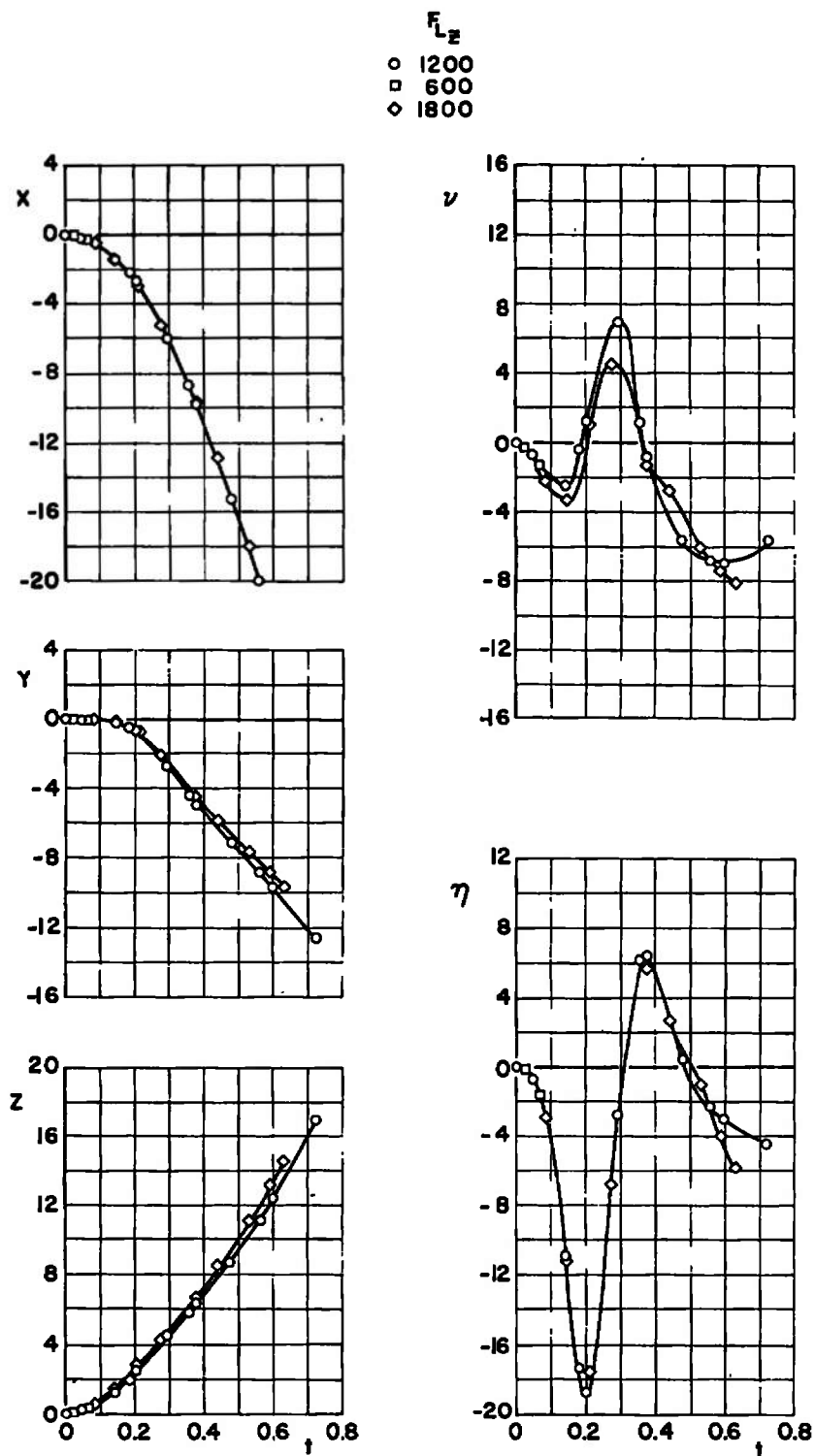


$F_{L2}$ 

○ 1200  
 □ 600  
 ◇ 1800



c.  $M_\infty = 1.10$   
 Fig. 22 Continued



d.  $M_\infty = 1.30$   
Fig. 22 Concluded

$I_{yy}$ 

○ 50  
□ 80

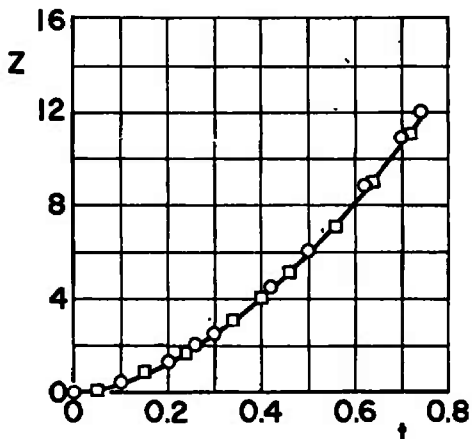
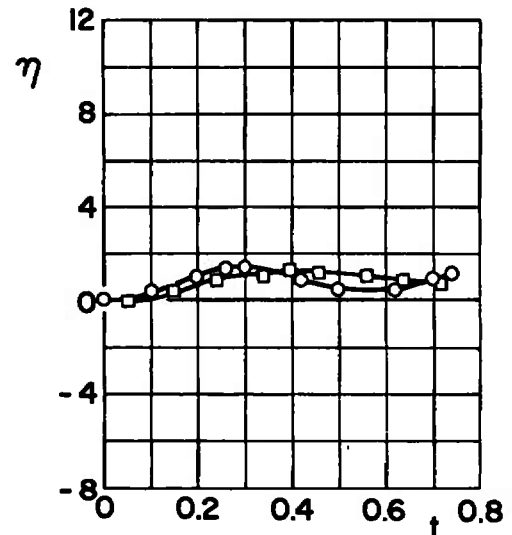
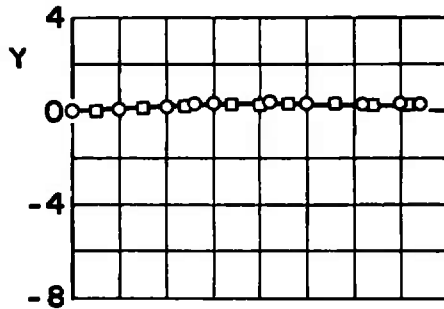
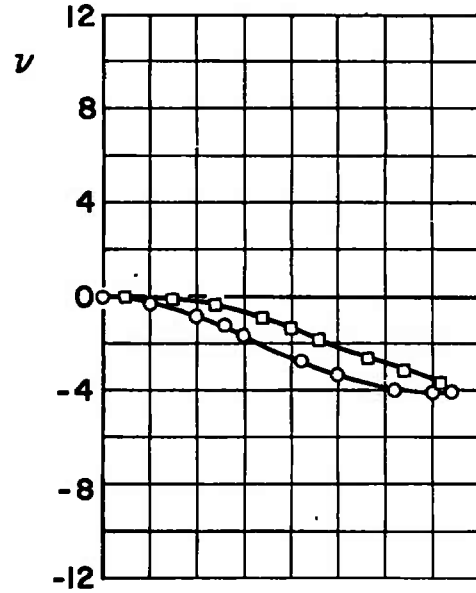
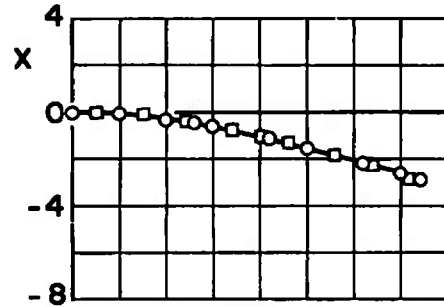
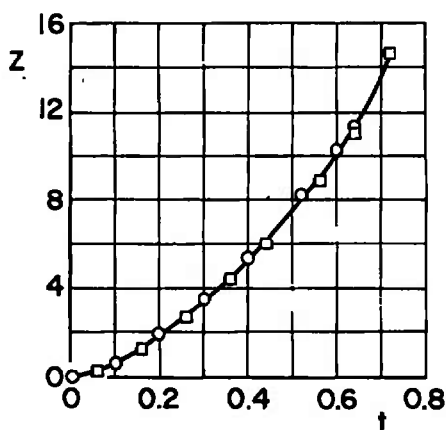
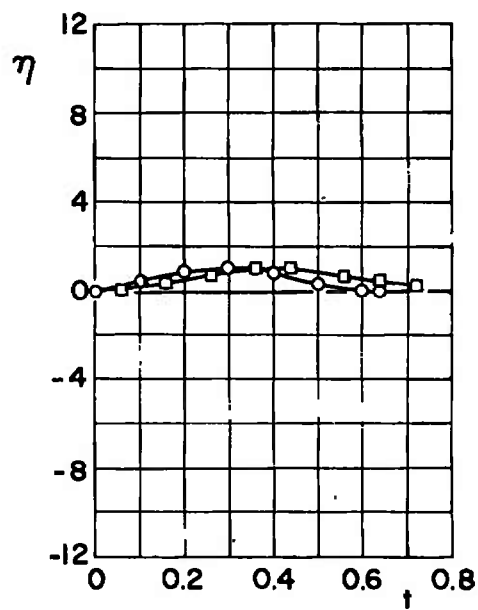
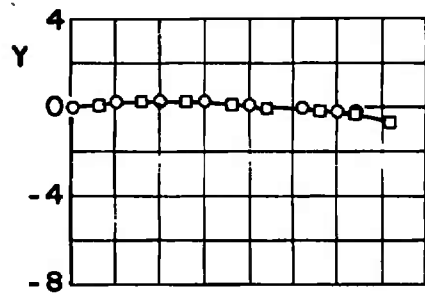
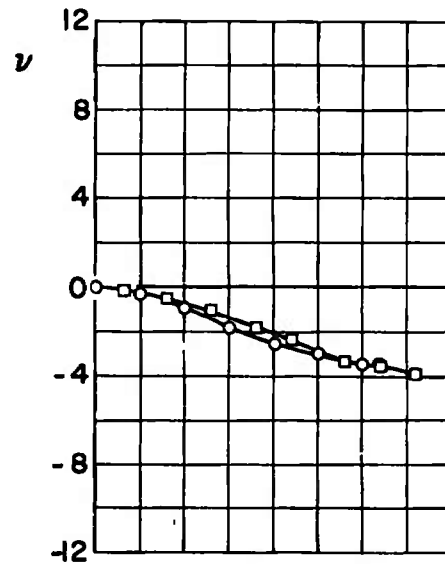
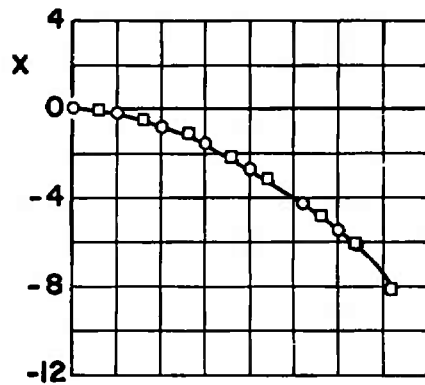
a.  $M_\infty = 0.70$ ,  $\bar{m} = 23.31$ 

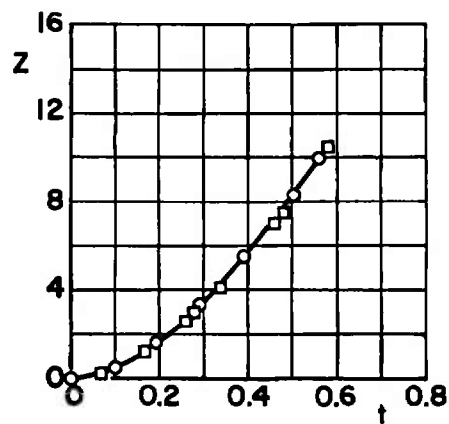
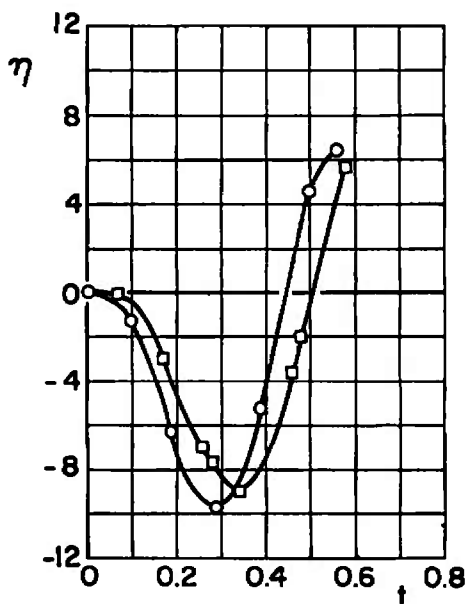
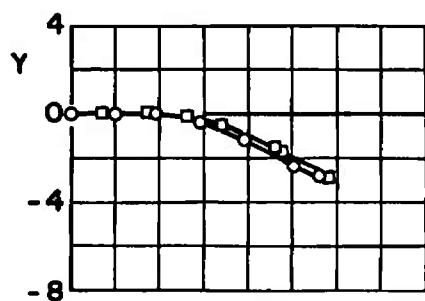
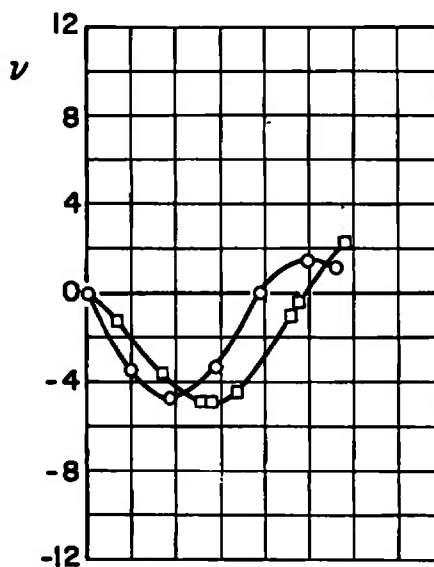
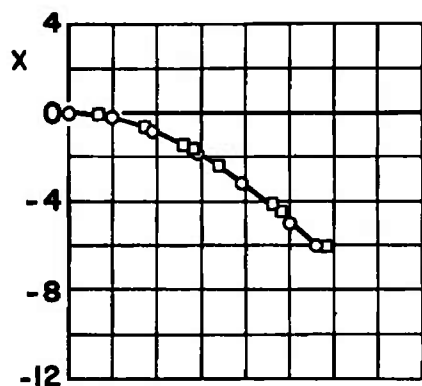
Fig. 23 Effect of Moment-of-Inertia Variation for Configuration III;  
 $X_{cg} = 2.74$ ,  $F_{LZ} = 1200$ ,  $\theta = 0$ ,  $h = 5000$

$I_{yy}$   
 ○ 30  
 □ 50

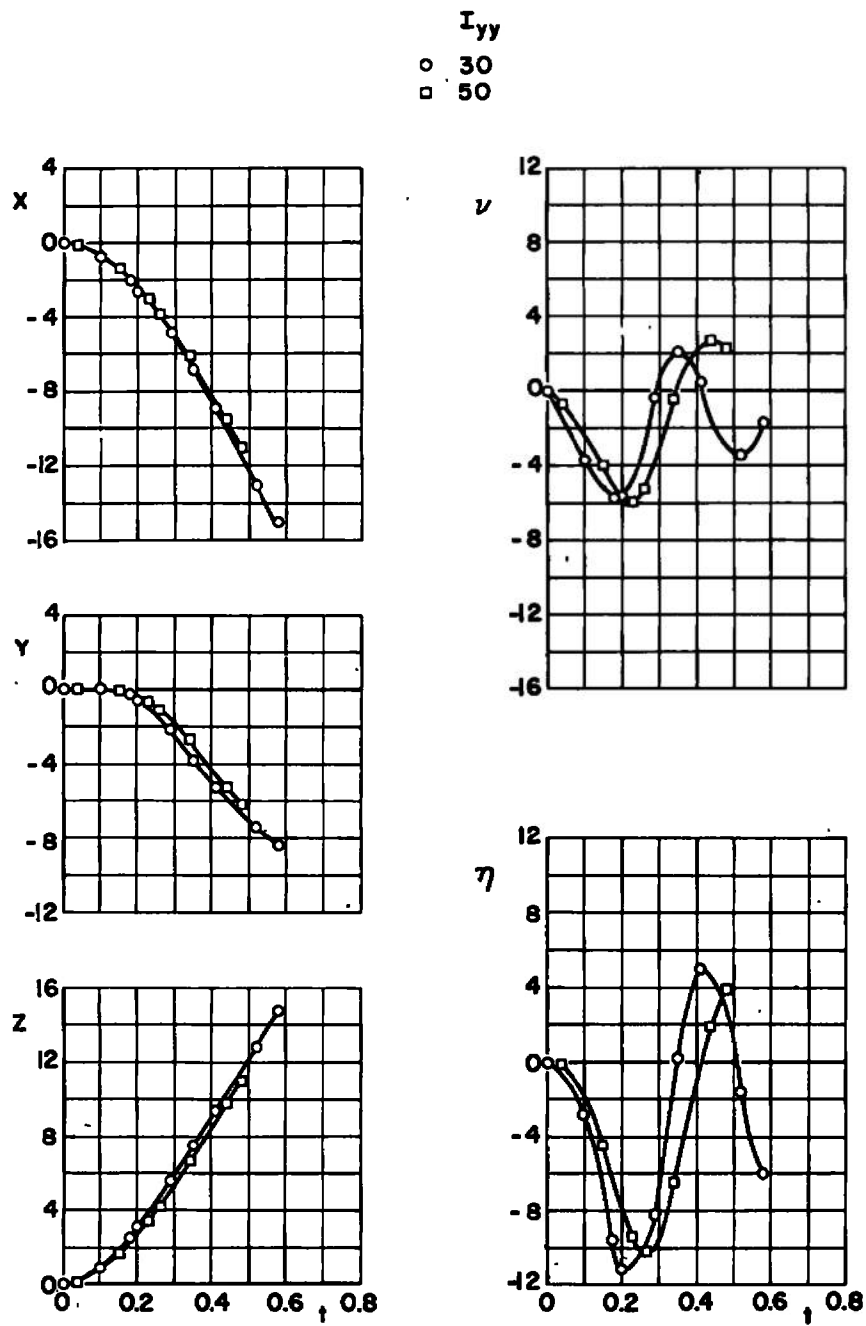


b.  $M_\infty = 0.70, \bar{m} = 7.771$   
 Fig. 23 Continued

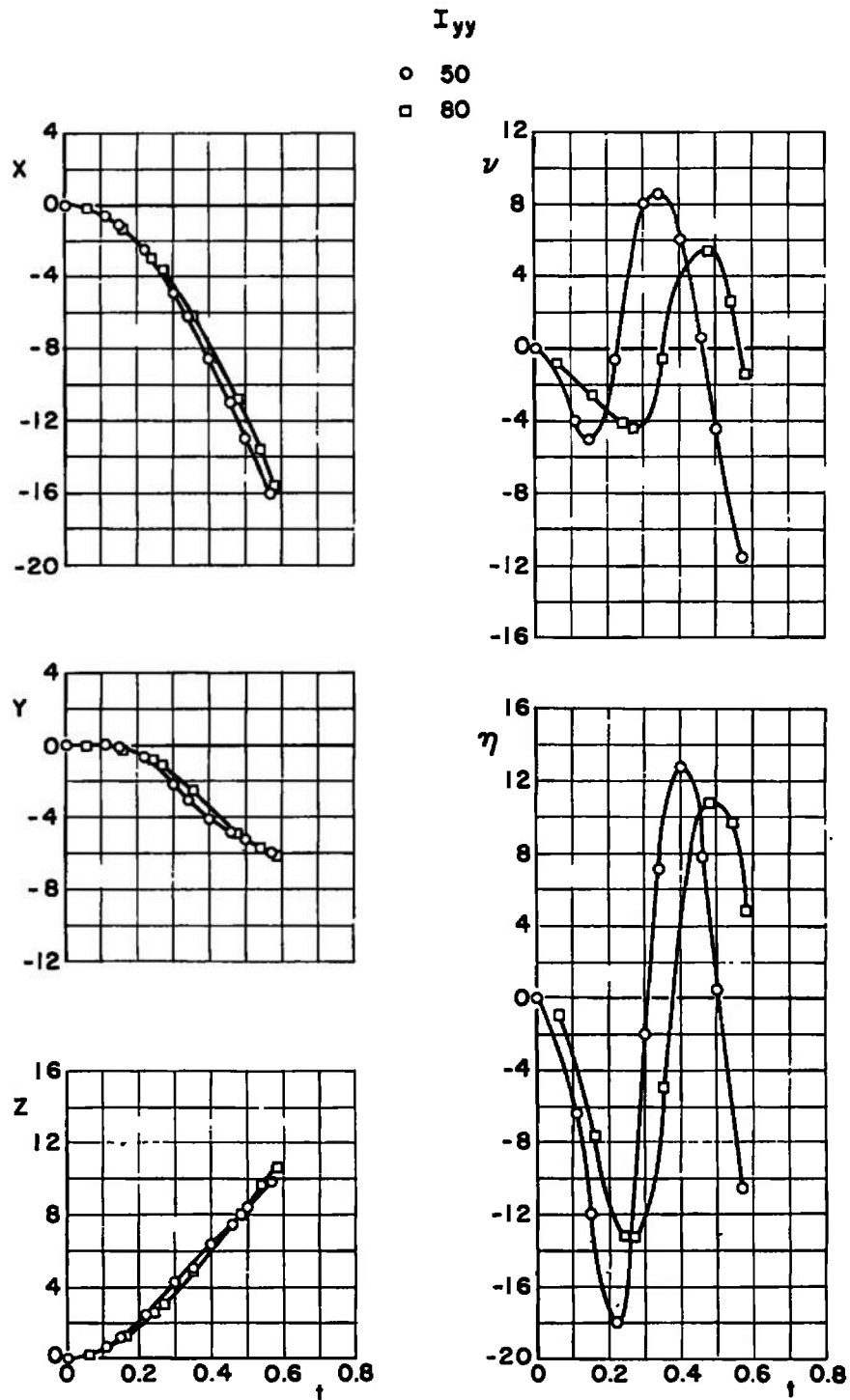
$I_{yy}$   
 ○ 50  
 □ 80



c.  $M_\infty = 0.90$ ,  $\bar{m} = 23.31$   
 Fig. 23 Continued

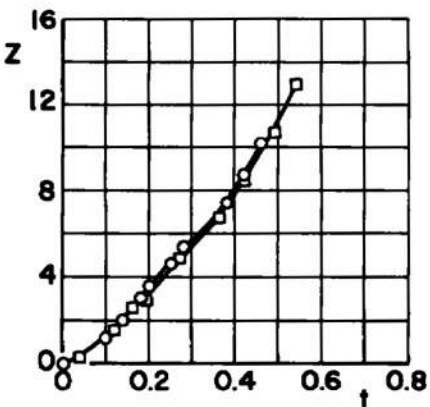
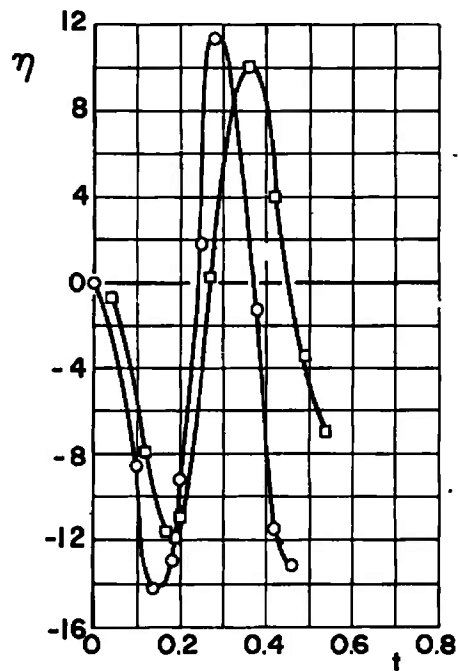
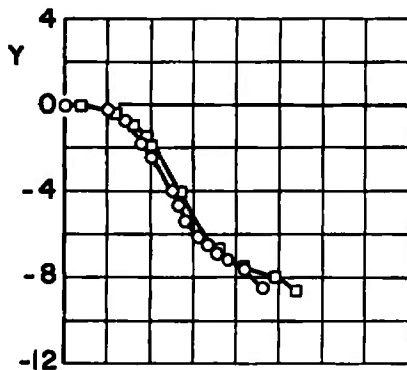
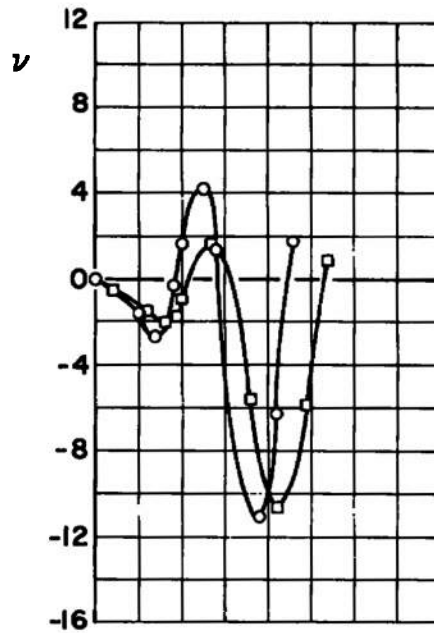
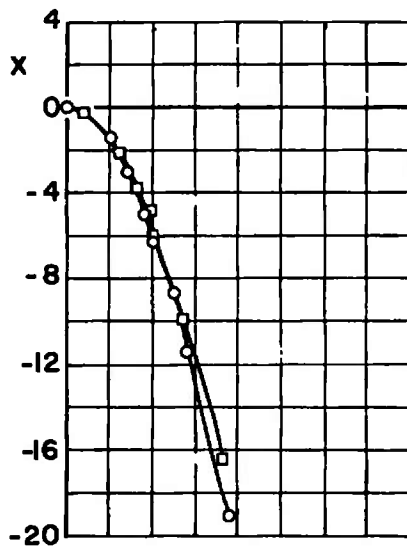


d.  $M_\infty = 0.90, \bar{m} = 7.771$   
Fig. 23 Continued



e.  $M_\infty = 1.10$ ,  $\bar{m} = 23.31$   
Fig. 23 Continued

$I_{yy}$   
 ○ 30  
 □ 50



f.  $M_\infty = 1.10$ ,  $\bar{m} = 7.771$   
 Fig. 23 Continued



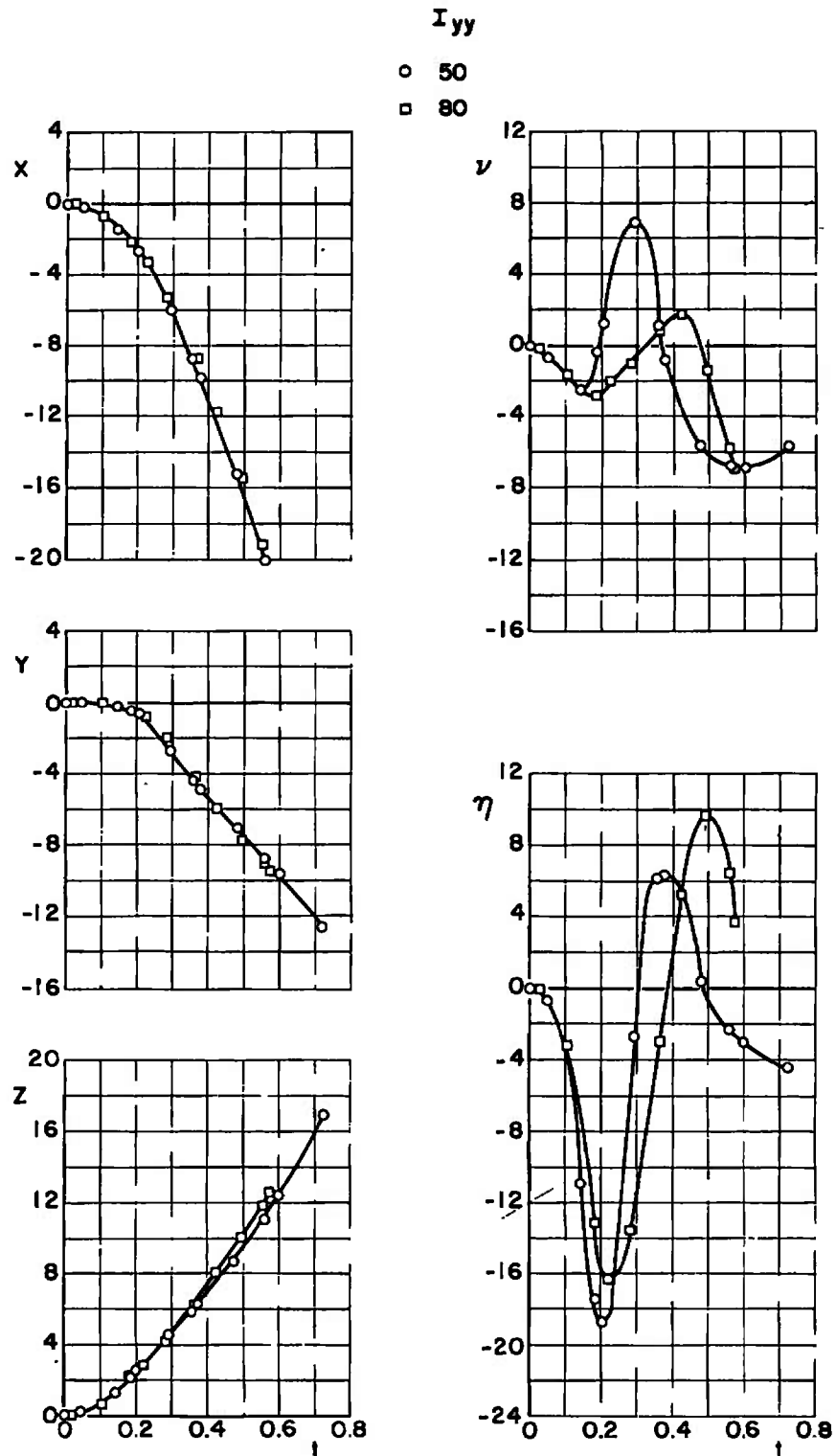
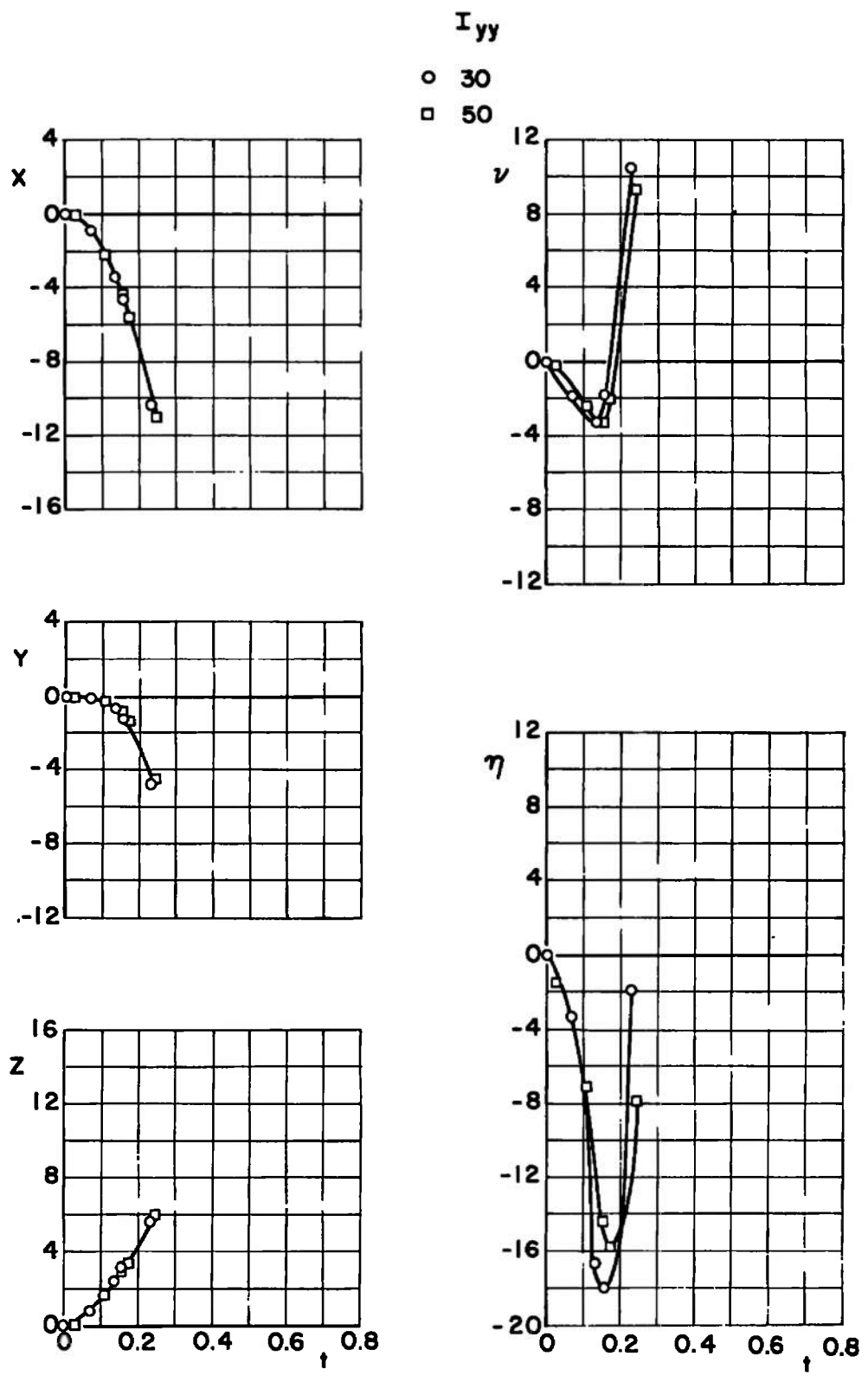
g.  $M_\infty = 1.30$ ,  $\bar{m} = 23.31$ 

Fig. 23 Continued



h.  $M_\infty = 1.30$ ,  $\bar{m} = 7.771$   
Fig. 23 Concluded

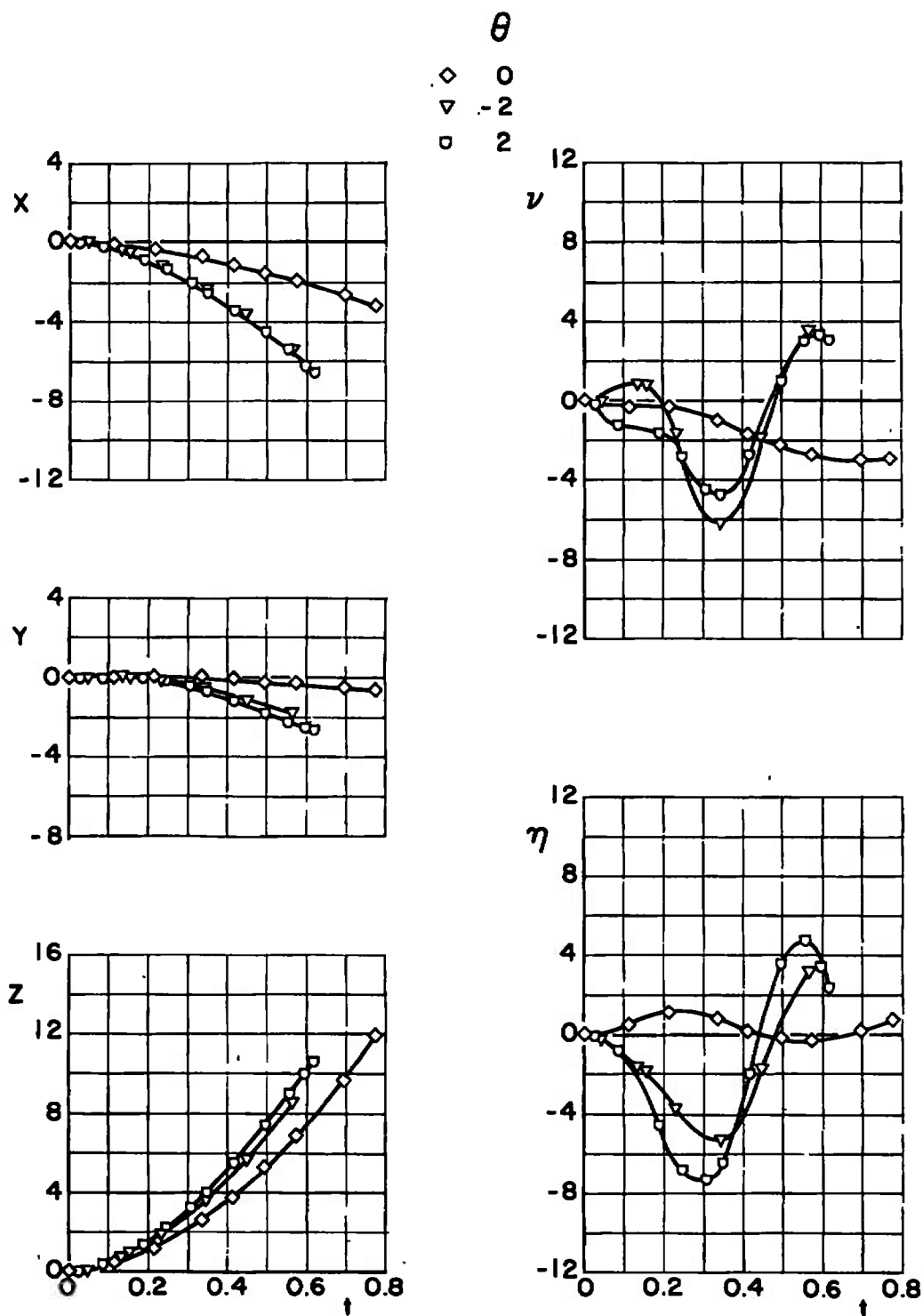
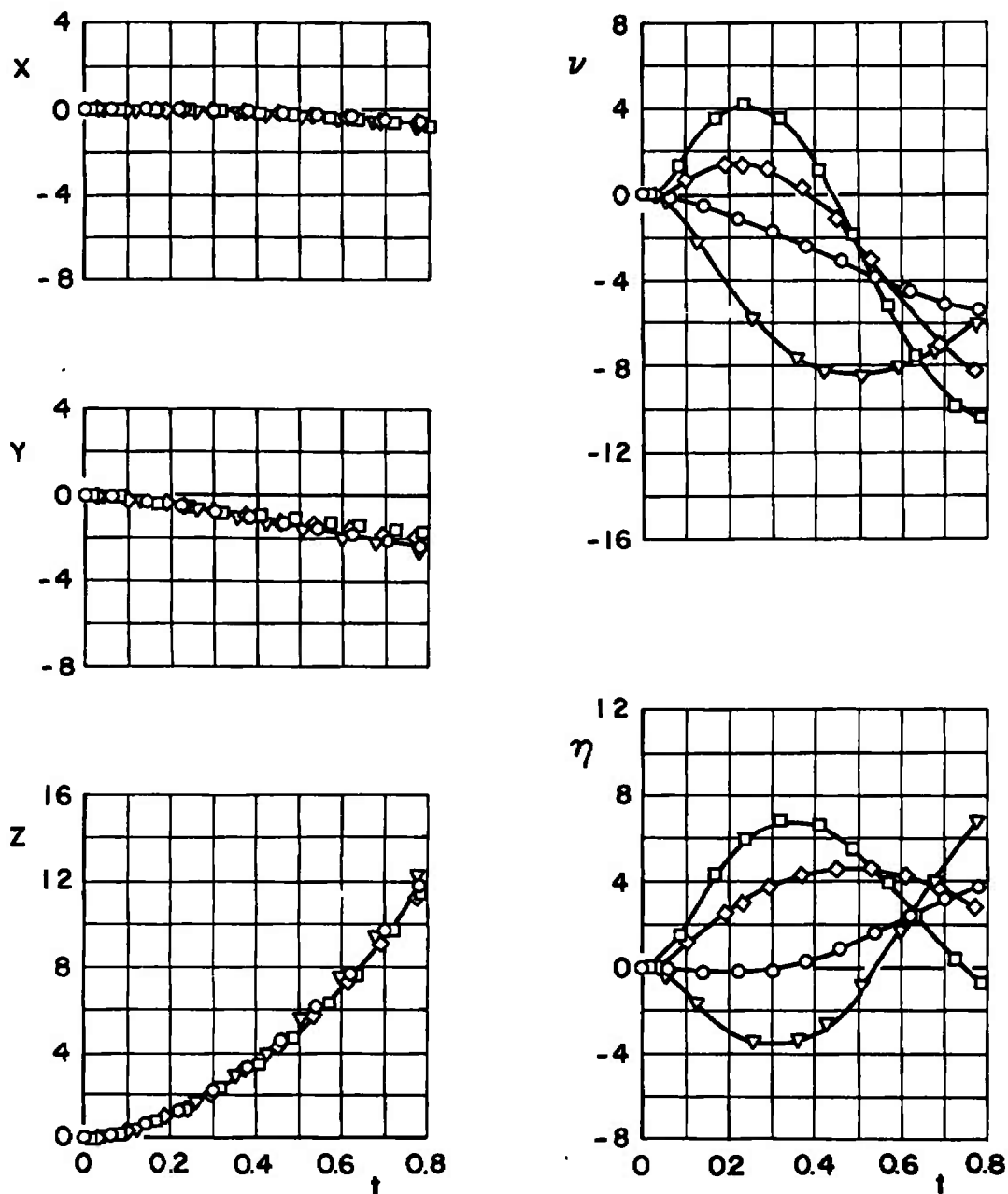


Fig. 24 Typical Effect of Initial Store Attitude for Configuration III;  
 $\bar{m} = 23.31$ ,  $X_{cg} = 2.74$ ,  $F_{LZ} = 1200$ ,  $I_{yy} = 50$ ,  $M_\infty = 0.90$ ,  $h = 5000$

	$x_{cg}$
○	2.74
□	2.24
◇	2.49
▽	2.99

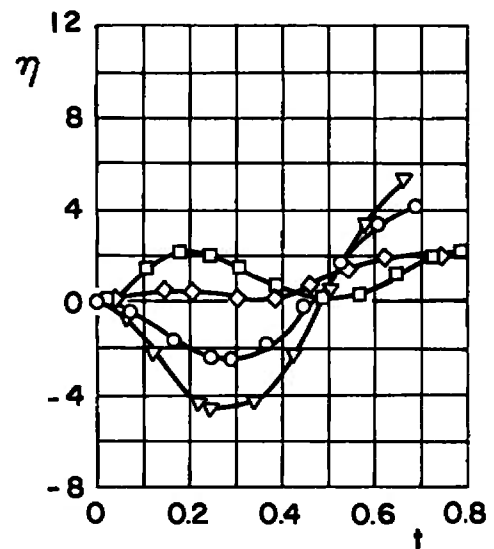
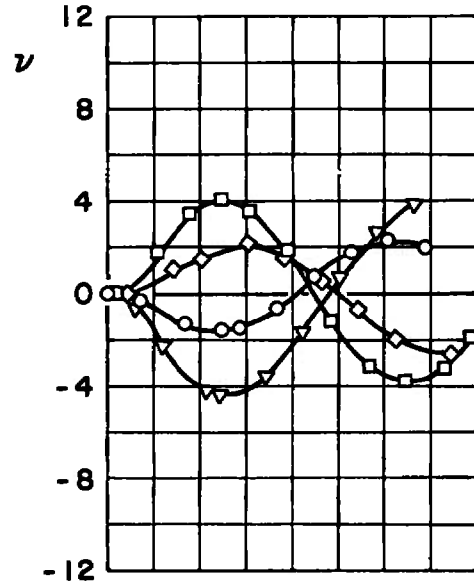
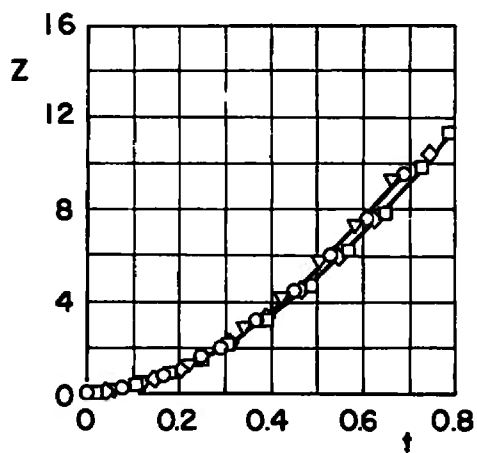
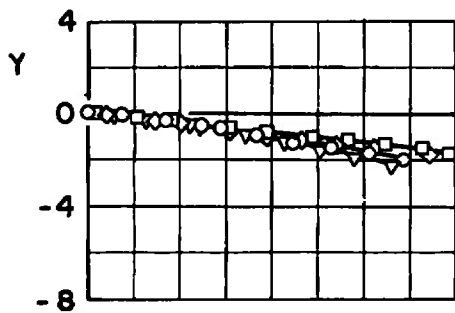
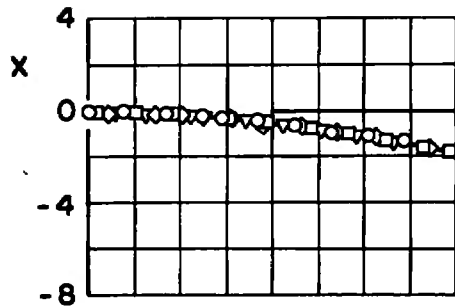


a.  $M_\infty = 0.50$

Fig. 25 Effect of Center-of-Gravity Variation for Configuration IV;  
 $\bar{m} = 23.31$ ,  $F_{LZ} = 1200$ ,  $\theta = 0$ ,  $I_{yy} = 50$ ,  $h = 20,000$

$X_{cg}$

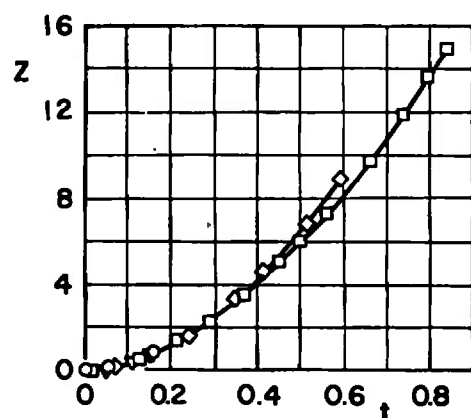
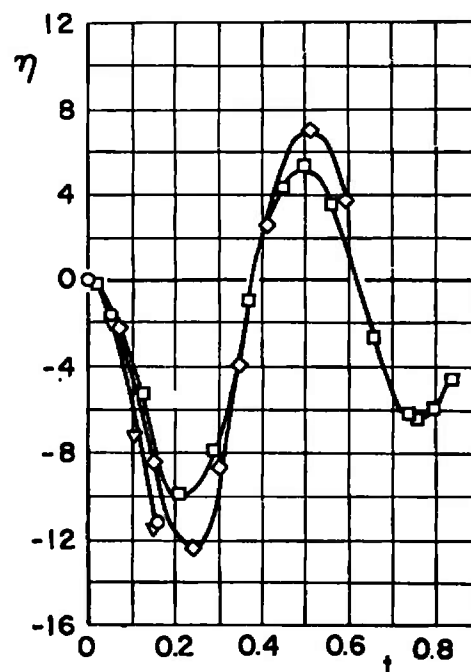
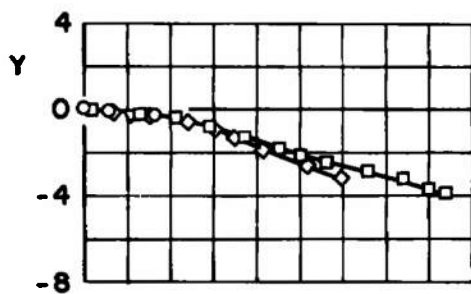
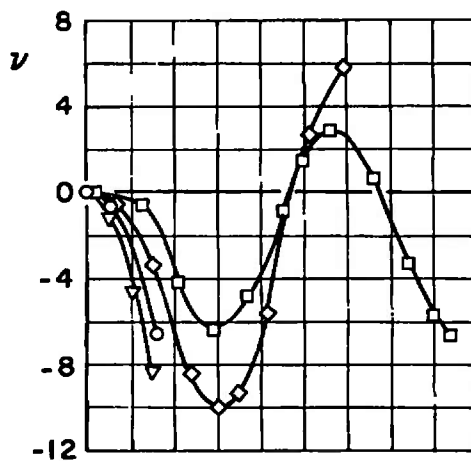
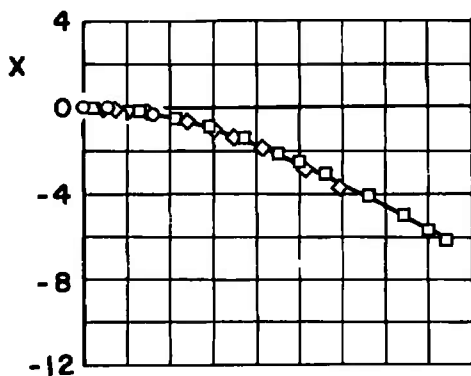
○	2.74
□	2.24
◇	2.49
▽	2.99



b.  $M_\infty = 0.70$   
Fig. 25 Continued

$X_{cg}$

○	2.74
□	2.24
◇	2.49
▽	2.99



c.  $M_\infty = 0.90$   
Fig. 25 Concluded

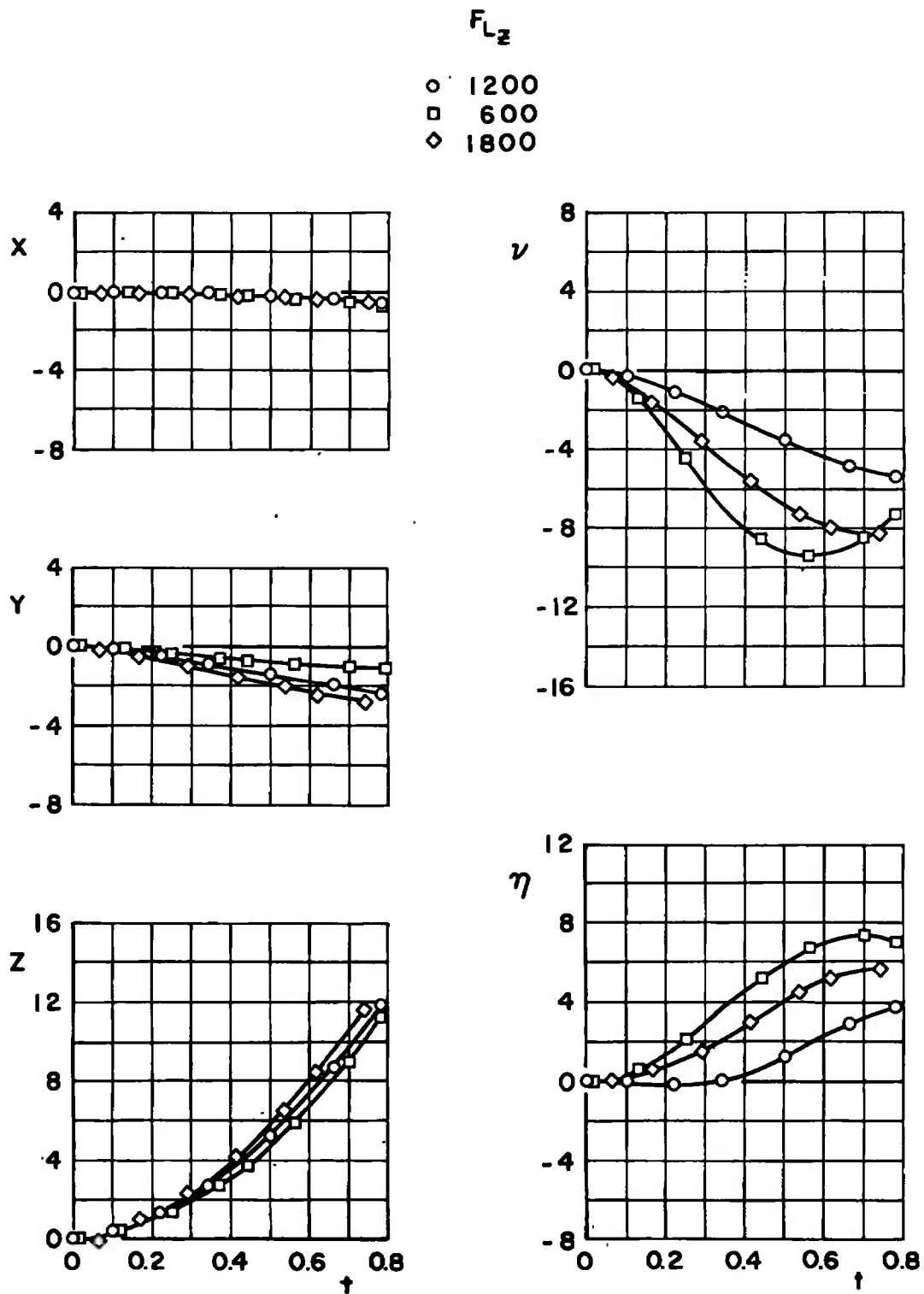
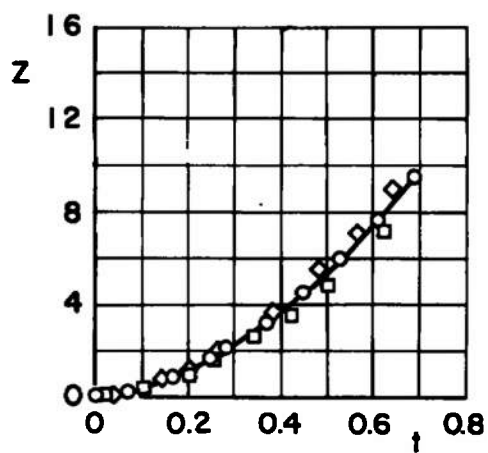
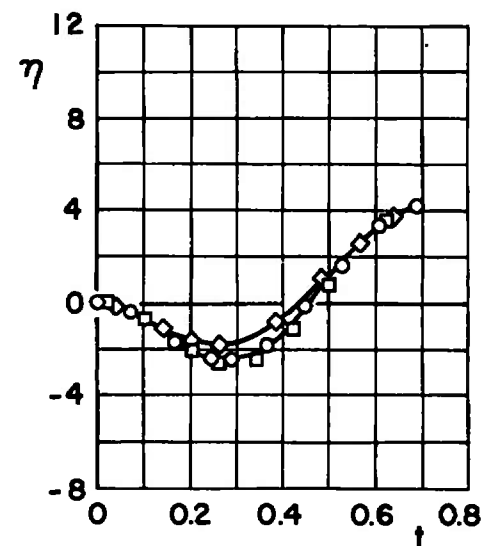
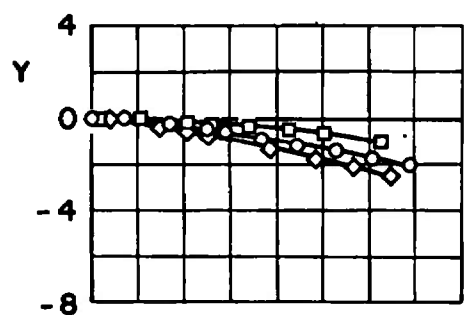
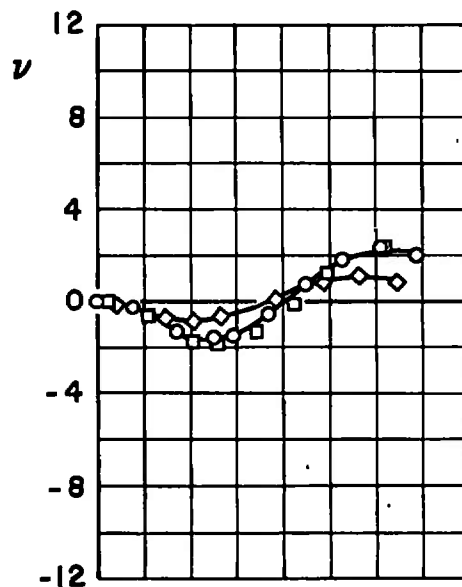
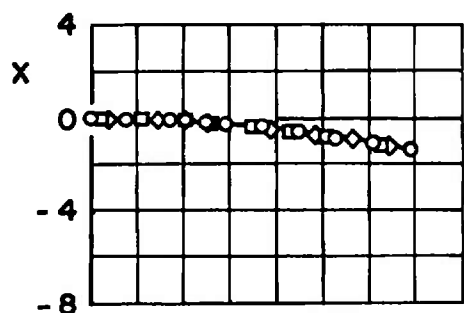
a.  $M_\infty = 0.50$ 

Fig. 26 Effect of Ejector-Force Variation for Configuration IV;  $\bar{m} = 23.31$ ,  
 $X_{cg} = 2.74$ ,  $\theta = 0$ ,  $I_{yy} = 50$ ,  $h = 20,000$

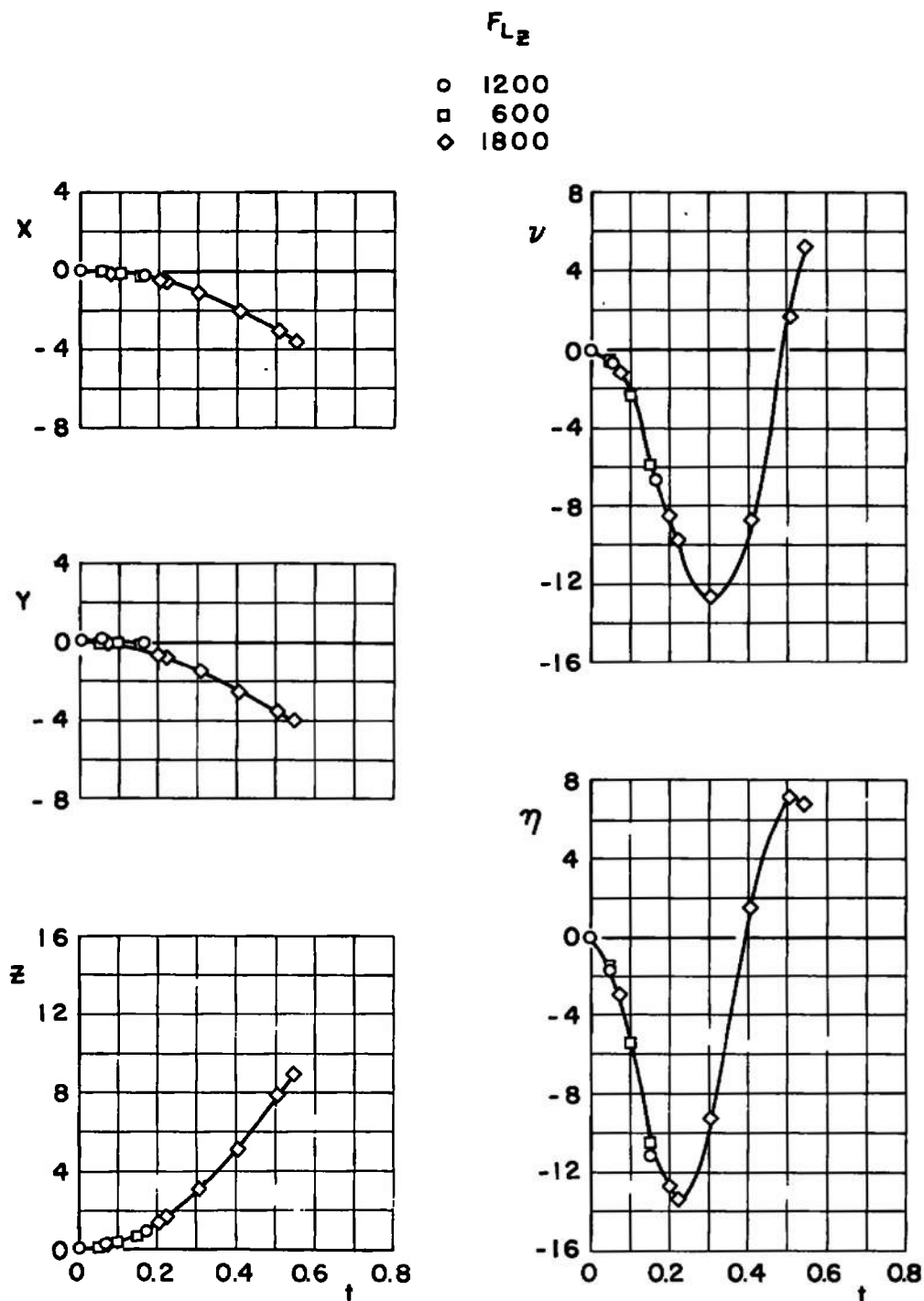
$F_{Lz}$

○ 1200  
□ 600  
◇ 1800

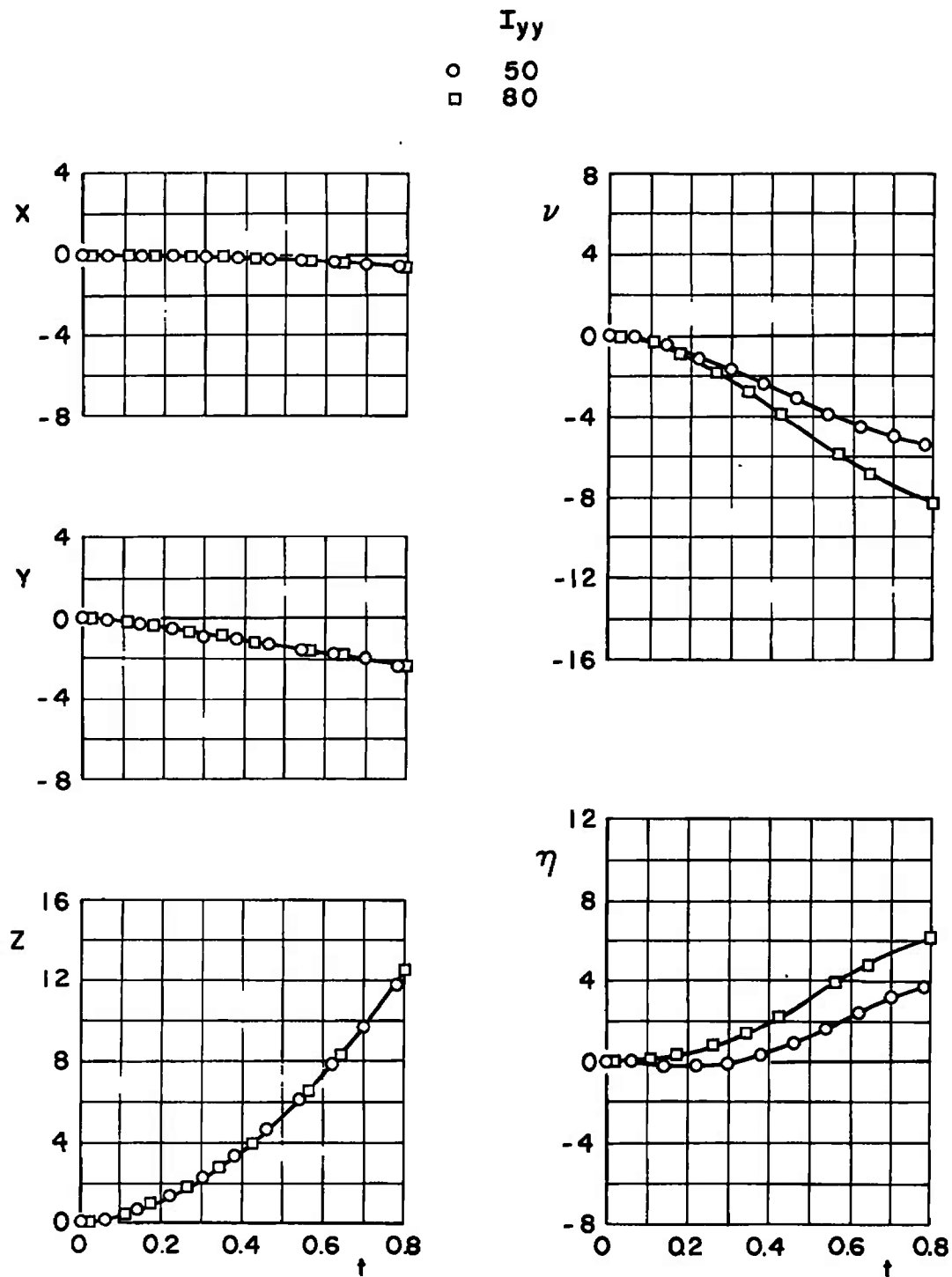


b.  $M_\infty = 0.70$   
Fig. 26 Continued





c.  $M_\infty = 0.90$   
Fig. 26 Concluded

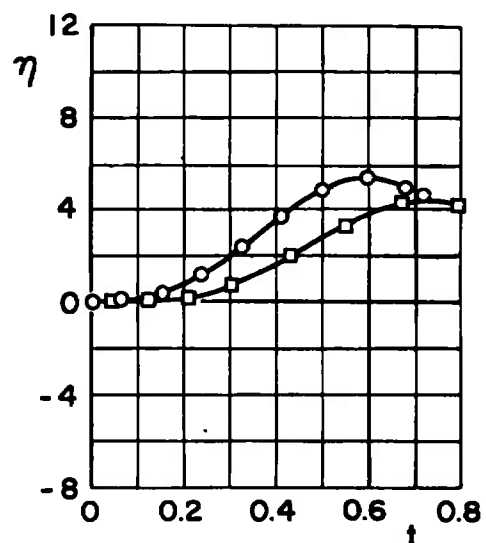
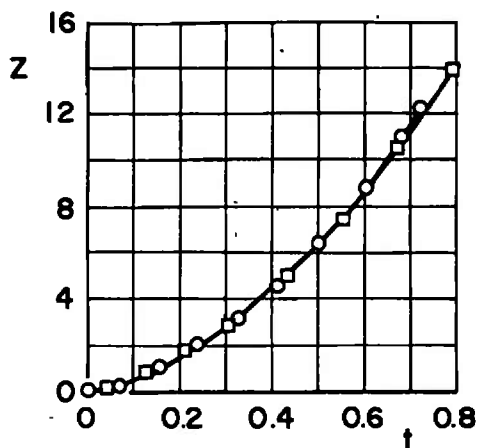
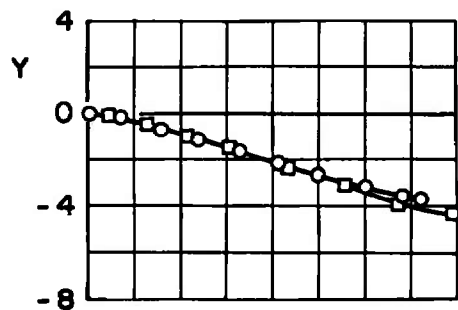
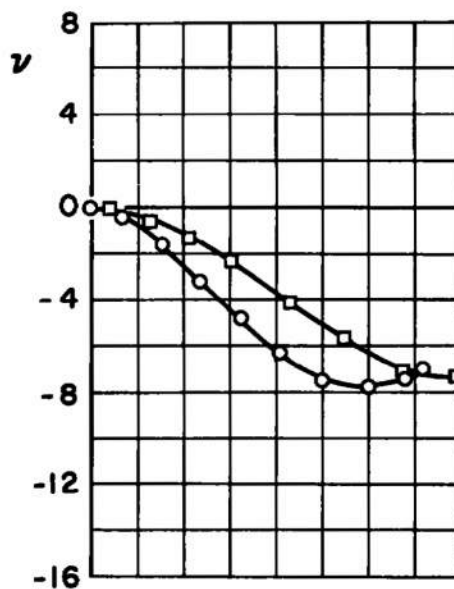
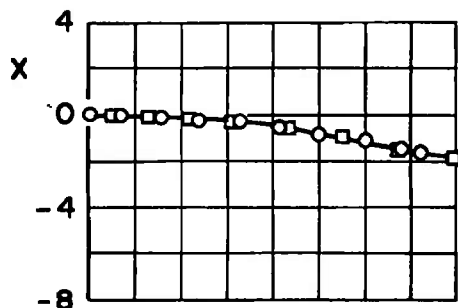


a.  $M_\infty = 0.50$ ,  $\bar{m} = 23.31$

Fig. 27 Effect of Moment-of-Inertia Variation for Configuration IV;  
 $X_{cg} = 2.74$ ,  $F_{Lz} = 0$ ,  $\theta = 0$ ,  $h = 20,000$

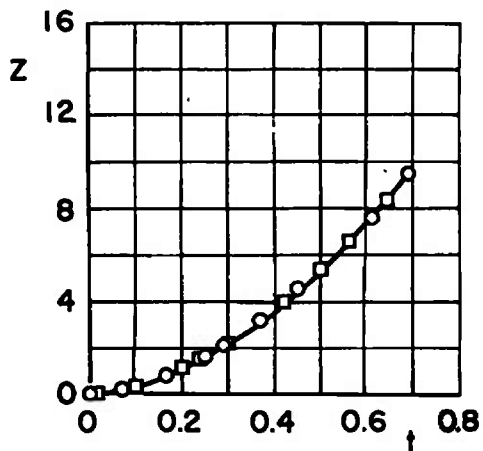
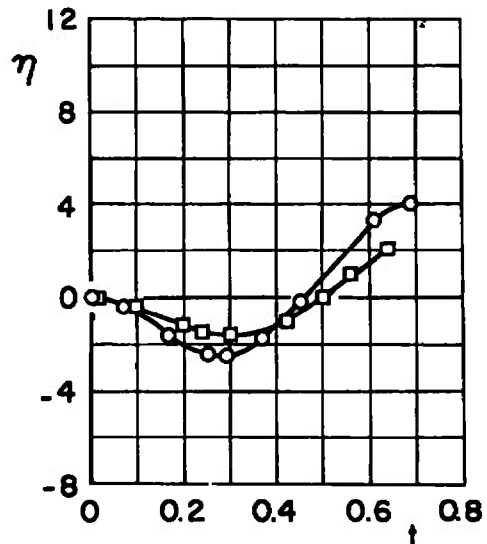
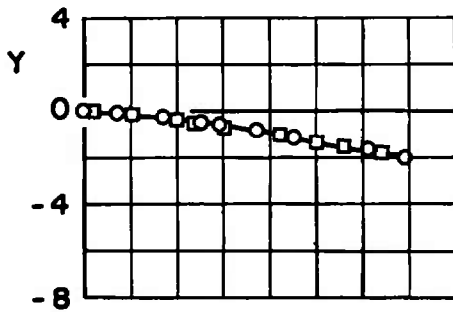
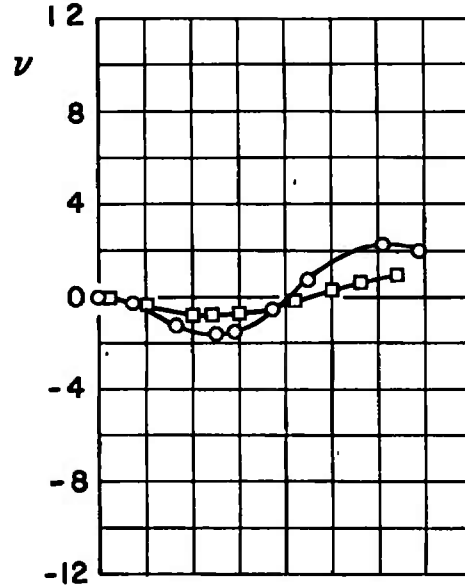
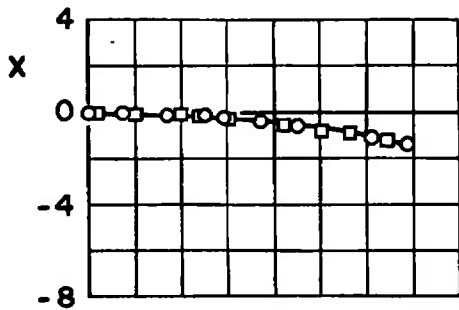
$I_{yy}$ 

○ 30  
 □ 50

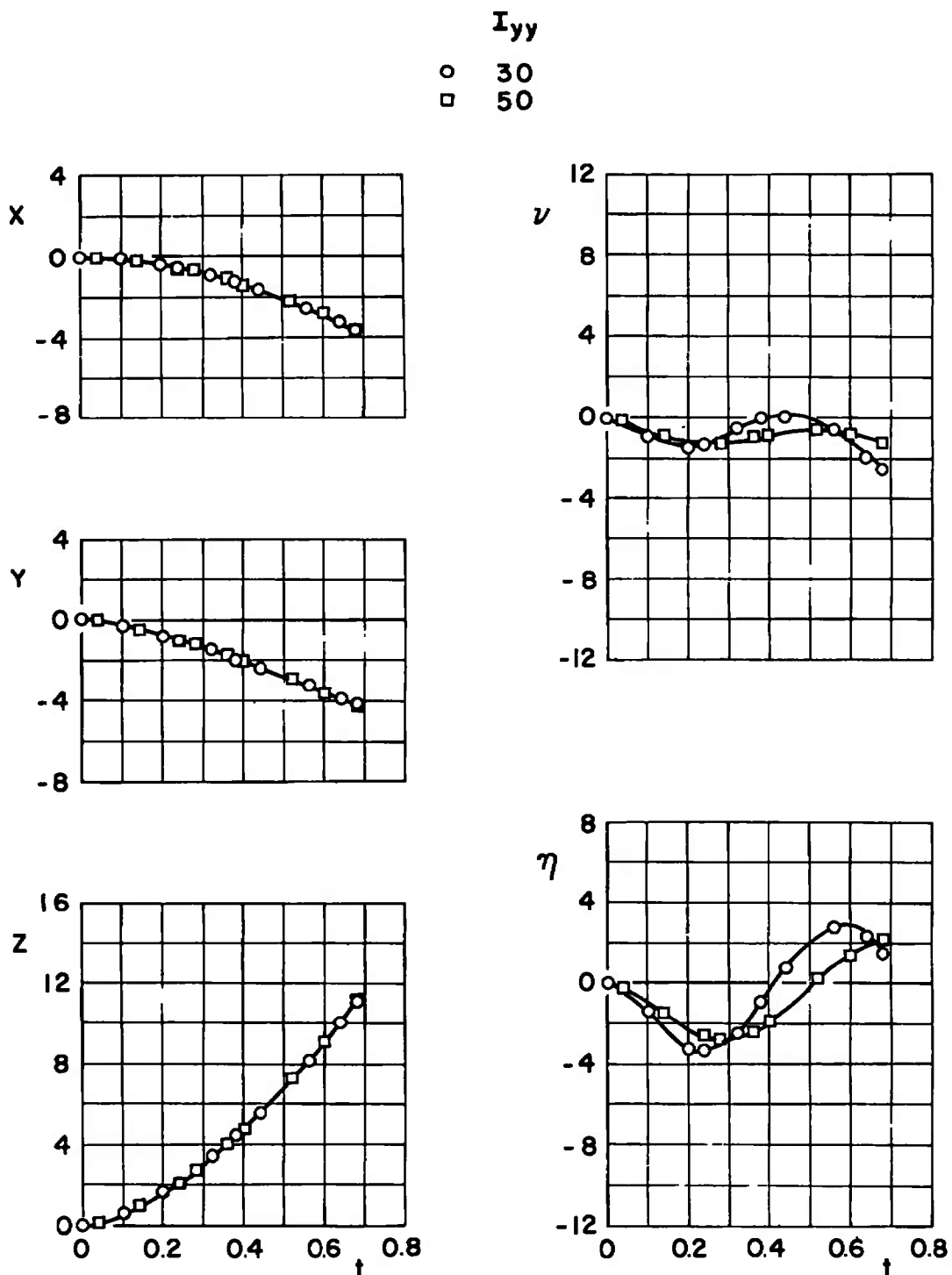


b.  $M_\infty = 0.50$ ,  $\bar{m} = 7.771$   
 Fig. 27 Continued

$I_{yy}$ 

○ 50  
□ 80


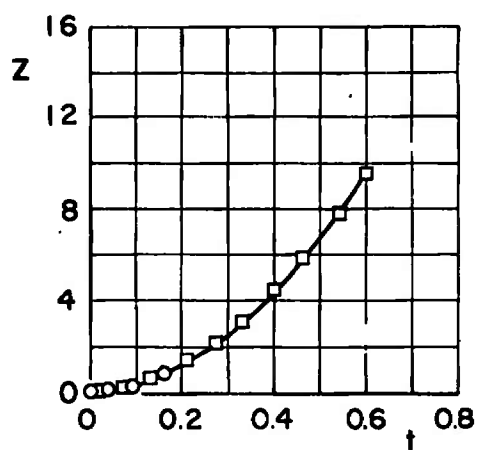
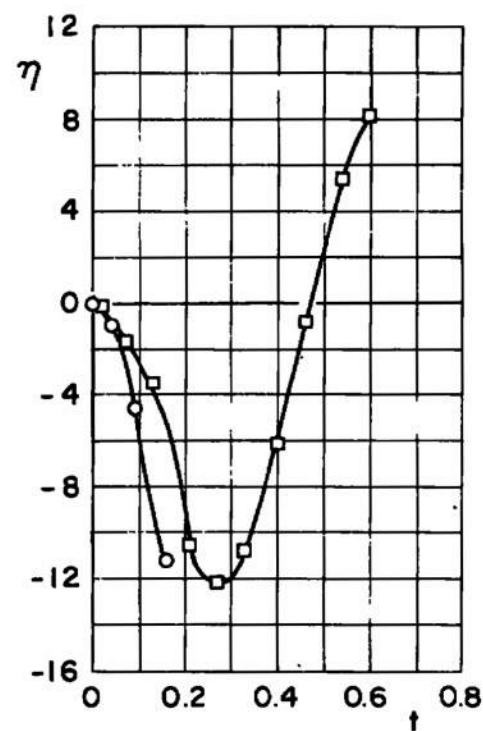
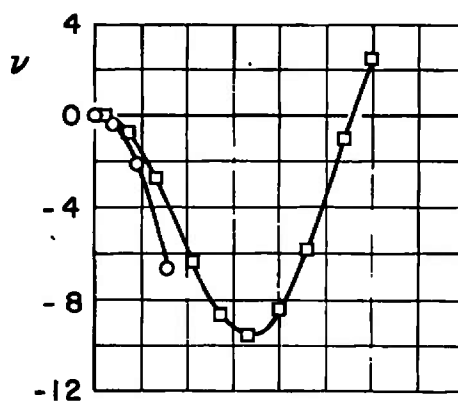
c.  $M_\infty = 0.70$ ,  $\bar{m} = 23.31$   
Fig. 27 Continued



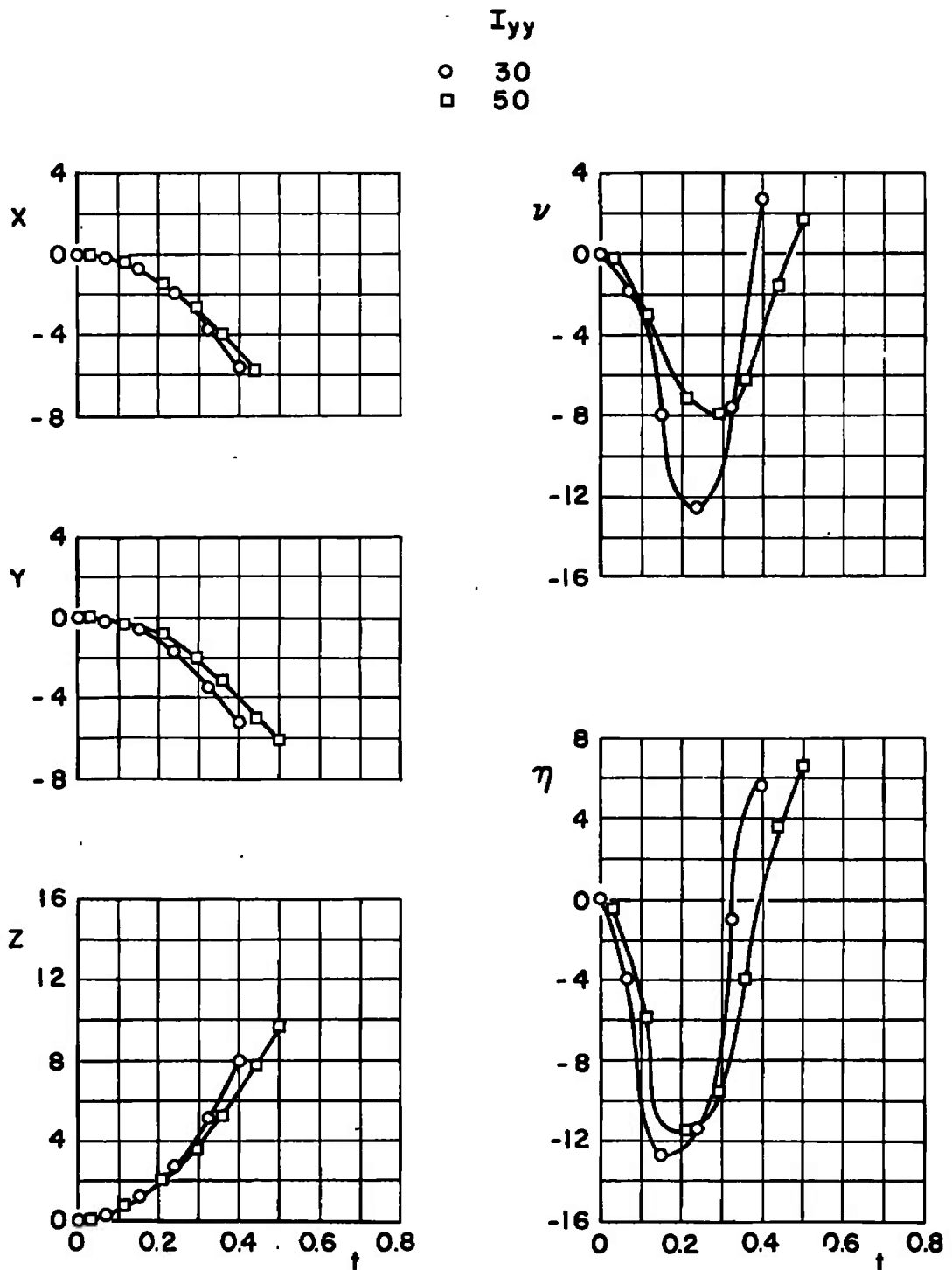
d.  $M_\infty = 0.70$ ,  $\bar{m} = 7.771$   
Fig. 27 Continued

$I_{yy}$ 

○ 50  
 □ 80



e.  $M_\infty = 0.90$ ,  $\bar{m} = 23.31$   
 Fig. 27 Continued



f.  $M_\infty = 0.90$ ,  $\bar{m} = 7.771$   
Fig. 27 Concluded

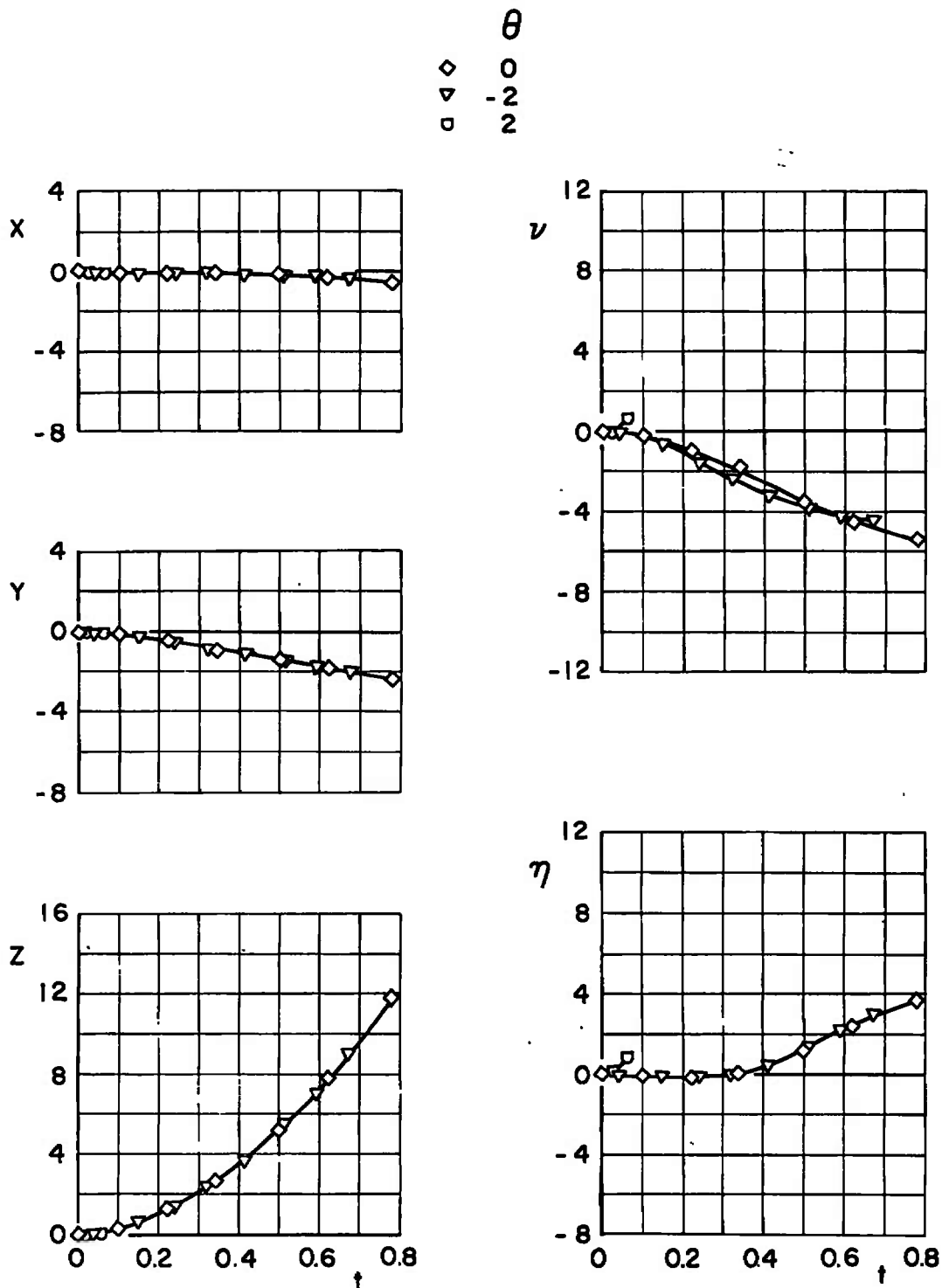
a.  $M_\infty = 0.50$ 

Fig. 28 Effect of Initial Store Attitude for Configuration IV;  $\bar{m} = 23.31$ ,  
 $X_{cg} = 2.74$ ,  $F_{Lz} = 1200$ ,  $I_{yy} = 50$ ,  $h = 20,000$



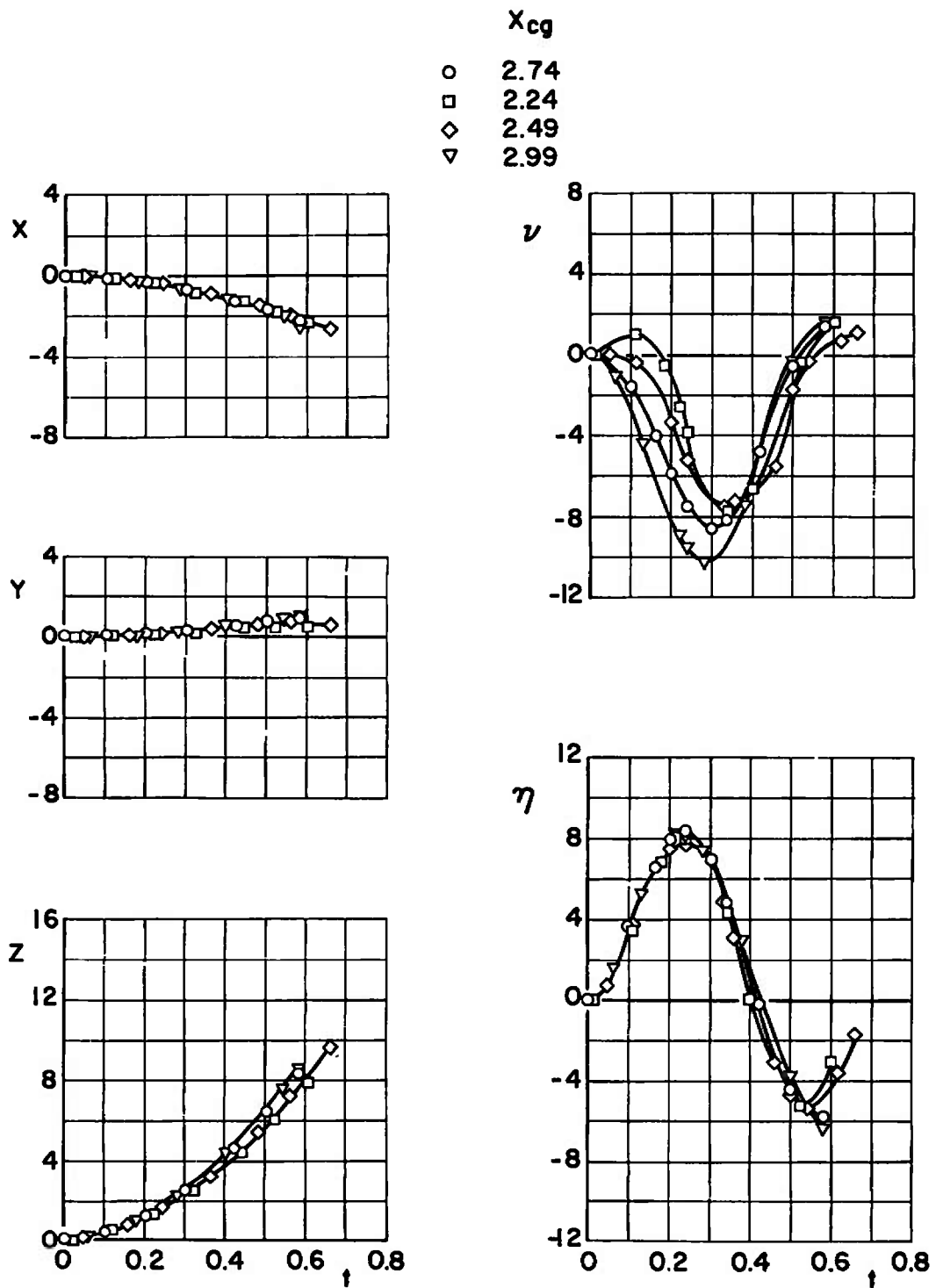


Fig. 29 Effect of Center-of-Gravity Variation for Configuration V;  $\bar{m} = 23.31$ ,  $F_{Lz} = 1200$ ,  $\theta = 0$ ,  $I_{yy} = 50$ ,  $M_\infty = 0.70$ ,  $h = 5000$

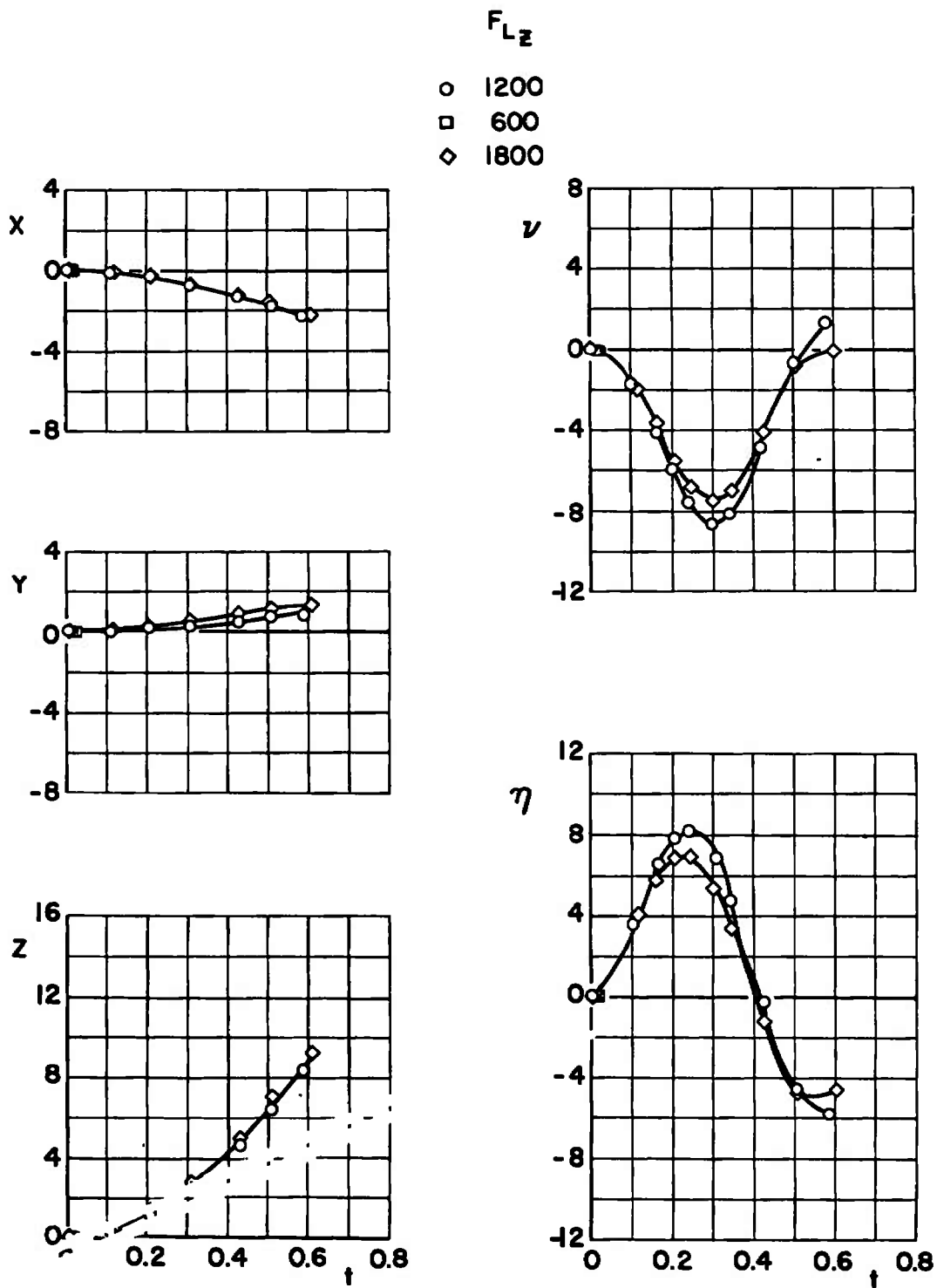
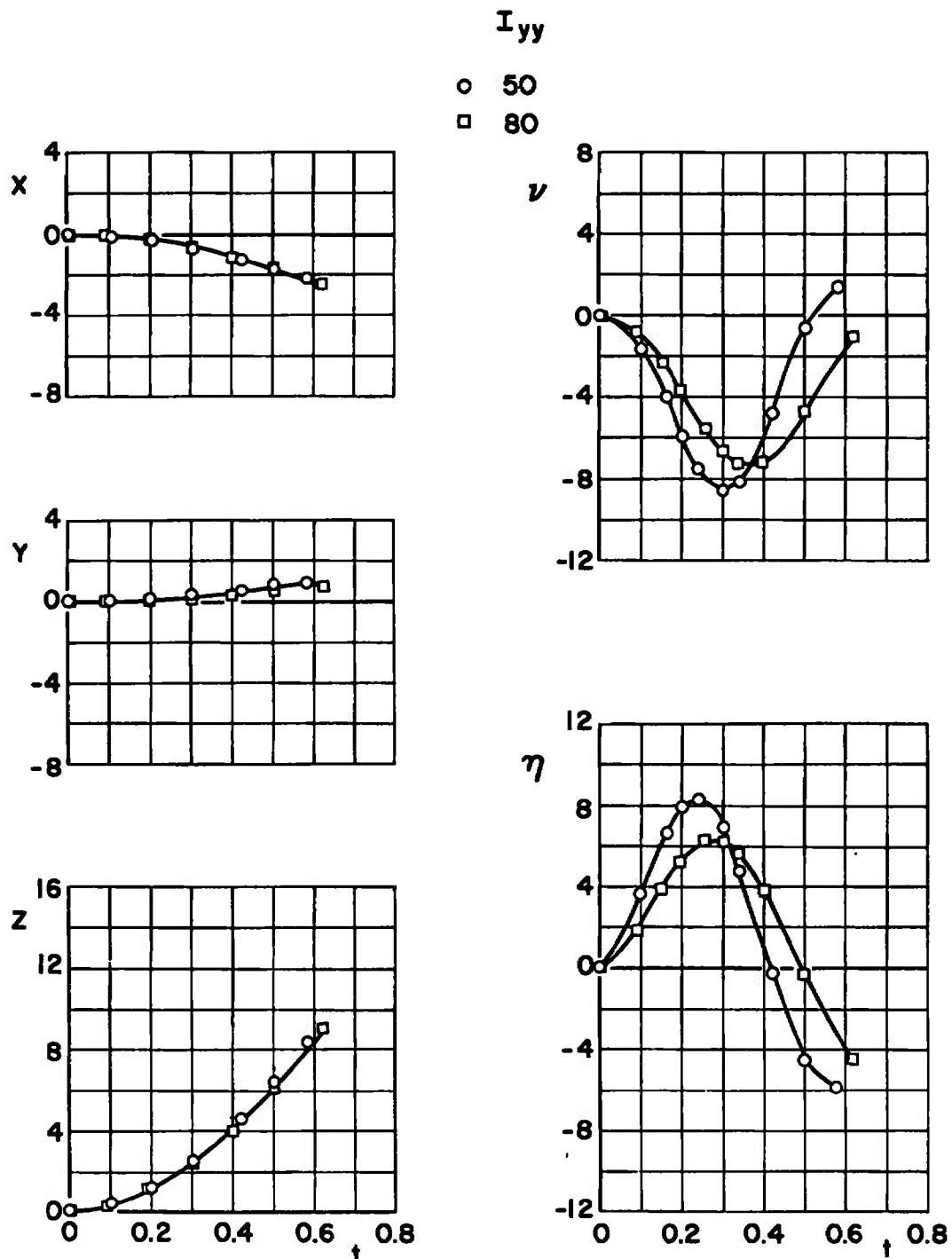
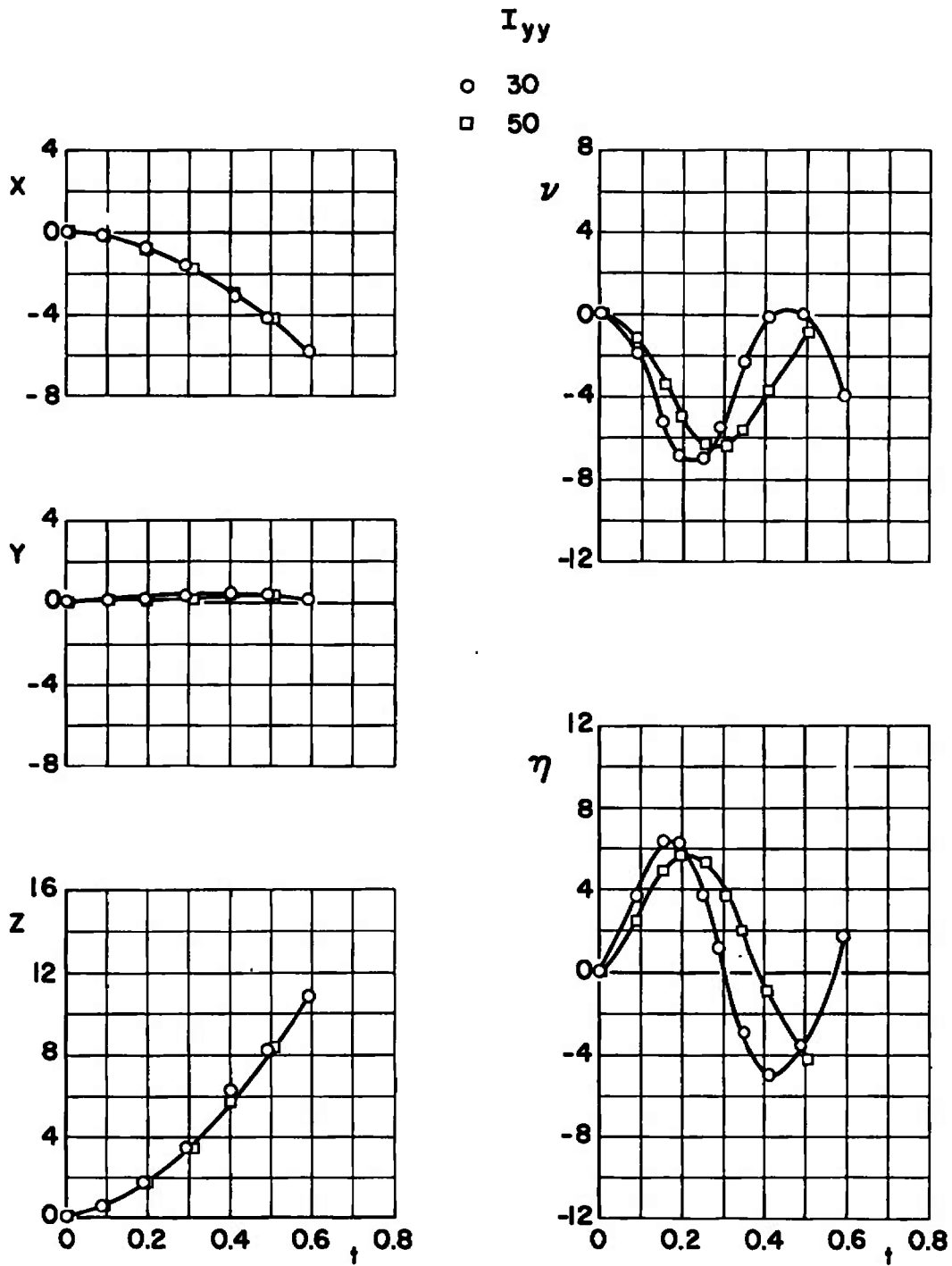


Fig. 30 Effect of Ejector-Force Variation for Configuration V;  $\bar{m} = 23.31$ ,  
 $X_{cg} = 2.74$ ,  $\theta = 0$ ,  $I_{yy} = 50$ ,  $M_\infty = 0.70$ ,  $h = 5000$



a.  $M_\infty = 0.70$ ,  $\bar{m} = 23.31$

Fig. 31 Effect of Moment-of-Inertia Variation for Configuration V;  
 $X_{cg} = 2.74$ ,  $F_{Lz} = 1200$ ,  $\theta = 0$ ,  $h = 5000$



b.  $M_\infty = 0.70$ ,  $\bar{m} = 7.771$   
Fig. 31 Concluded

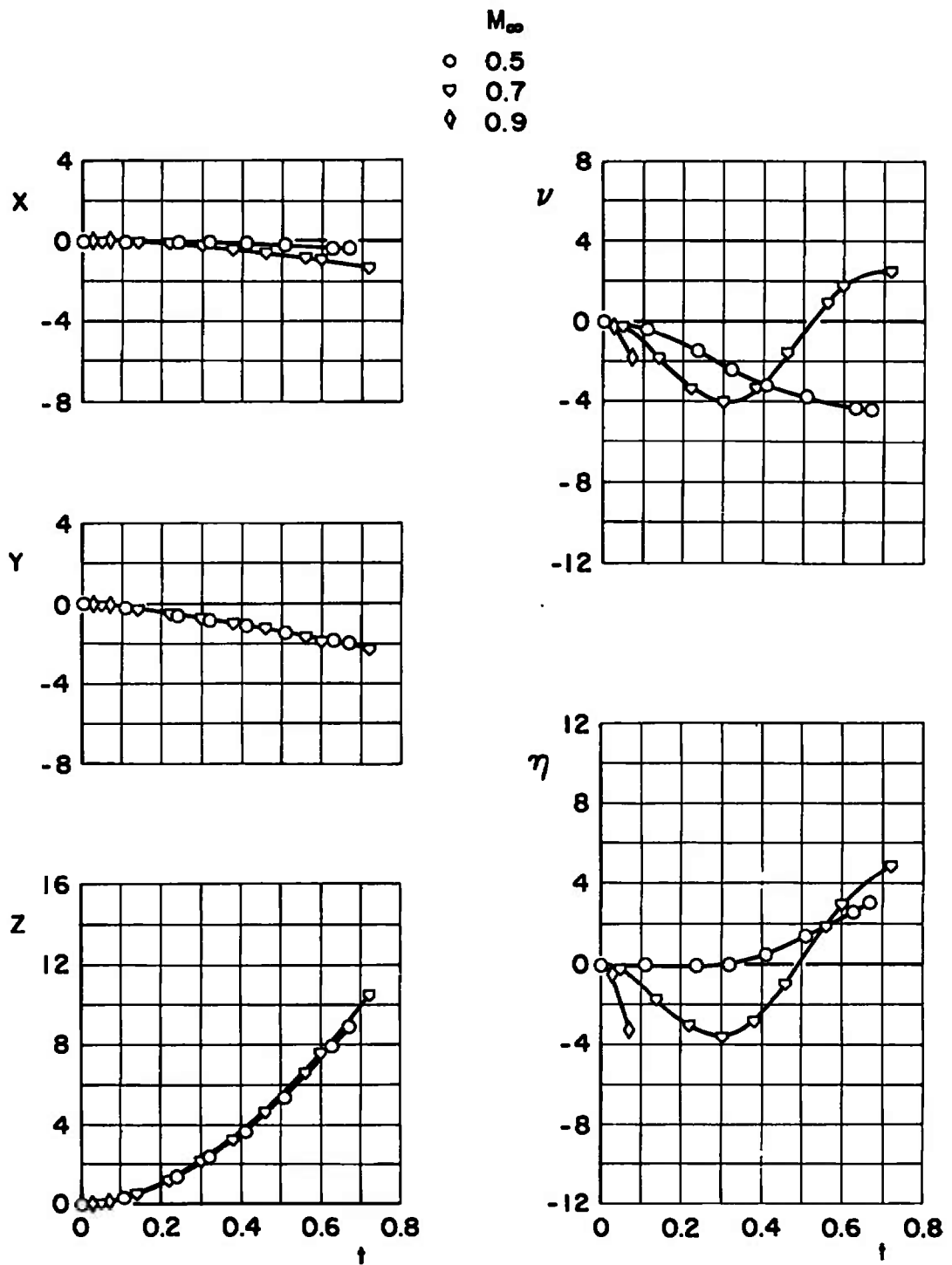
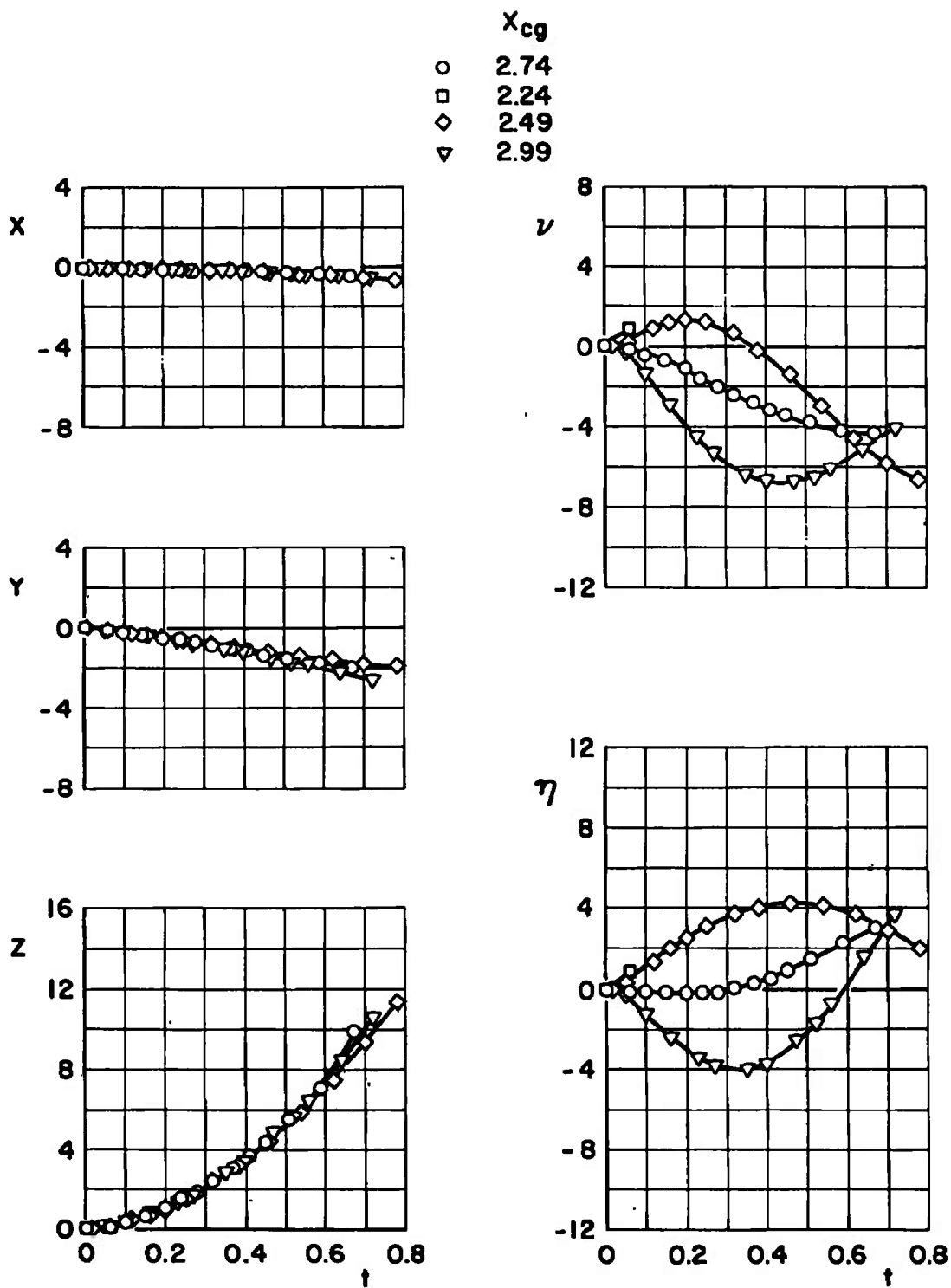
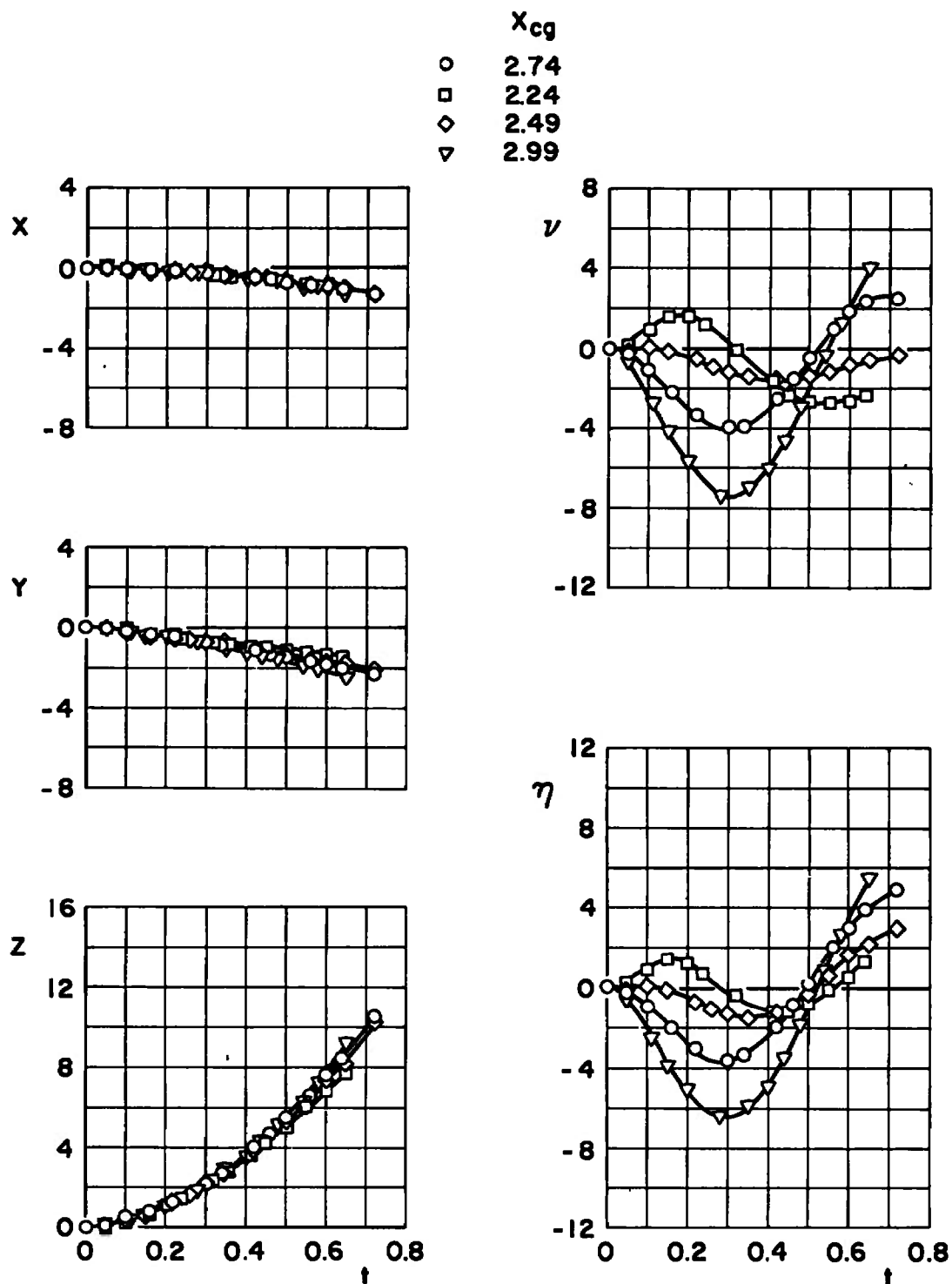


Fig. 32 Effect of Mach Number Variation for Configuration VI;  $\bar{m} = 23.31$ ,  
 $X_{cg} = 2.74$ ,  $F_{LZ} = 1200$ ,  $\theta = 0$ ,  $I_{yy} = 50$ ,  $h = 20,000$

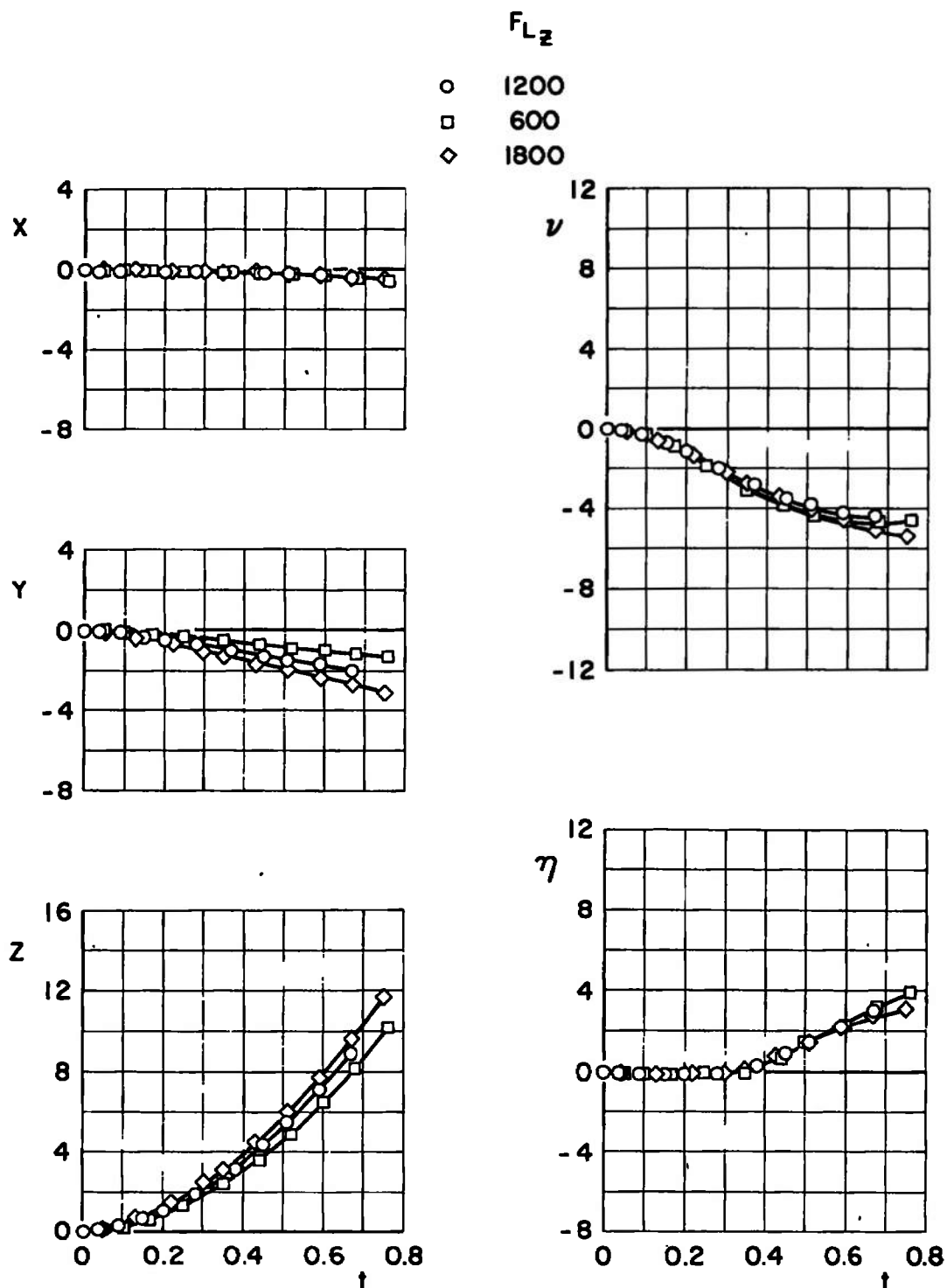


a.  $M_\infty = 0.50$

Fig. 33 Effect of Center-of-Gravity Variation for Configuration VI;  $\bar{m} = 23.31$ ,  $X_{cg} = 2.74$ ,  $F_{LZ} = 1200$ ,  $\theta = 0$ ,  $I_{yy} = 50$ ,  $h = 20,000$



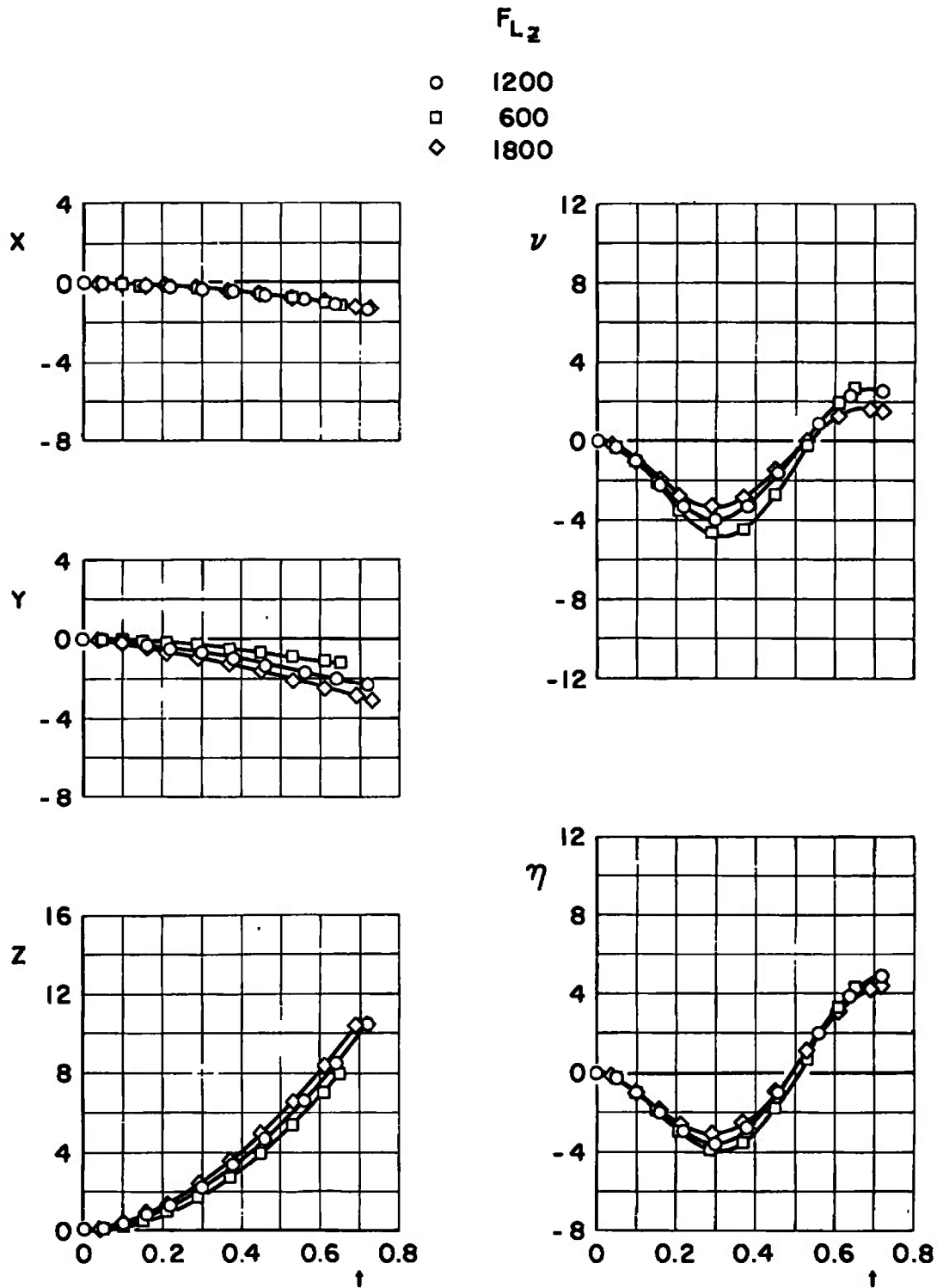
b.  $M_\infty = 0.70$   
 Fig. 33 Concluded



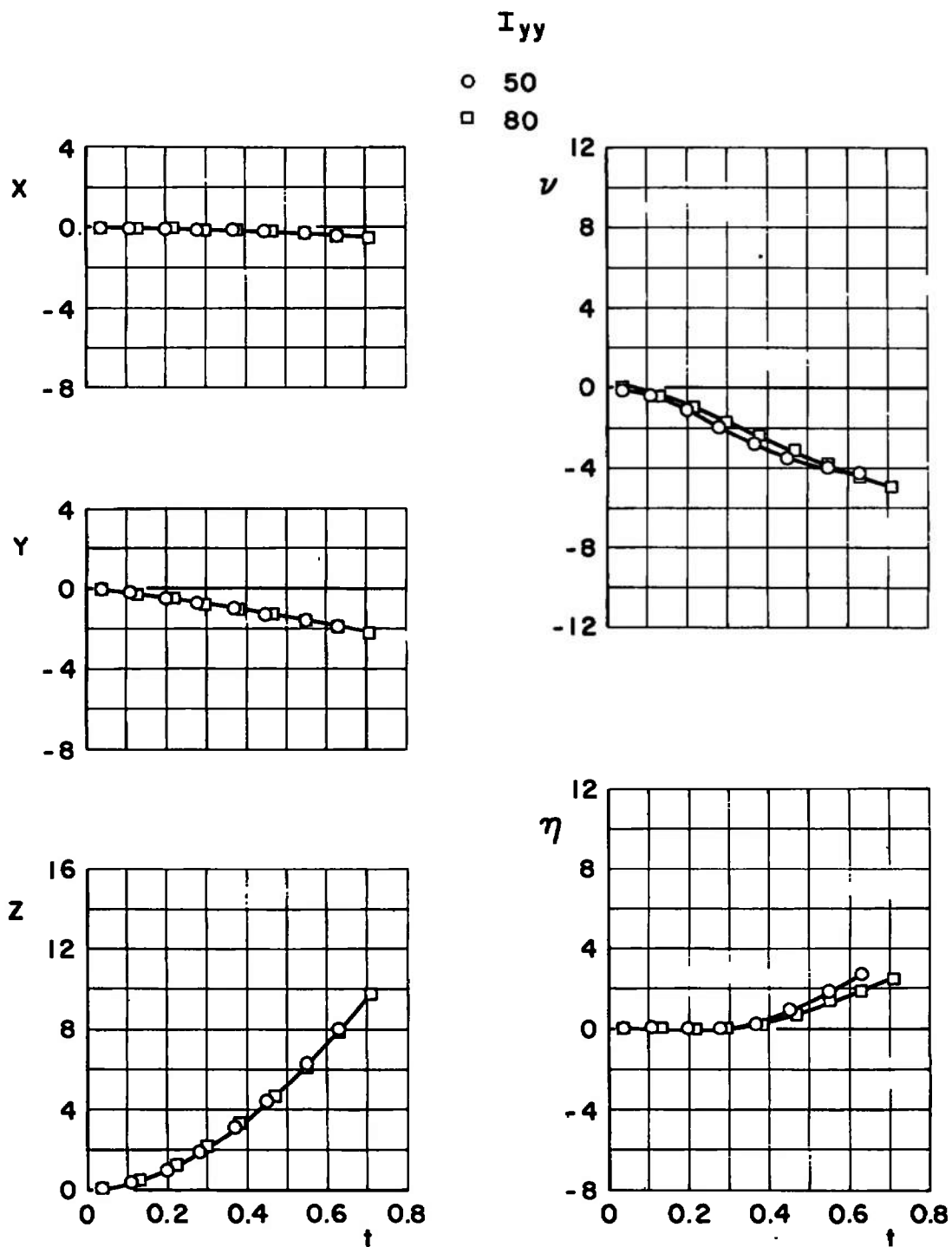
a.  $M_\infty = 0.50$

Fig. 34 Effect of Ejector-Force Variation for Configuration VI;  $\bar{m} = 23.31$ ,  
 $X_{cg} = 2.74$ ,  $\theta = 0$ ,  $I_{yy} = 50$ ,  $h = 20,000$



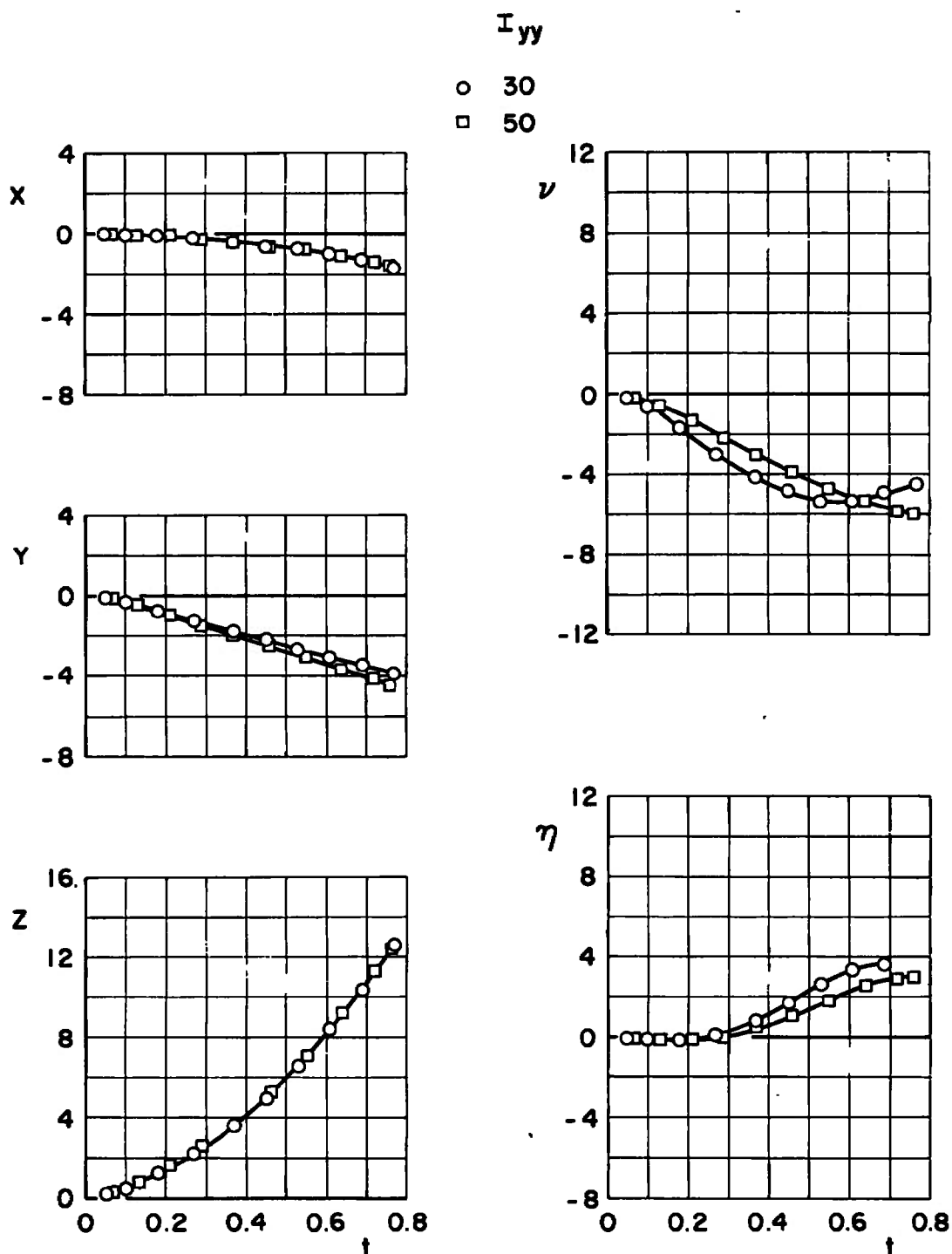


b.  $M_\infty = 0.70$   
Fig. 34 Concluded

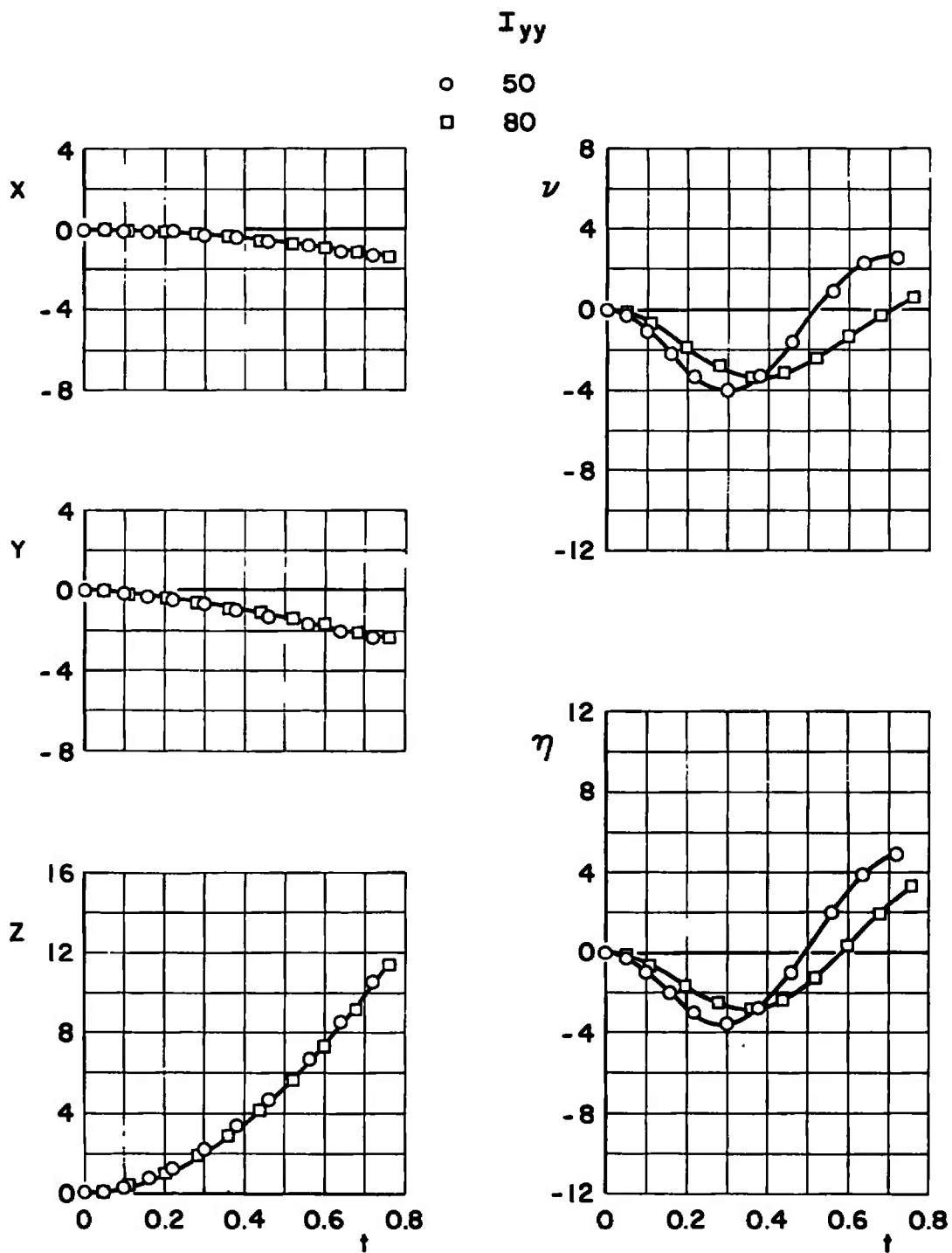


a.  $M_\infty = 0.50$ ,  $\bar{m} = 23.31$

Fig. 35 Effect of Moment-of-Inertia Variation for Configuration VI;  
 $X_{cg} = 2.74$ ,  $F_{Lz} = 1200$ ,  $\theta = 0$ ,  $h = 20,000$



b.  $M_\infty = 0.50$ ,  $\bar{m} = 7.771$   
Fig. 35 Continued



c.  $M_\infty = 0.70$ ,  $\bar{m} = 23.31$   
Fig. 35 Continued

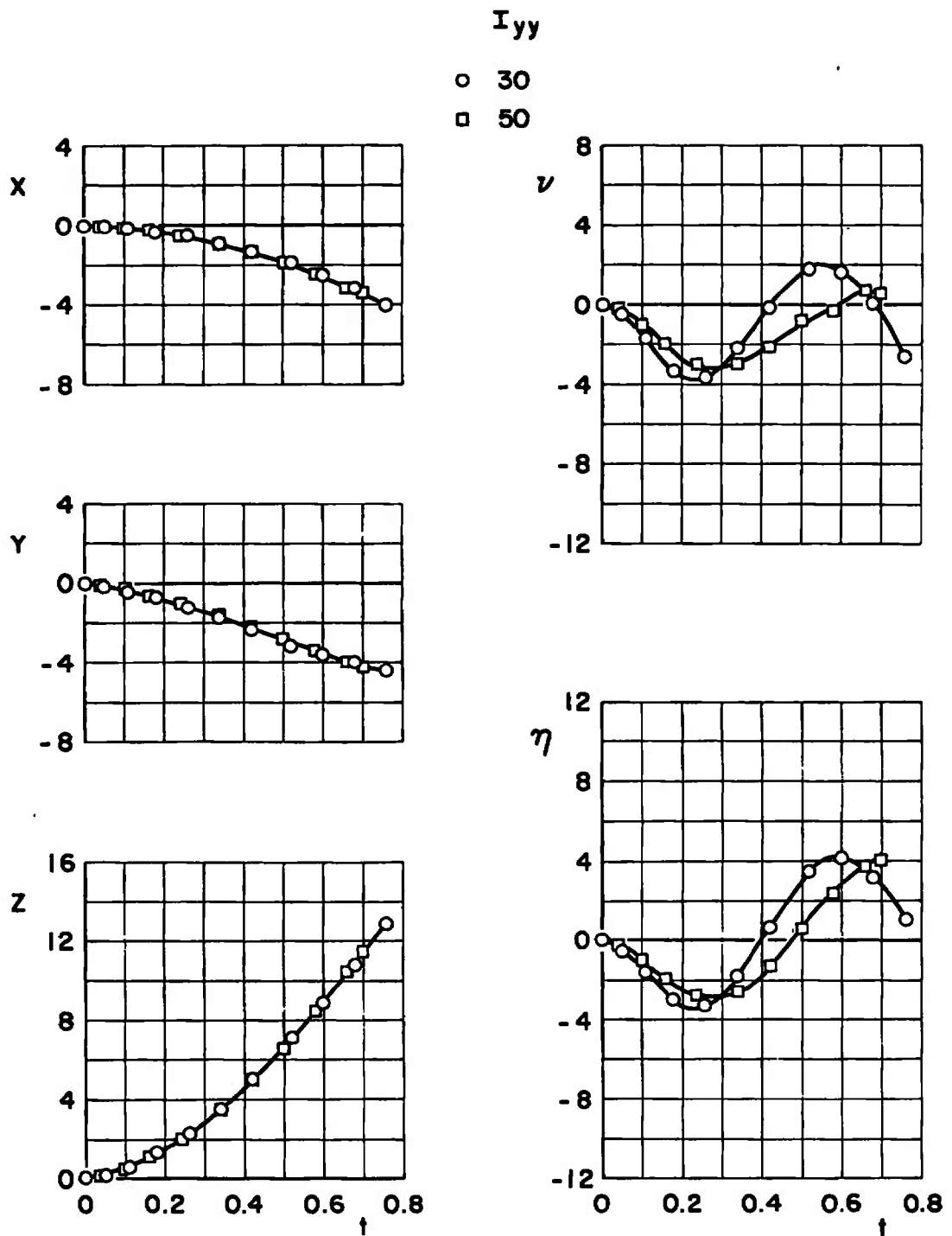
d.  $M_\infty = 0.70$ ,  $\bar{m} = 7.771$ 

Fig. 35 Concluded

	$\theta$
$\diamond$	0
$\nabla$	-2
$\square$	2

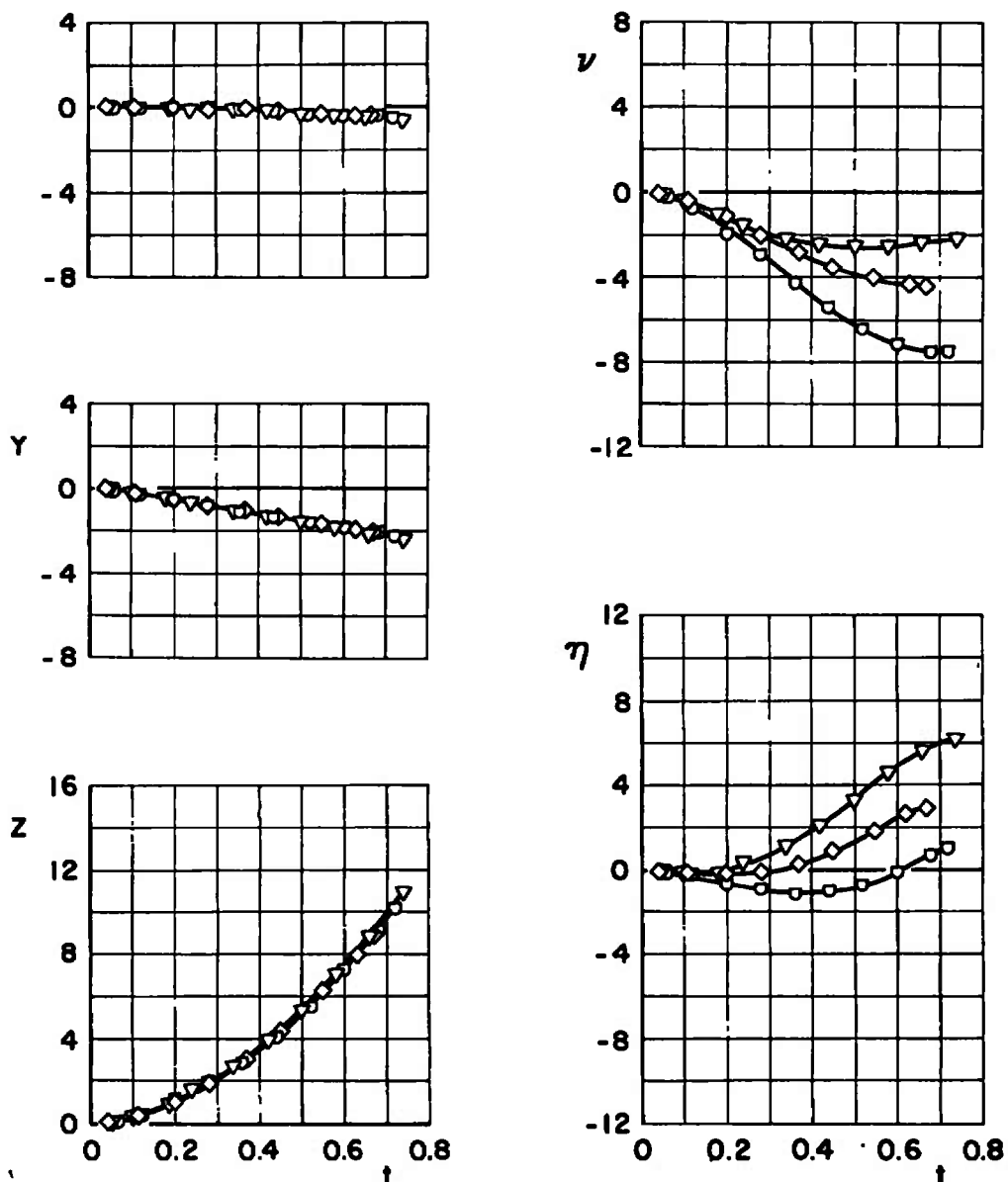
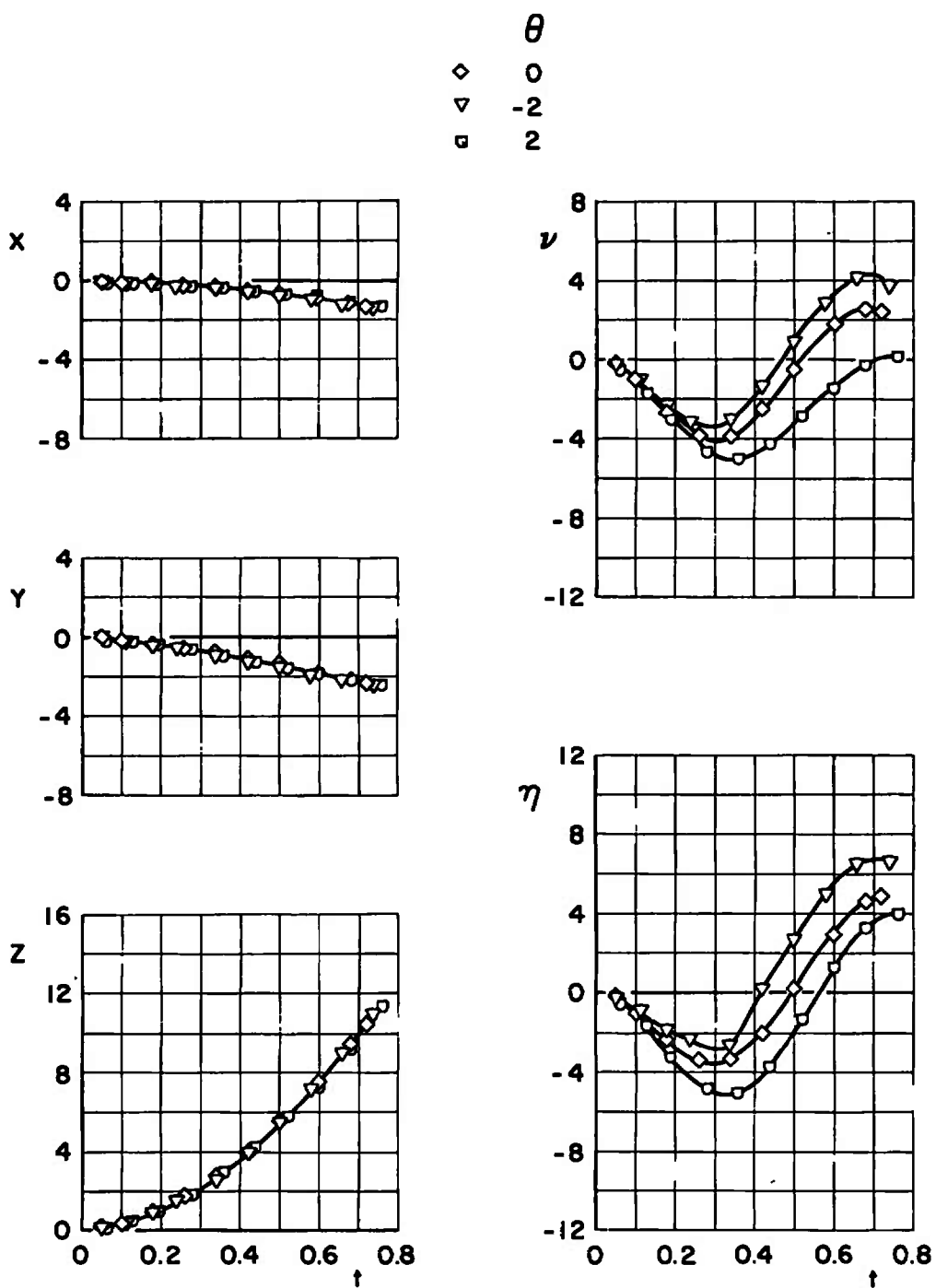
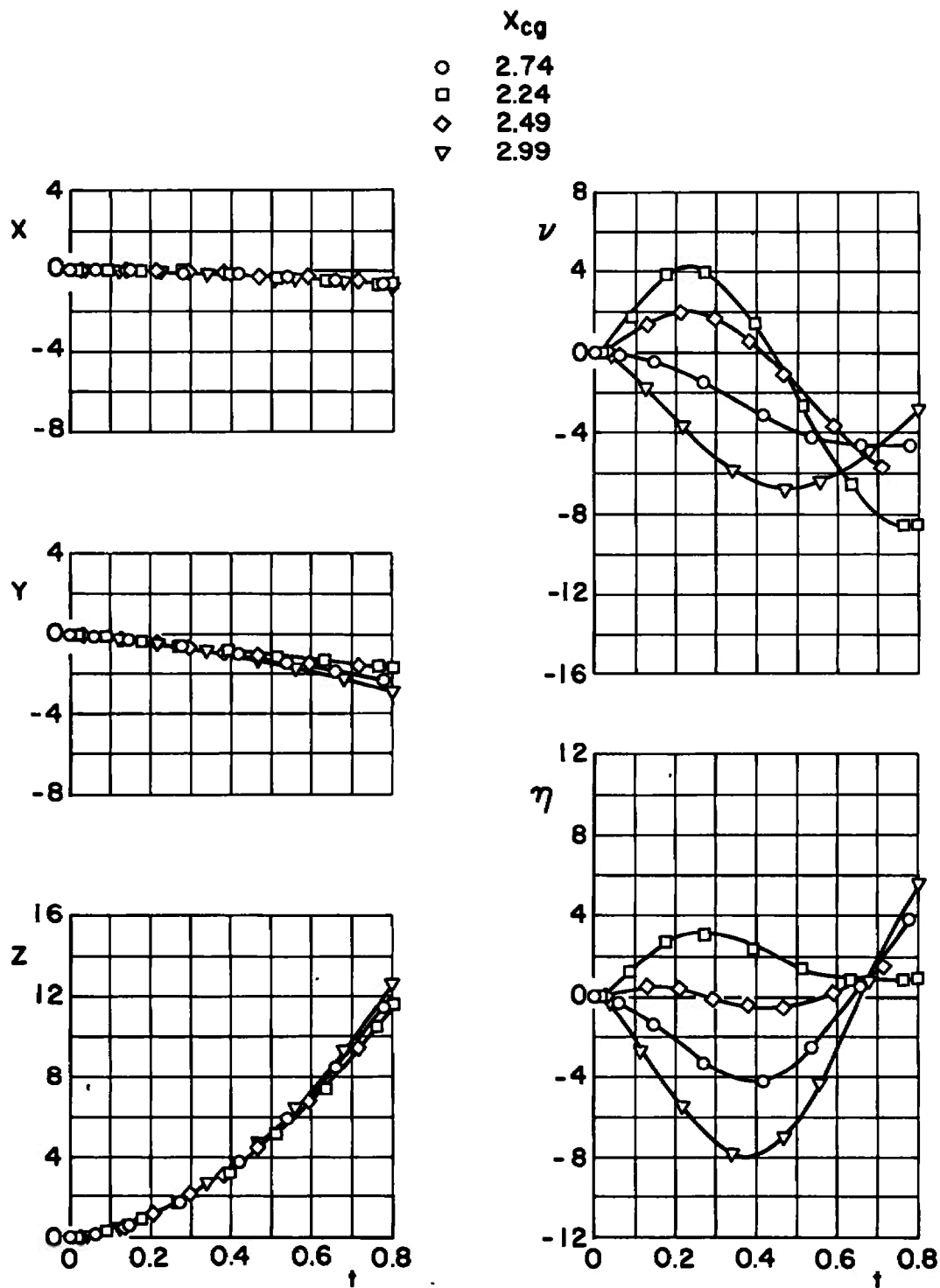
a.  $M_\infty = 0.50$ 

Fig. 36 Effect of Initial Store Attitude for Configuration VI;  $\bar{m} = 23.31$ ,  
 $X_{cg} = 2.74$ ,  $F_{LZ} = 1200$ ,  $I_{yy} = 50$ ,  $h = 20,000$



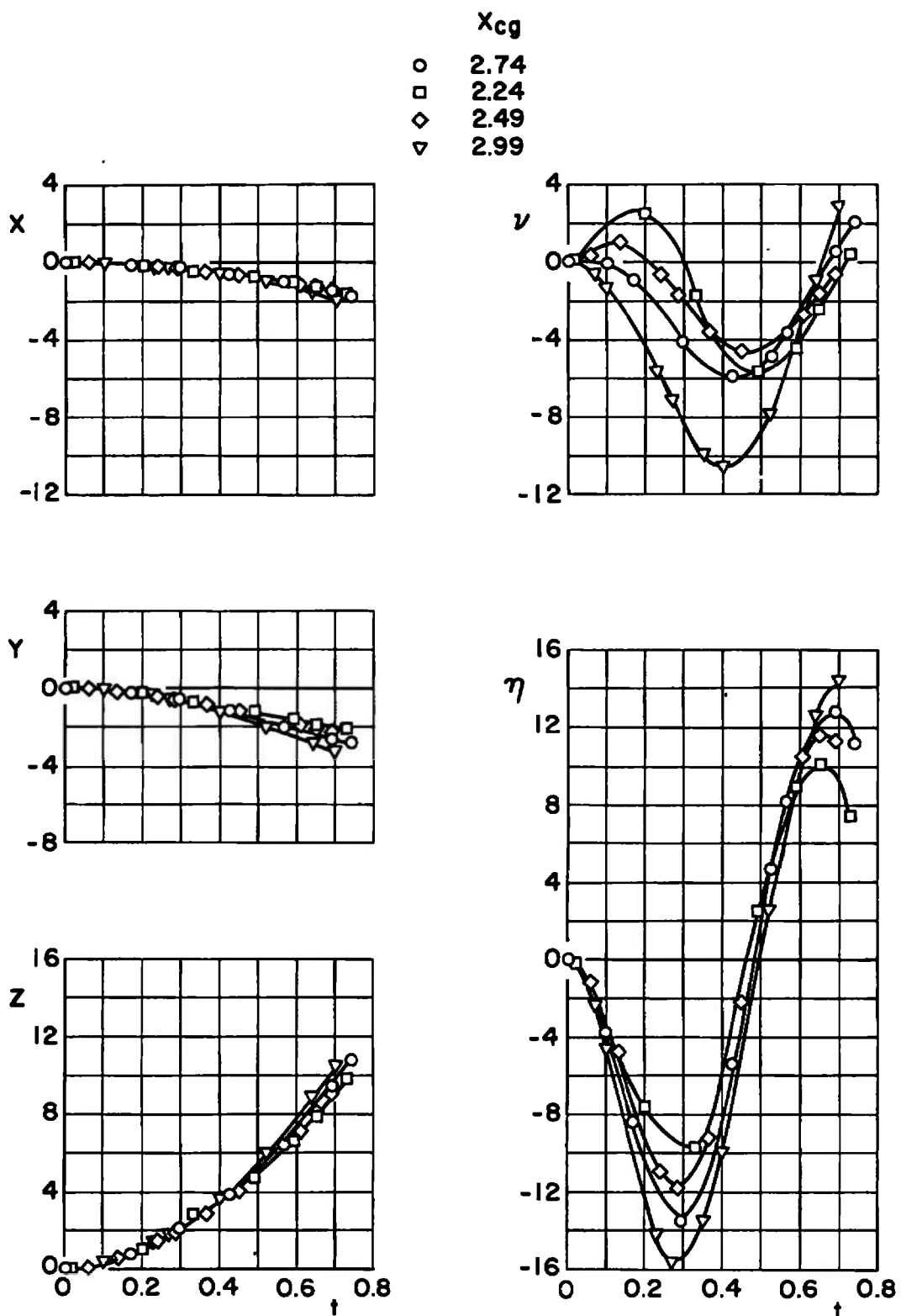
b.  $M_\infty = 0.70$   
Fig. 36 Concluded



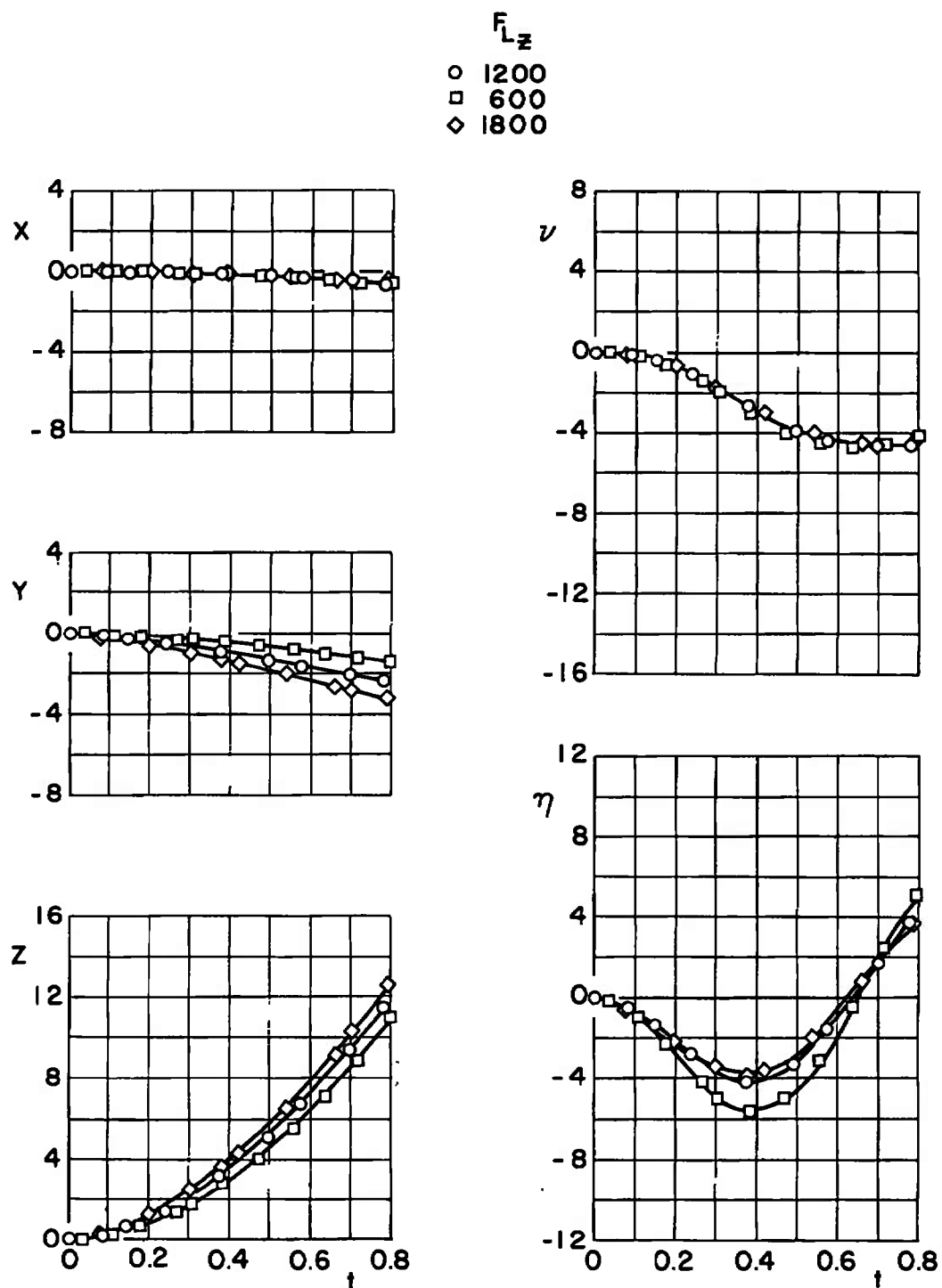
a.  $M_\infty = 0.50$

Fig. 37 Effect of Center-of-Gravity Variation for Configuration VII;  
 $\bar{m} = 23.31$ ,  $F_{Lz} = 1200$ ,  $\theta = 0$ ,  $I_{yy} = 50$ ,  $h = 20,000$





b.  $M_\infty = 0.70$   
 Fig. 37 Concluded

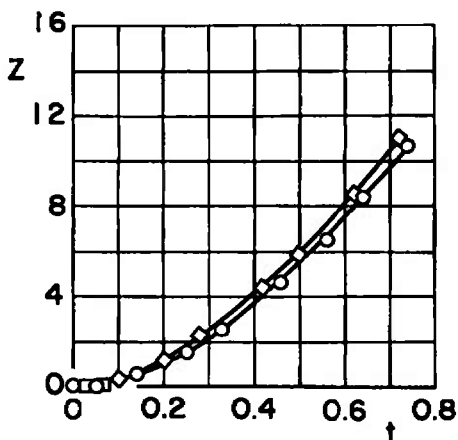
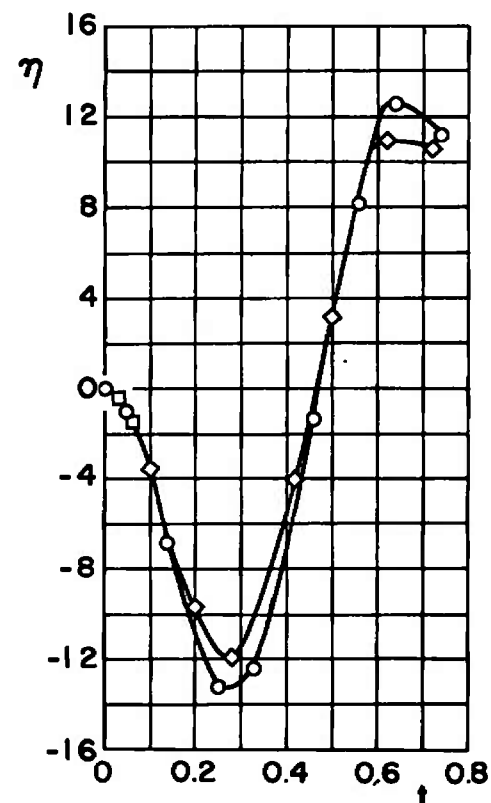
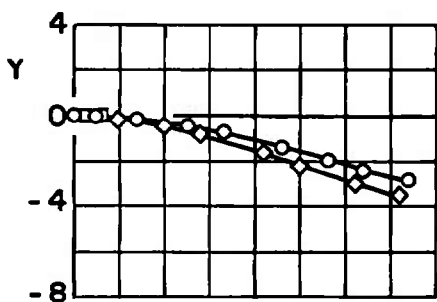
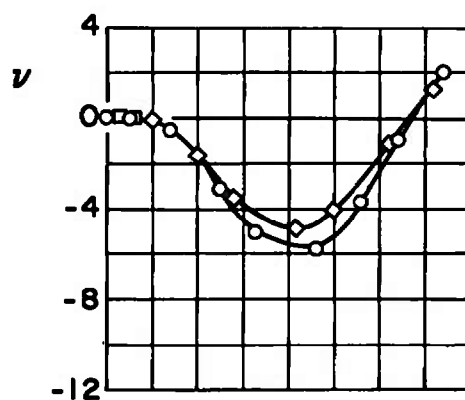
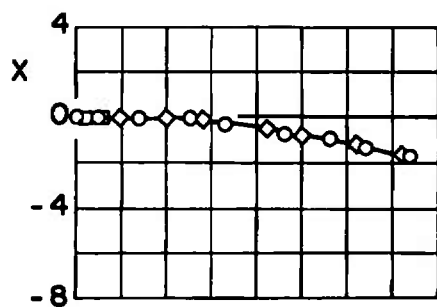


a.  $M_\infty = 0.50$

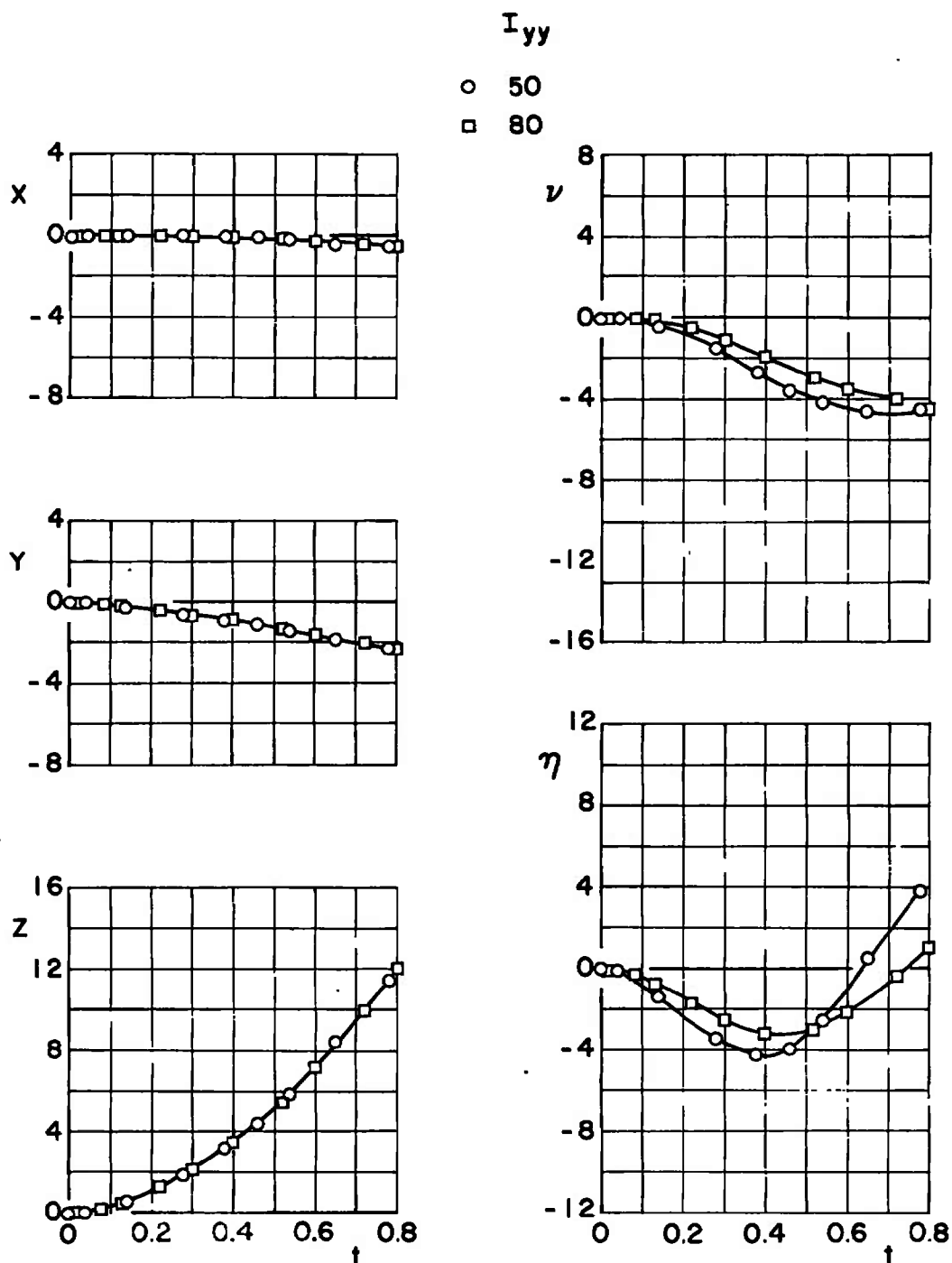
Fig. 38 Effect of Ejector-Force Variation for Configuration VII;  $\bar{m} = 23.31$ ,  $X_{cg} = 2.74$ ,  $\theta = 0$ ,  $I_{yy} = 50$ ,  $h = 20,000$

$F_{Lz}$ 

○ 1200  
 □ 600  
 ◇ 1800

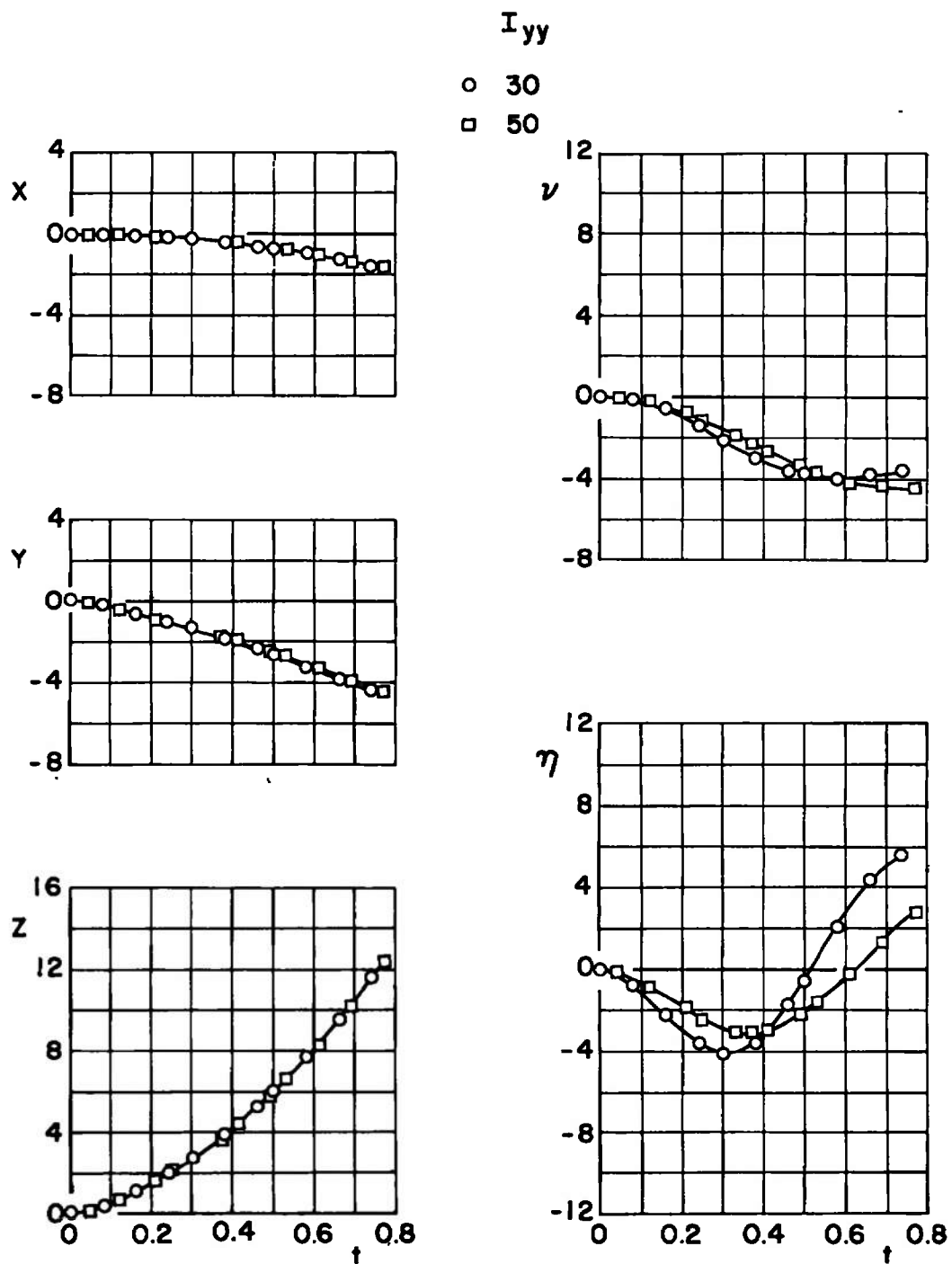


b.  $M_\infty = 0.70$   
 Fig. 38 Concluded

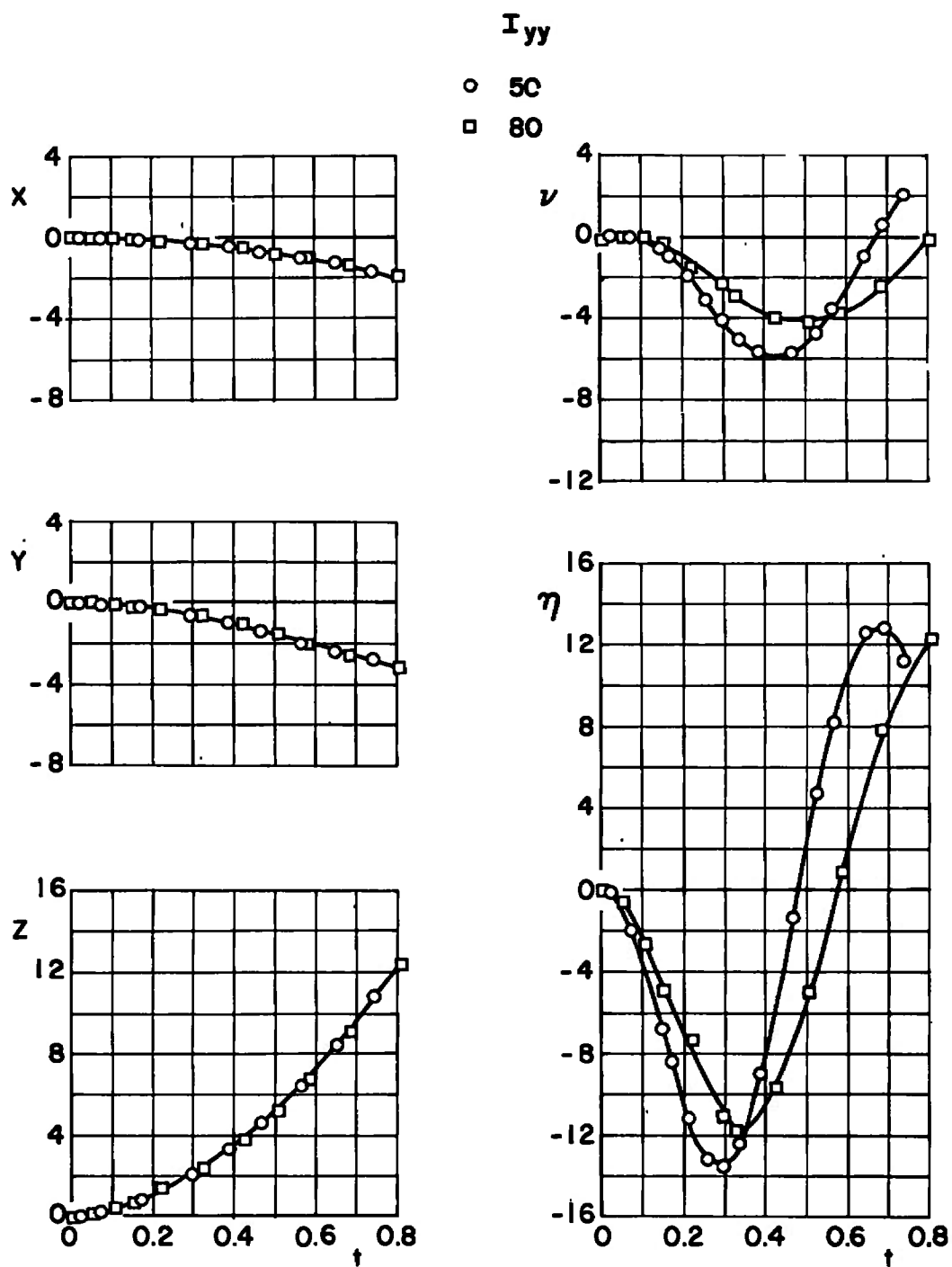


a.  $M_\infty = 0.50$ ,  $\bar{m} = 23.31$

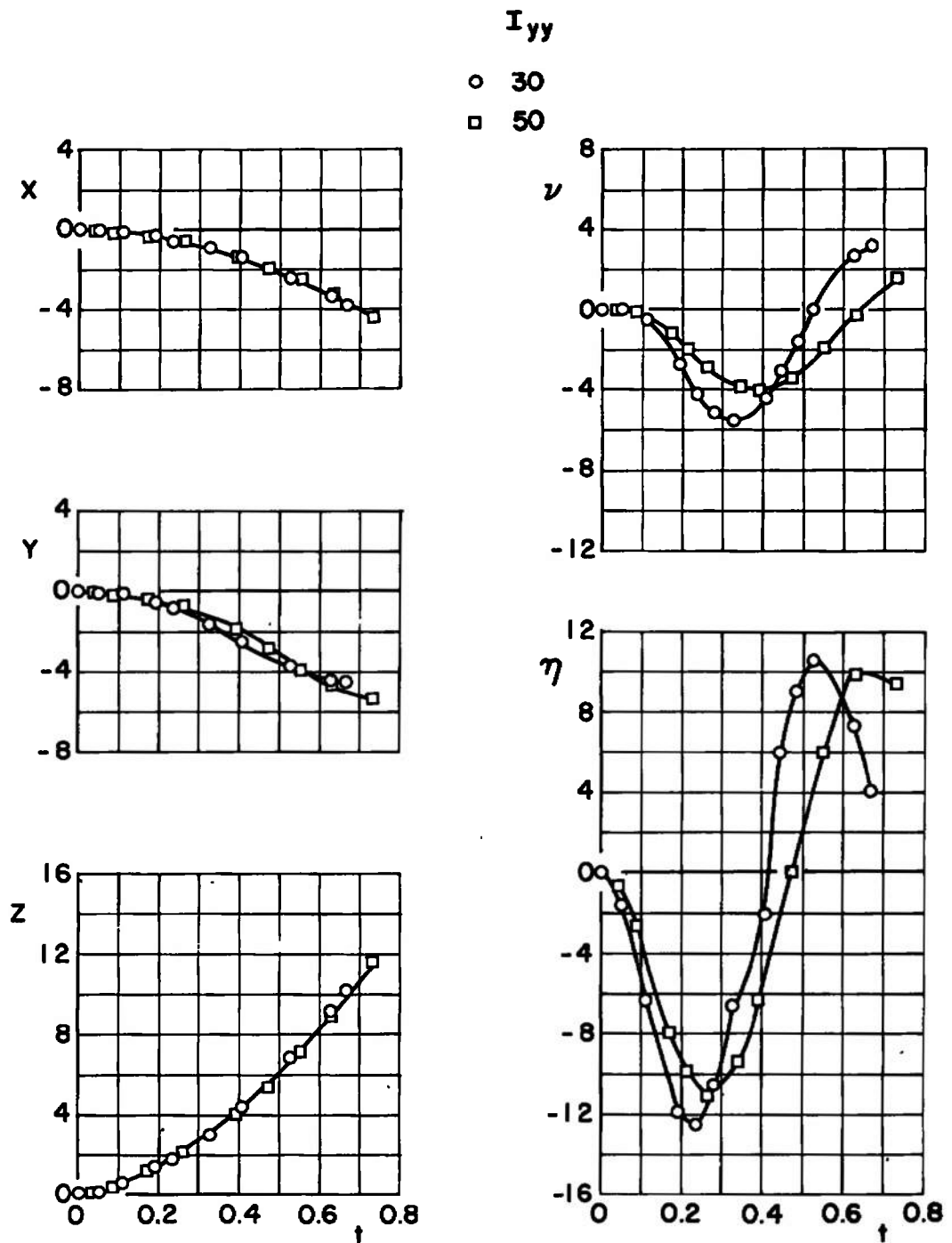
Fig. 39 Effect of Moment-of-Inertia Variation for Configuration VII;  
 $X_{cg} = 2.74$ ,  $F_{LZ} = 1200$ ,  $\theta = 0$ ,  $h = 20,000$



b.  $M_\infty = 0.50$ ,  $\bar{m} = 7.771$   
Fig. 39 Continued



c.  $M_\infty = 0.70$ ,  $\bar{m} = 23.31$   
Fig. 39 Continued



d.  $M_\infty = 0.70$ ,  $\bar{m} = 7.771$

Fig. 39 Concluded

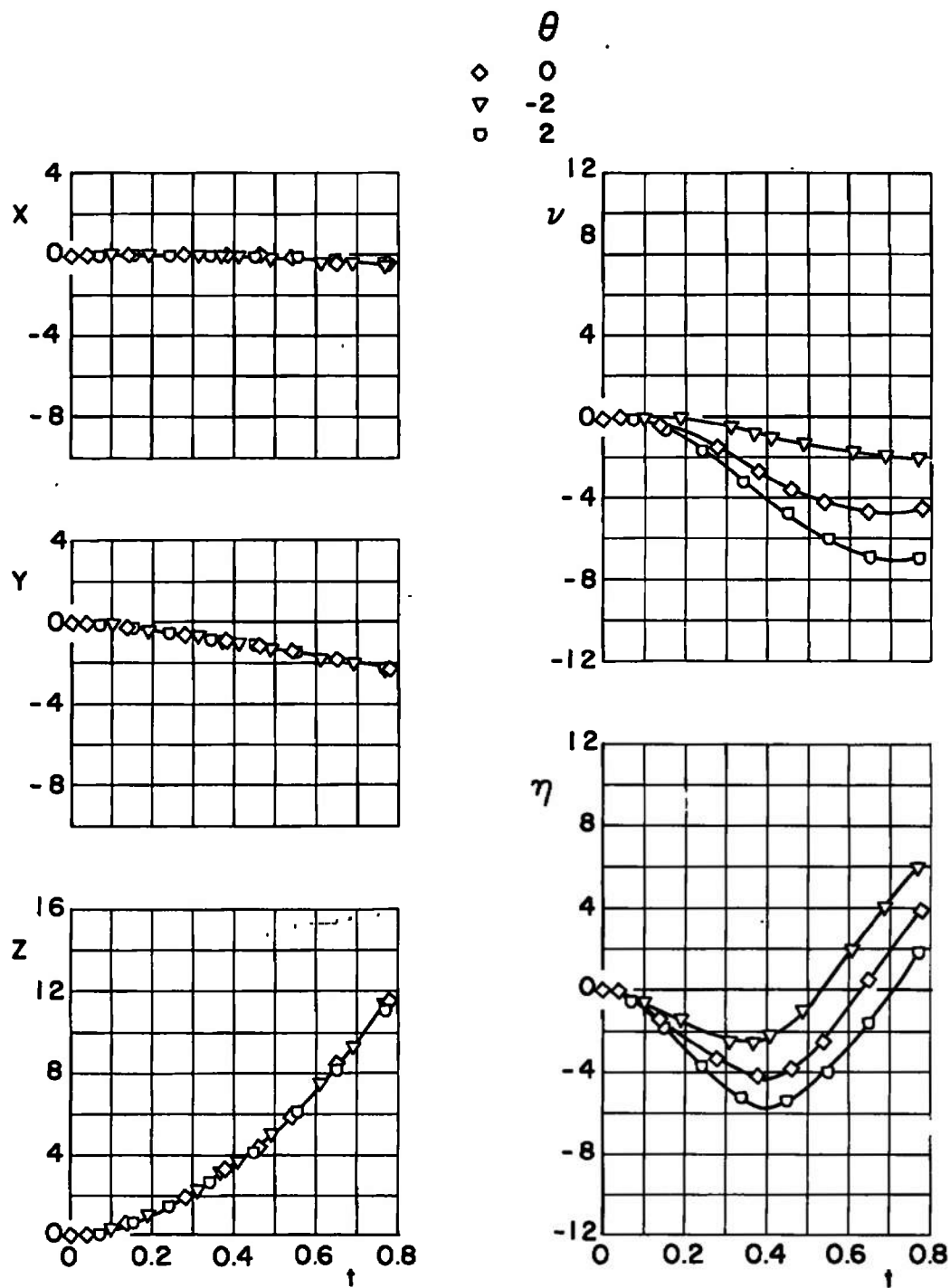
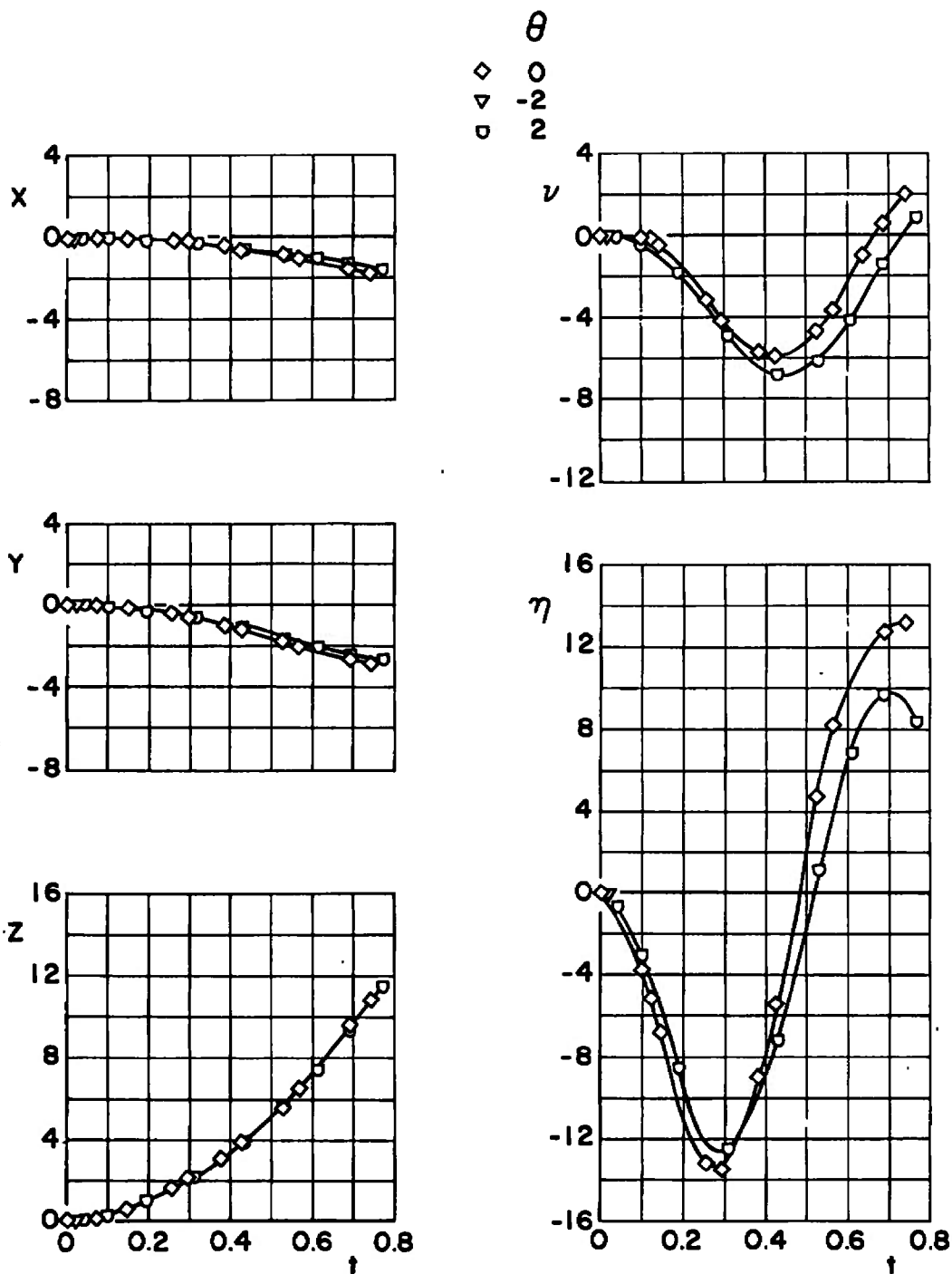
a.  $M_\infty = 0.50$ 

Fig. 40 Effect of Initial Store Attitude for Configuration VII;  $\bar{m} = 23.31$ ,  
 $X_{eq} = 2.74$ ,  $F_{LZ} = 1200$ ,  $I_{yy} = 50$ ,  $h = 20,000$





b.  $M_\infty = 0.70$   
 Fig. 40 Concluded

**TABLE I**  
**TEST CONSTANTS**

<u>Quantity</u>	<u>Dimensions, Full Scale</u>
Store roll moment of inertia, $I_{xx}$	40 slug-ft <sup>2</sup>
Store product of inertia, $I_{xz}$	0.0
Store lateral reference length, $b$	1.333 ft
Store longitudinal reference length, $\bar{c}$	7.325 ft
Store reference area, $S$	1.395 ft <sup>2</sup>
Model scale, $\lambda$	0.05
Ejector stroke length	0.2552 ft
Yaw-damping coefficient, $C_{n_r}$	-70/radian
Pitch-damping coefficient, $C_{m_q}$	-2.319/radian

	$M_\infty$	$\bar{m}$	$\theta$	$\alpha_p$	$I_{yy}/I_{zz}$	$FL_Z$	$X_{cg}$
250-lb M-117	0.5	7.771	0	3.0	30, 50	1000	2.74
	0.7	↓	↓	1.4	↓	↓	↓
	0.9			0.1			
	1.1			0.0			
	1.3			0.1			
750-lb M-117	0.5	23.31	0	3.0	50, 80**	600*, 1200, 1800*	2.24, 2.49, 2.74, 2.99
		↓	-2	↓	50	1200	2.74
			+2	↓	50	1200	2.74
	0.7		0	1.4	50, 80**	600*, 1200, 1800*	2.24, 2.49, 2.74, 2.99
			-2	↓	50	1200	2.74
			+2	↓	50	1200	2.74
	0.9		0	0.1	50, 80**	600*, 1200, 1800*	2.24, 2.49, 2.74, 2.99
			-2	↓	50	1200	2.74
			+2	↓	50	1200	2.74
	1.1		0	0.0	50, 80**	600*, 1200, 1800*	2.24, 2.49, 2.74, 2.99
			-2	↓	50	1200	2.74
			+2	↓	50	1200	2.74
	1.3		0	0.1	50, 80**	600*, 1200, 1800*	2.23, 2.49, 2.74, 2.99
			-2	↓	50	1200	2.74
			+2	↓	50	1200	2.74

**\*\*Run only with cg location of 2.74 and ejector force of 1200 lb**

UNCLASSIFIED

Security Classification

## DOCUMENT CONTROL DATA - R &amp; D

(Security classification of title, body of abstract and indexing annotation must be entered when the overall report is classified)

## 1. ORIGINATING ACTIVITY (Corporate author)

Arnold Engineering Development Center  
ARO, Inc., Operating Contractor  
Arnold Air Force Station, Tennessee

## 2a. REPORT SECURITY CLASSIFICATION

UNCLASSIFIED

## 2b. GROUP

N/A

## 3. REPORT TITLE

PARAMETRIC STUDY OF SEPARATION CHARACTERISTICS OF THE M-117 BOMB FROM  
THE F-4C AIRCRAFT AT TRANSONIC SPEEDS

## 4. DESCRIPTIVE NOTES (Type of report and inclusive dates)

August 12 through 16, 1969 - Final Report

## 5. AUTHOR(S) (First name, middle initial, last name)

E. G. Allee, Jr., ARO, Inc.

This document has been approved for public release  
its distribution is unlimited. *Per TAB 76-6  
D+H 12 March '76*

## 6. REPORT DATE

December 1969

## 7a. TOTAL NO. OF PAGES

110

## 7b. NO. OF REFS

1

## 8a. CONTRACT OR GRANT NO.

F40600-69-C-0001

## 9a. ORIGINATOR'S REPORT NUMBER(S)

AEDC-TR-69-248

b. Program Element 62701F

c. Program Area 327B

## 9b. OTHER REPORT NO(S) (Any other numbers that may be assigned this report)

N/A

## 10. DISTRIBUTION STATEMENT

This document is subject to special export controls and each transmittal to foreign governments or foreign nationals may be made only with prior approval of Air Force Armament Laboratory (AFATL) (ATII), Eglin Air Force Base, Florida 32542.

## 11. SUPPLEMENTARY NOTES

Available in DDC

## 12. SPONSORING MILITARY ACTIVITY

Air Force Armament Laboratory  
Eglin Air Force Base, Florida 32542

## 13. ABSTRACT

A parametric study was conducted to determine the separation characteristics of an M-117 bomb from a Triple Ejection Rack (TER) located on the left-wing inboard pylon of an F-4C aircraft. Data were obtained using 0.05-scale models at Mach numbers from 0.50 to 1.30 and at simulated altitudes of 5000 and 20,000 ft. The effects of variations in mass, moment of inertia, center-of-gravity location, ejector force, initial store attitude on the TER, and presence of adjacent stores were investigated.

This document is subject to special export controls and each transmittal to foreign governments or foreign nationals may be made only with prior approval of Air Force Armament Laboratory (AFATL) (ATII), Eglin Air Force Base, Florida 32542.

UNCLASSIFIED

Security Classification

14.

KEY WORDS

LINK A

LINK B

LINK C

ROLE

WT

ROLE

WT

ROLE

WT

transonic wind tunnels

F-4C aircraft

releasing

ejection

flight characteristics

external stores

altitude simulation

1 Bomb - - M-117.  
2 Airplanes - - Separation

4 Stores - - Separation

5 External " - - "

1-2

UNCLASSIFIED

Security Classification